SANDIA REPORT

SAND88—2936 • UC—70
Unlimited Release
Printed December 1988

Yucca Mountain Project

Technical Correspondence in Support of an Evaluation of the Hydrologic Effects of Exploratory Shaft Facility Construction at Yucca Mountain

Andrew C. Peterson, Roger R. Eaton,
Anthony J. Russo, John A. Lewin

Prepared by
Sandia National Laboratories
Albuquerque, New Mexico 87185 and Livermore, California 94550
for the United States Department of Energy
under Contract DE-AC04-76DP00789

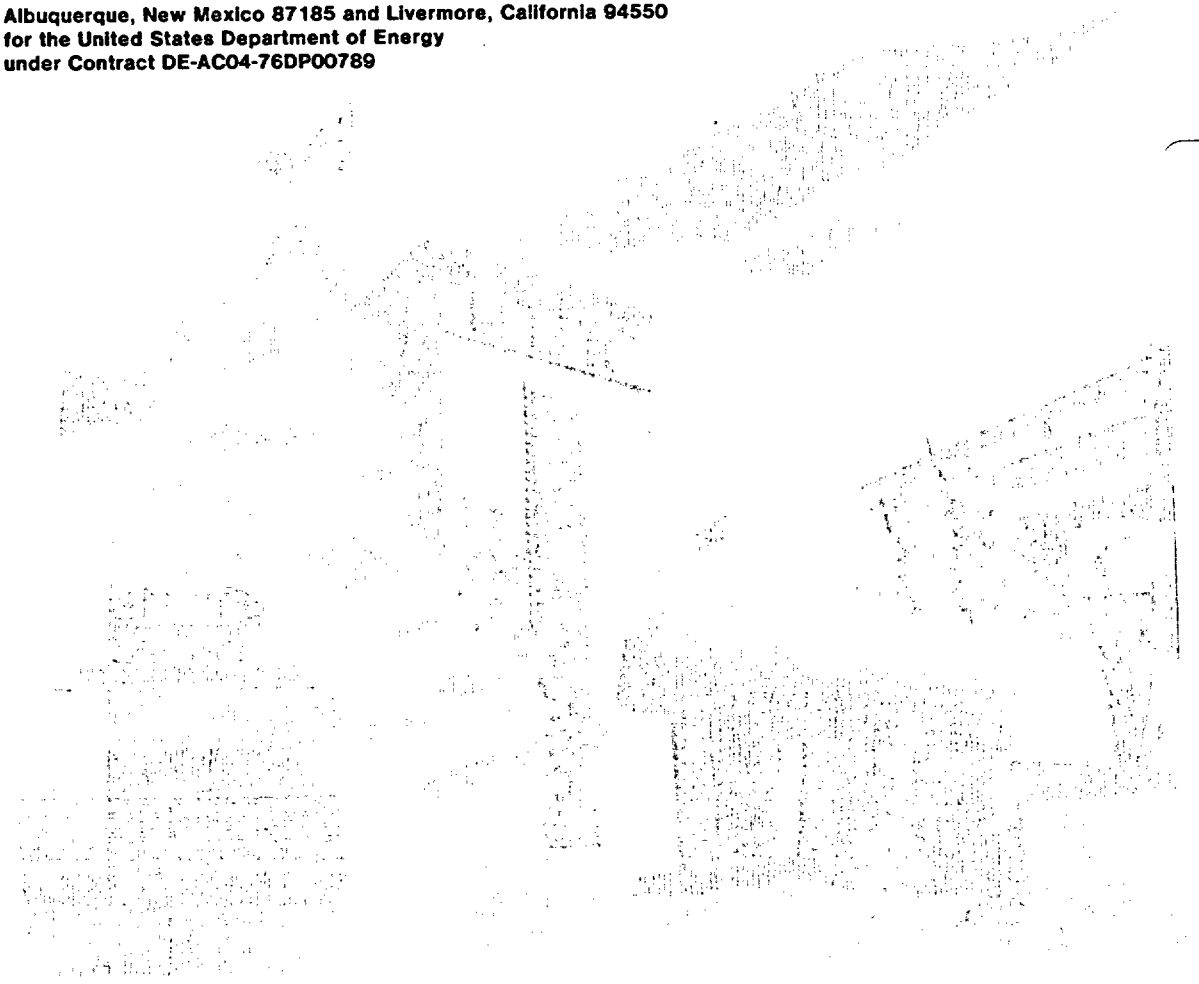

HYDROLOGY DOCUMENT NUMBER 459

"Prepared by Yucca Mountain Project (YMP) participants as part of the Civilian Radioactive Waste Management Program (CRWM). The YMP is managed by the Yucca Mountain Project Office of the U.S. Department of Energy, Nevada Operations Office (DOE/NV). YMP work is sponsored by the Office of Geologic Repositories (OGR) of the DOE Office of Civilian Radioactive Waste Management (OCRWM)."

Issued by Sandia National Laboratories, operated for the United States Department of Energy by Sandia Corporation.

Printed in the United States of America
Available from
National Technical Information Service
U.S. Department of Commerce
5285 Port Royal Road
Springfield, VA22161

NTIS price codes
Printed copy: A06
Microfiche copy: A01

SAND88-2936
Unlimited Release
Printed December 1988

Distribution
Category UC-70

TECHNICAL CORRESPONDENCE IN SUPPORT OF AN EVALUATION OF THE HYDROLOGIC EFFECTS OF EXPLORATORY SHAFT FACILITY CONSTRUCTION AT YUCCA MOUNTAIN

Andrew C. Peterson
Repository Performance Assessment Division

Roger R. Eaton, Anthony J. Russo, and John A. Lewin
Fluid Mechanics and Heat Transfer Division

Sandia National Laboratories
Albuquerque, NM 87185

ABSTRACT

This document comprises four letter reports containing information that has been used in preparing the plan to characterize the site of the prospective repository at Yucca Mountain. The Yucca Mountain Project is studying the feasibility of constructing a high-level nuclear waste repository in the Topopah Spring Unit of the Paintbrush Tuff. One activity of site characterization is the construction of two exploratory shafts. The information in this report pertains to (1) engineering calculations of the potential distribution of residual water from constructing the exploratory shafts and drifts, (2) numerical calculations predicting the movement of the residual construction water from the shaft walls into the rock, (3) numerical calculations of the movement of the residual water and how the movement is affected by ventilation, and (4) measurement of the movement of water into a welded tuff core when a pulse of water pressure is applied to a laboratory test sample for a short time (100 min).

QUALITY ASSURANCE LEVELS

Sections 1-3: Data gathered at QA Level III. Analyses performed at QA Level III.

Appendices A-E: Data gathered at QA Level III. Analyses performed at QA Level III.

CONTENTS

FOREWORD

This document contains four separate letter reports (Appendices A through D) that support information in the "Site Characterization Plan" (DOE, 1988) for the Yucca Mountain Project. The letter reports are collected in this document as a convenient means of referencing previously unpublished information cited in the "Site Characterization Plan."

ACKNOWLEDGMENT

The authors express their thanks to Carolyn Horne, LATA, and Susan Switzer, LATA, for editing throughout the revision cycles.

1.0 INTRODUCTION

The Yucca Mountain Project is currently investigating the feasibility of disposing of high-level radioactive waste in the unsaturated zone at Yucca Mountain in southern Nevada. Construction of the exploratory shaft facility (ESF), which includes the two shafts described in the "Site Characterization Plan" (DOE, 1988), will introduce additional water into the unsaturated zone. Experiments needed to characterize the unsaturated zone at the site require estimates of the potential effects of the construction water on the in situ experiments. Performance assessment of the Yucca Mountain site for postclosure radionuclide transport also requires estimates of the effects of construction water on the capability of the site to isolate and contain waste. Four letter reports, Appendices A-D, contribute to the evaluation of the potential effects of water from construction of the ESF and were initially prepared to support the "Exploratory Shaft Facility Fluids and Materials Evaluation" by K. A. West (1988).

Appendix A addresses the distance to which rock could be affected when up to 10% of the construction water is retained in the walls of the shafts and drifts. The engineering calculations in this report evaluate the radial distance that water would move from the shaft and drift walls when (1) the rock is initially unsaturated, (2) there is essentially no water in the fractures, and (3) the retained construction water enters the rock at a rate that initially saturated only the fractures. The affected distance has been determined by a geometric calculation based on the volume of retained water and the capacity of the initially unsaturated fractures. The change in saturation that would occur as a result of subsequent movement of the water, through capillary action, from the fractures into the matrix has also been calculated. Five hydrologic strata that represent Yucca Mountain were modeled in the analyses. The calculation indicated that at the Topopah Spring repository horizon the fractures within 24 m of the centerline of the shafts need to be saturated to contain 10% of the construction water. The maximum change in saturation was about 0.0014 at this same horizon when the construction water initially contained in the fractures came to equilibrium with the water in the rock matrix.

Appendix B provides analyses of the time-dependent, one-dimensional radial flow of the residual construction water in the rock matrix adjacent to the shaft liner. The retained water was initially assumed to be contained in the modified permeability zone (MPZ) around the shaft. The MPZ is the zone immediately surrounding an underground excavation in which the permeability of the rock mass has been altered as a result of stress redistribution and blast damage effects. The NORIA computer code (Bixler, 1985) has been used to calculate the changes in saturation out to a radius of 25 m from the shaft centerline for computed times of 1-1000 yr. It has been conservatively assumed for these calculations that the permeability of the matrix in the MPZ is 80 times larger than in the unmodified region. This conservative assumption results in a higher saturation at the MPZ outer boundary and an increased movement of water into the rock. In the analyses performed, the increase in saturation at radial distances greater than 5 m from the shaft centerline (0.6 m from the MPZ) was less than 0.03.

Appendix C is an extension of the analyses contained in the second letter report and includes the effects of drift ventilation on the movement of the residual construction water and in situ pore water. The NORIA code was used for these analyses. The results of these studies indicate that change in the saturation of the rock near the drift walls is completely dominated by the ventilation system and that in a matter of months the ventilation system can remove more water from the walls of the drifts than may be retained as a result of drift construction.

Appendix D provides laboratory data from experiments on the movement of water into tuff when a 100-min pulse of water is applied to one end of a core sample and is then allowed to redistribute isothermally. This data may be used to indicate the distance that construction water would penetrate the rock. Measurements of the saturation of a welded tuff sample showed that very little water penetrated the sample and that later redistribution of the water into the core was very slow.

2.0 CONCLUSIONS

The various analytical, numerical, and experimental approaches used in these studies indicate that saturation increases in the in situ rock mass from construction water would be small. The calculated changes in saturation may be less than the accuracy of the experiments and numerical calculations. However, these analyses did not consider the potential effects of local variations in strata properties that could occur. Thus, under these variations, the residual mining water could affect in situ experiments located some distance from the shaft. Without detailed knowledge of the variations in the strata, it is impossible to accurately model these situations.

3.0 REFERENCES

1. Bixler, N. E., 1985, "NORIA--A Finite Element Computer Program for Analyzing Water, Vapor, Air, and Energy Transport in Porous Media," SAND84-2057, Sandia National Laboratories, Albuquerque, NM.

2. DOE (U.S. Department of Energy), 1988, "Site Characterization Plan," DOE/RW-0199, Office of Civilian Radioactive Waste Management, Washington, DC.

3. West, K. A., 1988, "Exploratory Shaft Facility Fluids and Materials Evaluation," LA-111398, Los Alamos National Laboratory, Los Alamos, NM.

APPENDIX A

SLTR87-2001

DISTRIBUTION OF RESIDUAL SHAFT DRILLING AND DRIFT CONSTRUCTION WATER IN THE EXPLORATORY SHAFT FACILITY AT YUCCA MOUNTAIN

SLTR87-2001
Department 6310 Letter Report
Sandia National Laboratories
Nevada Nuclear Waste Storage
Investigations Project
Issued June 1987

DISTRIBUTION OF RESIDUAL SHAFT DRILLING AND DRIFT CONSTRUCTION WATER IN THE EXPLORATORY SHAFT FACILITY AT YUCCA MOUNTAIN

R. R. Eaton and A. C. Peterson

Introduction

The current plan for the shaft drilling and drift construction in the exploratory shaft facility (ESF) at the proposed Nevada Nuclear Waste Repository site includes the use of water for dust control and drilling purposes. During this operation, some of the water will be absorbed by the host rock. The presence of this water has generated concern about its effect on the undisturbed conditions of the rock; that is, can this water increase the saturation of the rock surrounding the shaft to a level that could have an adverse effect on in situ experiments or performance of the waste package?

This report is an initial attempt to address this issue and fulfills part of the analyses requested in Problem Definition Memo (PDM) 72-22. Two limiting cases are addressed to estimate the radial distance to which the rock is affected and the maximum increase in saturation that can be expected. For these analyses, it was assumed that the fractures had a small initial residual saturation and that the matrix initial saturation was low enough that when the water moved from the fractures into the matrix, the matrix did not become fully saturated. The hydrologic units that were included in these analyses were the Tiva Canyon welded, devitrified; Paintbrush vitric; Topopah Spring lithophysae-rich; Topopah Spring lithophysae-poor; and Calico Hills vitric. They are referred to in this report as Tiva Canyon, Paintbrush, Topopah Litho, Topopah Rep, and Calico Hills, respectively.

Calculations were performed for the shaft and drift geometries to determine the distance that water retained from construction could move from the surface into the rock if the water is assumed to initially saturate the fractures and not be absorbed into the matrix. The Case 1 analyses apply to the shaft, and Case 3 analyses apply to the drift. For both Case 1 and 3 analyses, the residual drilling water is assumed to enter the rock at a rate such that it initially stays in the fractures, uniformly filling them out to a radius, R, which is determined from the conservation of retained water. The change in the matrix saturation that would occur when the water from the fractures moved into the matrix was also

calculated. It is assumed that for longer times, the extremely large capillary forces that are found in tuff rock, pull the water from the fractures into the rock matrix, thus providing a means to approximate the expected increase in saturation in the host rock between the walls, R_o, and the radius, R.

To investigate the effect on the saturation level of the distance the retained water may move from the wall, calculations identified as Case 2 and Case 4 were performed. Water is considered to always be in fracture/matrix equilibrium and is therefore diffused as a result of the capillary pressure. Based on this premise, material saturation increase is calculated as a function of radius.

Cases 1 and 3 are limiting cases in that they calculate the maximum radial distance that water can travel into the saturated fractures of the matrix and the resulting equilibrium saturation increase. Cases 2 and 4 are limiting cases in that they calculate the maximum matrix saturation increase that may occur at any radial distance from the walls. Based on the output of these simplified parametric studies of the five hydrologic units in Yucca Mountain, recommendations for additional studies, which would be performed using the finite element code NORIA [1], are made. These calculations can be made for a few limiting cases and will provide additional bases for the assumptions made in Cases 1-4.

Case 1--Problem Definition

In this study it is assumed that the water infiltrates the region near the shaft sufficiently fast that the path of least resistance is through the natural fracture array that exists in the rock. It is assumed that the fractures saturate out to a distance R (Figure 1), which encompasses enough fracture volume to hold the water not removed during the drilling process. Equation 1, based on the assumption that the available volume in the fractures equals the volume of water retained for this scenario, is

$$R = \sqrt{\frac{nV}{\pi\phi_f(1 - s_{rf})} + R_0^2} \quad , \tag{1}$$

where R = the radius to which the fractures are saturated (m); n = the fraction of the construction water left in the rock (nd); V = the total volume of construction water used per meter (m^3/m); ϕ_f = porosity of conducting fractures (nd); s_{rf} = residual saturation of the fractures (nd); and R_0 = outside radius of the concrete shaft liner (m) (Figure 1).

In these calculations, the radius of the outside of the concrete liner was assumed to be 2.21 m. This is the same radius that was used in Reference 2, which analyzed the effects of the modified permeability zone around the shaft.

In the second part of Case 1, the saturation increases in the matrix after the water has left the fractures and was pulled, through capillary pressure, into the matrix in a volume based on the same total radius, R, was calculated. The equation for the saturation increase based on conservation of water volume is

$$(s_f - s_i)_m = \frac{\phi_f(1 - s_{rf})}{\phi_m} \quad , \tag{2}$$

where $(s_f - s_i)_m$ = matrix saturation increase (nd); $(1 - s_{rf})$ = fracture saturation decrease (nd); ϕ_f = fracture porosity (nd); and ϕ_{m2} = matrix porosity (nd). As shown by Equation 2, the increase in saturation does not depend on the radius to which the fractures are saturated. The increase is dependent on the fracture porosity and residual saturation and the matrix porosity. To investigate the effect of the matrix porosity on the change in saturation for each hydrologic unit, calculations were performed using the fracture characteristics listed in Table 1 for matrix porosities ranging from 0.05 to 0.5. This range includes the reference matrix porosity listed in Table 1. (The values from Reference 3 are within the range of values provided in the Reference Information Base (RIB),

Reference 3, except for the matrix porosity for the Calico Hills Unit. The matrix porosity was larger by 0.01 than the range indicated in the RIB. This value of matrix porosity was used because previous calculations, Reference 3, had been performed using this value and the conclusions in the present analyses would not be affected by this small difference.)

The FORTRAN program used to evaluate Equations 1 and 2 for the shaft is listed in Attachment A.

Case 1--Results

Results obtained using Equations 1 and 2 for all five hydrologic strata are given in Attachment B. These are based on 3.02 m^3/m of drilling water and the material properties given in Table 1. Preliminary estimates of the amount of construction water that may be retained were about 10%. Therefore, calculations were performed for up to 10% retained water. Figure 2 shows a plotted summary of the calculations based on Equation 1. It can be seen from this figure that when 10% of the drilling water is retained in the fractures, the fractures saturate to a radial distance, R, between 27 and 47 m for the five strata. The radius is the smallest for the Topopah Rep because the fracture porosity was the highest in this unit of the hydrologic strata analyzed.

Figure 3 shows a plotted summary of the results of Equation 2. It can be seen from this figure that the maximum increase in saturation, if the hydrologic strata porosities were as low as 0.05, is less than 0.004. The change in saturation for the reference value of matrix porosity of each hydrologic strata is also shown in Figure 3. The largest increase would occur in the Tiva Canyon unit and would be about 0.0017.

Case 2--Problem Definition

In this case it is assumed that the primary driving force for the transport of water into the rock is capillarity. Additionally, it is assumed that the water distributed between R and R_0 is at a uniform

saturation, as indicated in Figure 4. Equation 3 is an expression for the conservation of water under these assumptions.

$$(s_f - s_i)_m = \frac{nV}{\phi_m \pi (R^2 - R_0^2)} \quad . \tag{3}$$

This equation was also evaluated for the shaft using the FORTRAN program listed in Attachment A.

Case 2--Results

A tabulated display of the results of Equation 3 is given in Attachment B for all five units, assuming that 10% of the drilling water was retained in the rock. Saturation increases for a range of radial distances between 10 and 110 m are given. Figure 5 shows calculated saturation increases up to 0.013. The maximum saturation increase, which occurs in the Tiva Canyon strata, is calculated to be 0.013 at a radial distance of 10 m. This radial distance would be 7.8 m from the outside of the concrete liner. At a radius of 20 m, the maximum increase in saturation would be 0.003. For the Topopah Spring strata the saturation increase would be 0.009 at a radial distance of 10 m.

Case 3--Problem Definition

This case is identical to Case 1 except that it applies to a drift. For these analyses the drift geometry shown in Figure 6 was used as the basis for the calculations. The drift was analyzed as a right circular cylinder having the same circular area as the drift shown in Figure 6. This resulted in the drift being analyzed as a circle with a radius of 3.38 m. Equation 1 was also used for this case with the inside radius of the drift wall, R_0, equaling 3.38 m.

The calculation of the change in the matrix saturation after the water retained from drift construction was pulled from the fractures into the matrix would be the same for a drift as for the shaft. Therefore, the

results discussed for Case 1 and shown in Figure 3 would also apply to the drifts.

The FORTRAN program used to evaluate Equation 1 for the drifts is listed in Attachment C.

Case 3--Results

The calculated radii applicable to the drift geometry for five hydrologic strata are listed in Attachment D. Results are given for all the strata, even though drifts are only planned for the Topopah Spring and Calico Hills units. These results were based on 1.65 m^3/m of water being used during drift construction and the material properties listed in Table 1. The results are also plotted in Figure 7, which shows that when 10% of the construction water is retained in the fractures, the fractures will be saturated to a radial distance between 18 and 45 m for the five strata analyzed. The largest radius was in the Calico Hills unit and the smallest radius was in the Topopah Spring repository unit.

Case 4--Problem Definition

This case is identical to Case 22, except that it is also based on the drift geometry discussed for Case 3. Therefore, in Equation 3, an inside radius of 3.38 m was used.

The FORTRAN program used to evaluate Equation 3 for the drifts is listed in Attachment C.

Case 4--Results

The increase in saturation (calculated using Equation 3) applicable to the drift geometry assuming 10% of the construction water was retained in each of the five hydrologic units is listed in Attachment D. These results, also shown in Figure 8, indicate a maximum calculated increase in saturation of about 0.007 for a radius of 10 m in the Tiva Canyon unit.

The increase in saturation for the Topopah Spring and Calico Hills units for a 10-m radius was 0.0054 and 0.0013, respectively.

Conclusions and Additional Calculations

The results for the analyses discussed in the document indicate that the change in saturation would be quite small when the retained water was uniformly distributed in the rock. The largest calculated increase in saturation was 0.013 when 10% of the drilling water was retained in the Tiva Canyon unit around the shaft at a distance of 10.0 m from the shaft center (7.8 m from the concrete liner). For representative matrix and fracture porosities for the hydrologic strata the exploratory shaft will be constructed in, the maximum change in saturation was 0.0017. These changes in saturation may be less than the accuracy of experiments and numerical calculations. These analyses did not consider potential effects of local variations in strata properties that could occur.

These analyses assumed the distribution of the retained water was uniform. However, Figure 4 illustrates that the initial distribution will probably not be uniform. Therefore, to investigate the potential effects of the initial distribution of the retained water, it is recommended that time-dependent, one-dimensional radial calculations be performed using the NORIA finite element computer code for the significant cases. These calculations will show the movement of the retained water from the surface.

References

1. N. E. Bixler, "NORIA--A Finite Element Computer Program for Analyzing Water, Vapor, Air, and Energy Transport in Porous Media," SAND84-2057, Sandia National Laboratories, Albuquerque, NM, August 1985.

2. J. A. Fernandez, T. E. Hinkebein, and J. B. Case, "Selected Analyses to Evaluate the Effect of the Exploratory Shaft on Repository Performance of Yucca Mountain," SAND85-0598, Sandia National Laboratories, Albuquerque, NM, 1988.

3. DOE (U.S. Department of Energy), "The Nevada Nuclear Waste Storage Investigations Project Reference Information Base," Version 03.001, Washington, DC, December 1987.

Table 1

Material Properties

Unit	ϕ_m	s_{rf}	$\phi_f \cdot 10^3$
Tiva Canyon	0.08		0.140
Paintbrush	0.4		0.027
Topopah Litho	0.11		0.041
Topopah Rep	0.11		0.18
Calico Hills	0.46		0.046
fractures		0.0395	

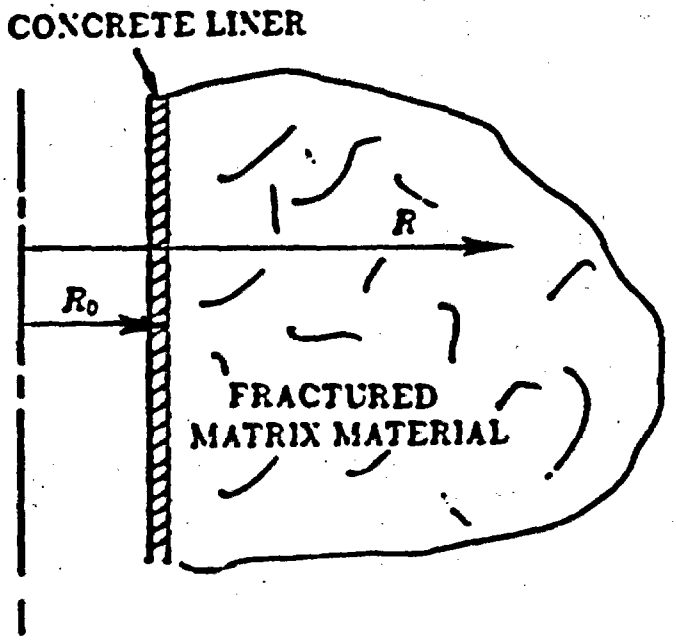

Figure 1. Outline of Problem Geometry.

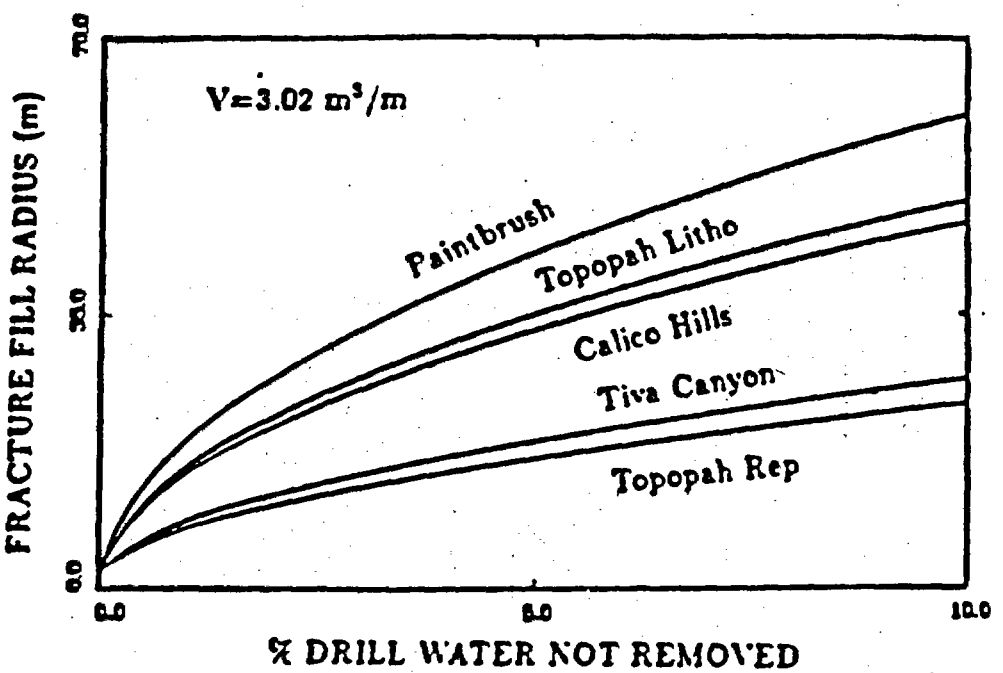

Figure 2. Radius to Which Fractures Would Fill to Accommodate All Residual Drilling Water, Case 1a.

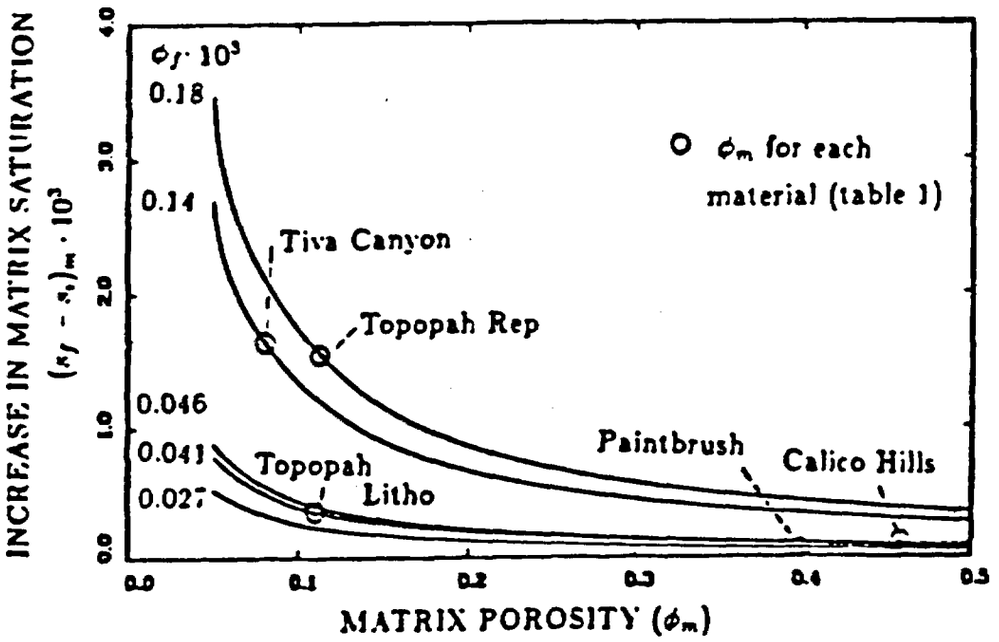

Figure 3. Increase in Matrix Saturation Assuming All Residual Drilling Water Was Originally in Fractures, Case 1b.

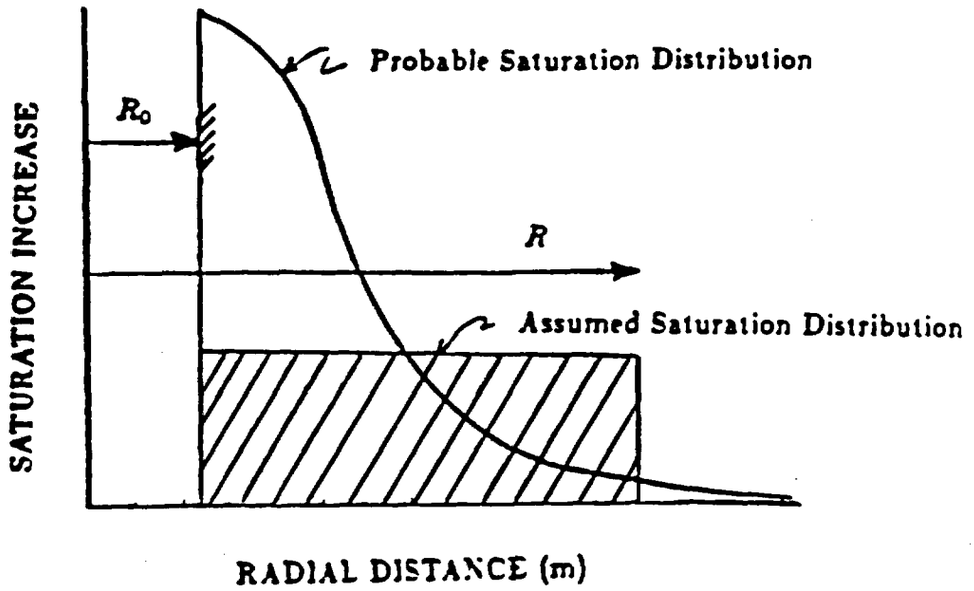

Figure 4. Probable and Assumed Water Distribution, Case 2.

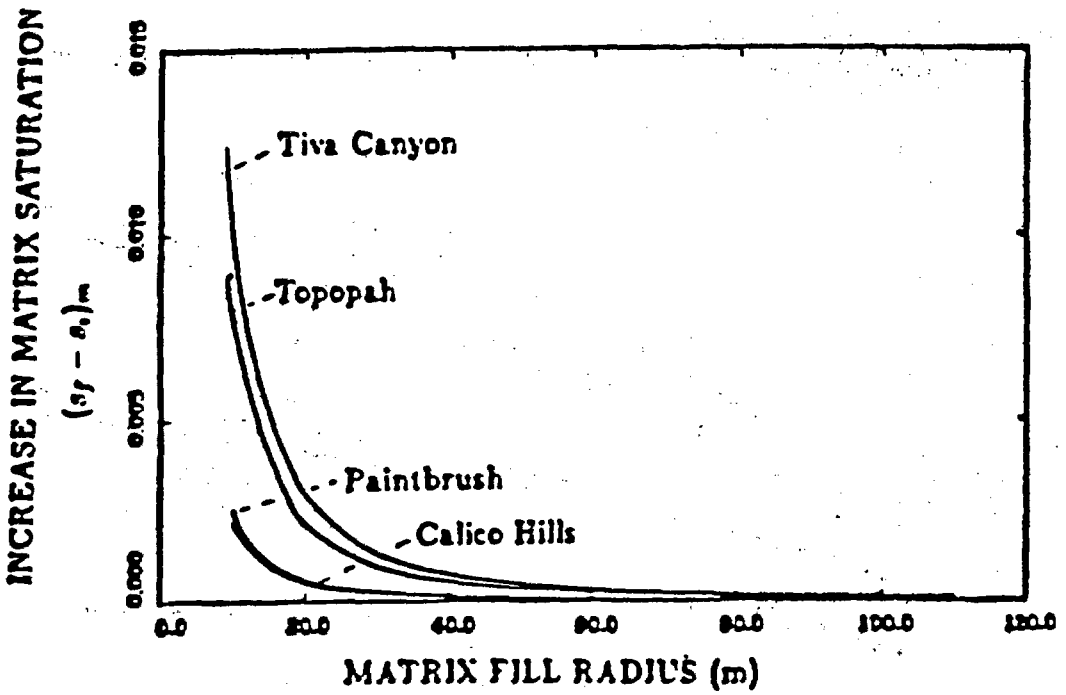

Figure 5. Increase in Matrix Saturation Assuming Residual Drilling Water To Be Evenly Distributed in Matrix Between R_0 and R, Case 2.

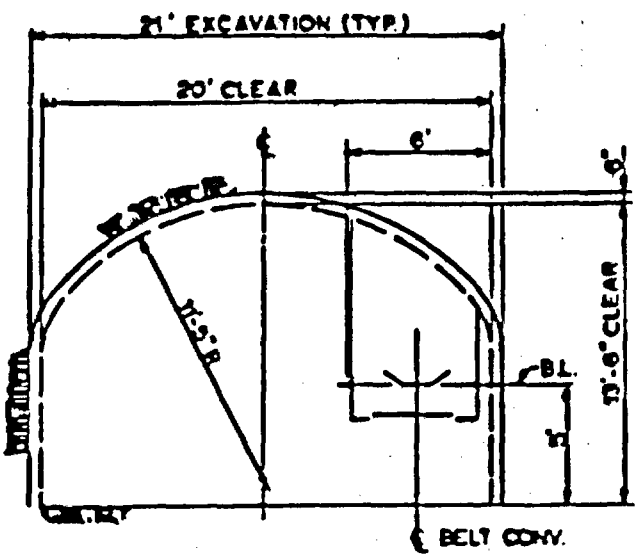

Figure 6. Drift Geometry Used in Analyses.

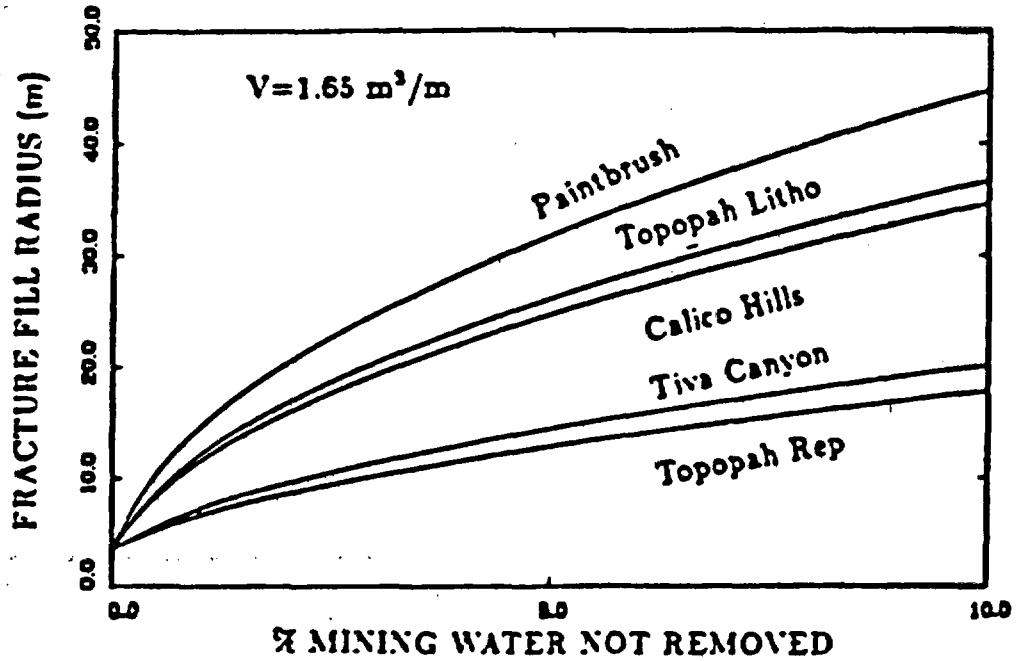

Figure 7. Radius to Which Fractures Would Fill To Accommodate All Residual Drift Construction Water, Case 3.

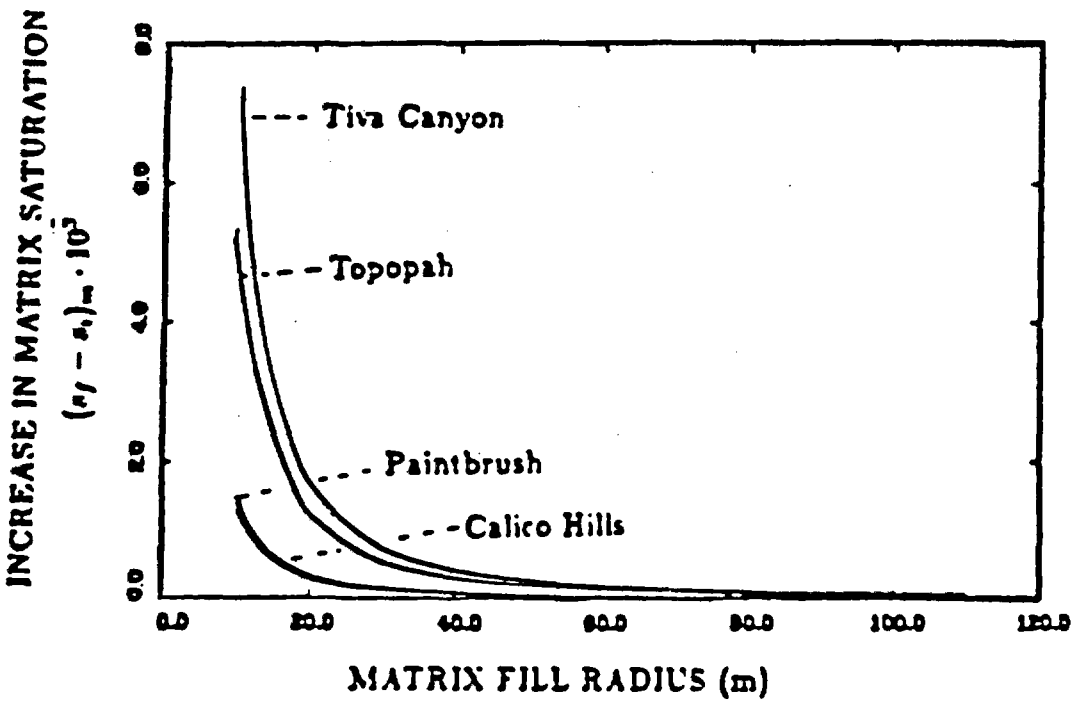

Figure 8. Increases in Matrix Saturation Assuming Residual Drift Construction Water To Be Uniformly Distributed in Matrix Between R_0 and R, Case 4.

Attachment A

The FORTRAN program listed below solves Equations 1, 2, and 3 for several parametric sets of conditions. The program is complete and needs no additional input to generate the output listed in Attachment B.

```
C  PROGRAM TO CALCULATE THE RADIUS OF FRACTURE FILL
C  AND THE CHANGE OF SATURATION IN MATRIX
C  RD = RADIUS OF DRILL SHAFT (M)
C  VF = RELATIVE VOLUME OF FRACTURES (nd)
C  W  = DRILL WATER PER METER  (3.02 m**2 = 32.5 ft**2)
C  DX = FRACTION OF TOTAL WATER
C  POR = POROSITY
C  DPOR = CHANGE IN POROSITY
C  SRF= RESIDUAL SATURATION OF FRACTURES
C
      DIMENSION VF(10),PORM(10)
      OPEN (UNIT=1,NAME='RAD.PDAT',TYPE='NEW')
      OPEN (UNIT=2,NAME='RAD.DAT',TYPE='NEW')
      DATA (VF(I),I=1,5)/1.4E-4, 2.75E-5, 4.1E-5, 1.8E-4, 4.6E-5/
      DATA (PORM(I),I=1,5)/ .08, .40, .11, .11, .46/
      RD = 2.21
      SRF=0.039
      NP=11
      NPM1=NP-1
      W = 3.02
      DX = 0.01
      DR = .10
      DO 10 I = 1,5
      X = -DX
      XP = X*100
      WRITE(2,*)
      WRITE(2,*) 'FRACTURE POROSITY= ', VF(I)
      WRITE(1,*) 'X DRILL WATER     FILL RADIUS (m) '
      WRITE(1,*) I,NP
      DO 10  J = 1,NP
      X=X+DX
      XP=X*100
      RF = (X*W/(3.14159*VF(I)*(1-SRF)) + RD**2)**0.5
      WRITE(2,*) XP,RF
      WRITE(1,*) XP,RF
10    CONTINUE
C
      DPOR = 0.05
      DO 20 I = 1,5
      WRITE(2,*)
      WRITE(2,*) 'FRACTURE POROSITY =', VF(I)
      WRITE(2,*) 'POROSITY          CHANGE IN SATURATION'
      POR = 0
      WRITE(1,*) I+5,NPM1
      DO 20 J = 1,NPM1
      POR = POR + DPOR
      DS = VF(I)*(1-SRF)/POR
      WRITE(2,*) POR,DS
      WRITE(1,*) POR,DS
20    CONTINUE
C
      WRITE(2,*)
      WRITE(2,*) 'MATRIX SATURATION INCREASE TO RADIUS FILL '
      X=0
      DO 30 I = 1,5
      R=0
      WRITE(2,*)
      WRITE(2,*) 'MATRIX POROSITY =', PORM(I)
      WRITE(2,*) 'FILL RADIUS    SATURATION INCREASE '
      WRITE(1,*) I+10,NP
      DO 30  J = 1,NP
      R=R+DR
      DS = (X*W/(3.14159*PORM(I)*(R**2 - RD**2)) )
      WRITE(2,*) R,DS
      WRITE(1,*) R,DS
30    CONTINUE
      CLOSE (UNIT=1,DISP='SAVE')
      CLOSE (UNIT=2,DISP='SAVE')
      END
```

Attachment B

The Computer program listed in Attachment A was used to generate the data listed below for Case 1a. The FILL RADIUS (m) is the radius to which the fractures would fill for a given percentage of drill water left in the shaft after drilling. This assumes no water is initially absorbed by the matrix material.

Tiva Canyon

FRACTURE POROSITY= 1.40000000E-04

% DRILL WATER	FILL RADIUS (m)
0.00000000E+00	2.210000
1.000000	8.736974
2.000000	12.15670
3.000000	14.80662
4.000000	17.04953
5.000000	19.02550
6.000000	20.82277
7.000000	22.47306
8.000000	24.01019
9.000000	25.45466
9.999999	26.82145

Paintbrush

FRACTURE POROSITY= 2.75000000E-05

% DRILL WATER	FILL RADIUS (m)
0.00000000E+00	2.210000
1.000000	19.19581
2.000000	27.08254
3.000000	33.10785
4.000000	38.20835
5.000000	42.70395
6.000000	46.76939
7.000000	50.50865
8.000000	54.00356
9.000000	57.25924
9.999999	60.35205

Topopah Litho

FRACTURE POROSITY= 4.09999995-05

% DRILL WATER	FILL RADIUS (m)
0.00000000E+00	2.210000
1.000000	15.47235
2.000000	22.19999
3.000000	27.14435
4.000000	31.31765
5.000000	34.99675
6.000000	38.32428
7.000000	41.38512
8.000000	44.23467
9.000000	46.91144
9.999999	49.44352

Topopah Rep

FRACTURE POROSITY= 1.80000008-04

% DRILL WATER	FILL RADIUS (m)
0.00000000E+00	2.210000
1.000000	7.725397
2.000000	10.77170
3.000000	13.09970
4.000000	15.07232
5.000000	16.81510
6.000000	18.36349
7.000000	19.84674
8.000000	21.20051
9.000000	22.47306
9.999999	23.67723

Calico Hills

FRACTURE POROSITY= 4.60000018-05

% DRILL WATER	FILL RADIUS (m)
0.00000000E+00	2.210000
1.000000	14.91115
2.000000	20.81143
3.000000	25.63707
4.000000	29.57563
5.000000	33.04809
6.000000	36.18887
7.000000	39.07804
8.000000	41.76783
9.000000	44.29458
9.999999	46.68477

The output data for Case 1b is given below. The change in saturation of the matrix (CHANGE IN SATURATION) was obtained by assuming that the water in the fractures between the shaft wall and the FILL RADIUS, calculated in Case 1a, is absorbed into the matrix material through capillary pressure.

Tiva Canyon

FRACTURE POROSITY = 1.40000000E-04

POROSITY	CHANGE IN SATURATION
5.0000001E-02	2.6908202E-03
0.1000000	1.5254051E-03
0.1500000	8.6533337E-04
0.2000000	5.2270506E-04
0.2500000	3.3616003E-04
0.3000000	2.2462462E-04
0.3500000	1.5439999E-04
0.4000000	1.0855000E-04
0.4500000	7.7777777E-05
0.5000001	5.6907899E-05

Paintbrush

FRACTURE POROSITY = 2.75000000E-05

POROSITY	CHANGE IN SATURATION
5.0000001E-02	5.2855001E-04
0.1000000	2.9427500E-04
0.1500000	1.7961333E-04
0.2000000	1.1213750E-04
0.2500000	7.4571000E-05
0.3000000	5.1561666E-05
0.3500000	3.6477136E-05
0.4000000	2.6065744E-05
0.4500000	1.8955772E-05
0.5000001	1.3854994E-05

Topopah Litho

FRACTURE POROSITY = 4.09999998E-05

POROSITY	CHANGE IN SATURATION
5.0000001E-02	7.8852003E-04
0.1000000	4.3901031E-04
0.1500000	2.6767333E-04
0.2000000	1.6700501E-04
0.2500000	1.0760401E-04
0.3000000	7.1536666E-05
0.3500000	4.8757429E-05
0.4000000	3.3824968E-05
0.4500000	2.3977772E-05
0.5000001	1.8831697E-05

Topopah Rep

FRACTURE POROSITY = 1.80000000E-04

POROSITY	CHANGE IN SATURATION
5.0000001E-02	3.4626003E-03
0.1000000	1.9285501E-03
0.1500000	1.1333000E-03
0.2000000	6.8540027E-04
0.2500000	4.3152005E-04
0.3000000	2.7462333E-04
0.3500000	1.7642857E-04
0.4000000	1.1424999E-04
0.4500000	7.4222222E-05
0.5000001	4.8960000E-05

Calico Hills

FRACTURE POROSITY = 4.60000001E-05

POROSITY	CHANGE IN SATURATION
5.0000001E-02	8.8412000E-04
0.1000000	4.9206000E-04
0.1500000	3.0070667E-04
0.2000000	1.9103000E-04
0.2500000	1.2682400E-04
0.3000000	8.4733333E-05
0.3500000	5.8026857E-05
0.4000000	4.0514999E-05
0.4500000	2.8755555E-05
0.5000001	2.0641695E-05

Attachment B (concluded)

The data listed below, for Case 2, give the matrix saturation increase (SATURATION INCREASE) between the shaft wall and FILL RADIUS for 10% residual water. In this calculation, it was assumed that the water in this region is at constant saturation.

MATRIX SATURATION INCREASE TO RADIUS FILL

Tiva Canyon

MATRIX POROSITY = 7.9999998E-02

FILL RADIUS	SATURATION INCREASE
10.00000	1.2633228E-02
20.00000	3.0411857E-03
30.00000	1.3424192E-03
40.00000	7.5331255E-04
50.00000	4.8158914E-04
60.00000	3.3423706E-04
70.00000	2.4547343E-04
80.00000	1.8789666E-04
90.00000	1.4843775E-04
100.0000	1.2022030E-04
110.0000	9.9347605E-05

Paintbrush

MATRIX POROSITY = 0.4000000

FILL RADIUS	SATURATION INCREASE
10.00000	2.5266458E-03
20.00000	6.0823717E-04
30.00000	2.6848388E-04
40.00000	1.5066253E-04
50.00000	9.6317835E-05
60.00000	6.6847402E-05
70.00000	4.9094688E-05
80.00000	3.7579332E-05
90.00000	2.9697551E-05
100.0000	2.4044160E-05
110.0000	1.9869522E-05

Topopah Litho

MATRIX POROSITY = 0.1100000

FILL RADIUS	SATURATION INCREASE
10.00000	9.1678027E-03
20.00000	2.2117714E-03
30.00000	9.7630499E-04
40.00000	5.4786372E-04
50.00000	3.5024667E-04
60.00000	2.4330148E-04
70.00000	1.7852614E-04
80.00000	1.3665212E-04
90.00000	1.0795473E-04
100.0000	8.7433305E-05
110.0000	7.2252806E-05

Topopah Rep

MATRIX POROSITY = 0.1100000

FILL RADIUS	SATURATION INCREASE
10.00000	9.1678027E-03
20.00000	2.2117714E-03
30.00000	9.7630499E-04
40.00000	5.4786372E-04
50.00000	3.5024667E-04
60.00000	2.4330148E-04
70.00000	1.7852614E-04
80.00000	1.3665212E-04
90.00000	1.0795473E-04
100.0000	8.7433305E-05
110.0000	7.2252806E-05

Calico Hills

MATRIX POROSITY = 0.4600000

FILL RADIUS	SATURATION INCREASE
10.00000	2.1670833E-03
20.00000	5.2690187E-04
30.00000	2.3346422E-04
40.00000	1.3101058E-04
50.00000	8.3754635E-05
60.00000	5.8128178E-05
70.00000	4.2661034E-05
80.00000	3.2677683E-05
90.00000	2.5815263E-05
100.0000	2.0907964E-05
110.0000	1.7277844E-05

Attachment C

The FORTRAN program listed below solves Equations 1, 2, and 3 for several parametric sets of conditions. The program is complete and needs no additional input to generate the output listed in Attachment D.

```
C  PROGRAM TO CALCULATE THE RADIUS OF FRACTURE FILL
C  AND THE CHANGE OF SATURATION IN MATRIX
C  RO = EQUIVALENT RADIUS OF DRIFT (M)
C  VF = RELATIVE VOLUME OF FRACTURES (nd)
C  W  =  DRILL WATER PER METER  (1.65 m**2 = 17.8 ft**2)
C  DX = FRACTION OF TOTAL WATER
C  POR = POROSITY
C  DPOR = CHANGE IN POROSITY
C  SRF= RESIDUAL SATURATION OF FRACTURES
C
      DIMENSION VF(10),PORM(10)
      OPEN (UNIT=1,NAME='RAD.DAT',TYPE='NEW')
      OPEN (UNIT=2,NAME='RAD.DAT',TYPE='NEW')
      DATA (VF(I),I=1,5)/1.4E-4, 2.75E-5, 4.1E-5, 1.8E-4, 4.6E-5/
      DATA (PORM(I),I=1,5)/ .08, .40, .11, .11, .46/
      RO = 3.38
      SRF=0.035
      NP=11
      NPM1=NP-1
      W = 1.65
      DX = 0.01
      DR = .10
      DO 10 I = 1,5
      X = -DX
      XP = X*100
      WRITE(2,*)
      WRITE(2,*) 'FRACTURE POROSITY= ', VF(I)
      WRITE(2,*) '% DRILL WATER     FILL RADIUS (m) '
      WRITE(1,*) I,NP
      DO 10 J = 1,NP
      X=X+DX
      XP=X*100
      RF = (X*W/(3.14159*VF(I)*(1-SRF)) + RO**2)**0.5
      WRITE(2,*) XP,RF
      WRITE(1,*) XP,RF
10    CONTINUE
C
      DPOR = 0.05
      DO 20 I = 1,5
      WRITE(2,*)
      WRITE(2,*) 'FRACTURE POROSITY =', VF(I)
      WRITE(2,*) 'POROSITY        CHANGE IN SATURATION'
      POR = 0
      WRITE(1,*) I+5,NPM1
      DO 20 J = 1,NPM1
      POR = POR + DPOR
      DS = VF(I)*(1-SRF)/POR
      WRITE(2,*) POR,DS
      WRITE(1,*) POR,DS
20    CONTINUE
C
      WRITE(2,*)
      WRITE(2,*) 'MATRIX SATURATION INCREASE TO RADIUS FILL '
      X=0
      DO 30 I = 1,5
      R=0
      WRITE(2,*)
      WRITE(2,*) 'MATRIX POROSITY =',  PORM(I)
      WRITE(2,*) 'FILL RADIUS   SATURATION INCREASE '
      WRITE(1,*) I+10,NP
      DO 30  J = 1,NP
      R=R+DR
      DS = (X*W/(3.14159*PORM(I)*(R**2 - RO**2)) )
      WRITE(2,*) R,DS
      WRITE(1,*) R,DS
30    CONTINUE
      CLOSE (UNIT=1,DISP='SAVE')
      CLOSE (UNIT=2,DISP='SAVE')
      END
```

Attachment D

The computer program listed in Attachment C was used to generate the data listed below for Case 3. The FILL RADIUS (m) is the radius to which the fractures would fill for a given percentage of water left in the drift after mining. This assumes no water is initially absorbed by the matrix material.

Tiva Canyon

FRACTURE POROSITY= 1.4000000E-04

% DRILL WATER	FILL RADIUS (m)
0.0000000E+00	3.380000
1.000000	7.103661
2.000000	9.460422
3.000000	11.33742
4.000000	12.94507
5.000000	14.37402
6.000000	15.67322
7.000000	16.87269
8.000000	17.99236
9.000000	19.04633
9.999999	20.04496

Paintbrush

FRACTURE POROSITY= 2.7500000E-05

% DRILL WATER	FILL RADIUS (m)
0.0000000E+00	3.380000
1.000000	14.45694
2.000000	20.22123
3.000000	24.65025
4.000000	28.39558
5.000000	31.70345
6.000000	34.69647
7.000000	37.45106
8.000000	40.01648
9.000000	42.42706
9.999999	44.70785

Topopah Litho

FRACTURE POROSITY= 4.0999999E-05

% DRILL WATER	FILL RADIUS (m)
0.0000000E+00	3.380000
1.000000	12.03011
2.000000	16.67401
3.000000	20.28107
4.000000	23.33711
5.000000	26.03689
6.000000	28.48150
7.000000	30.73301
8.000000	32.83012
9.000000	34.80105
9.999999	36.66627

Topopah Rep

FRACTURE POROSITY= 1.8000000E-04

% DRILL WATER	FILL RADIUS (m)
0.0000000E+00	3.380000
1.000000	6.464284
2.000000	8.494089
3.000000	10.12483
4.000000	11.52713
5.000000	12.77643
6.000000	13.91402
7.000000	14.96537
8.000000	15.94757
9.000000	16.87269
9.999999	17.74955

Calico Hills

FRACTURE POROSITY= 4.6000001E-05

% DRILL WATER	FILL RADIUS (m)
0.0000000E+00	3.380000
1.000000	11.41203
2.000000	15.78114
3.000000	19.17953
4.000000	22.06048
5.000000	24.60640
6.000000	26.91254
7.000000	29.03609
8.000000	31.01459
9.000000	32.87423
9.999999	34.63416

The data listed below, for Case 4, give the matrix saturation increase (SATURATION INCREASE) between the drift wall and FILl RADIUS for 10% residual water. In this calculation, it was assumed that the water in this region is at constant saturation.

Tiva Canyon

MATRIX SATURATION INCREASE TO RADIUS FILL

MATRIX POROSITY = 7.9999998E-02

FILL RADIUS	SATURATION INCREASE
10.00000	7.4119135E-03
20.00000	1.6695417E-03
30.00000	7.3883934E-04
40.00000	4.1322537E-04
50.00000	2.6361144E-04
60.00000	1.8264875E-04
70.00000	1.3429570E-04
80.00000	1.0276386E-04
90.00000	8.1165579E-05
100.0000	6.5726553E-05
110.0000	5.4308690E-05

Paintbrush

MATRIX POROSITY = 0.4000000

FILL RADIUS	SATURATION INCREASE
10.00000	1.4823628E-03
20.00000	3.3385357E-04
30.00000	1.4776789E-04
40.00000	8.2654515E-05
50.00000	5.2732287E-05
60.00000	3.6589150E-05
70.00000	2.6855141E-05
80.00000	2.0565772E-05
90.00000	1.6255134E-05
100.0000	1.3165313E-05
110.0000	1.0861738E-05

Topopah Litho

MATRIX POROSITY = 0.1100000

FILL RADIUS	SATURATION INCREASE
10.00000	5.3904530E-03
20.00000	1.2287576E-03
30.00000	5.3733774E-04
40.00000	3.0056186E-04
50.00000	1.9186285E-04
60.00000	1.3305146E-04
70.00000	9.7665596E-05
80.00000	7.4737356E-05
90.00000	5.9029587E-05
100.0000	4.7801135E-05
110.0000	3.9497230E-05

Topopah Rep

MATRIX POROSITY = 0.1100000

FILL RADIUS	SATURATION INCREASE
10.00000	5.3904530E-03
20.00000	1.2287576E-03
30.00000	5.3733774E-04
40.00000	3.0056186E-04
50.00000	1.9186285E-04
60.00000	1.3305146E-04
70.00000	9.7665596E-05
80.00000	7.4737356E-05
90.00000	5.9029587E-05
100.0000	4.7801135E-05
110.0000	3.9497230E-05

Calico Hills

MATRIX POROSITY = 0.4600000

FILL RADIUS	SATURATION INCREASE
10.00000	1.2892284E-03
20.00000	2.9383338E-04
30.00000	1.2849364E-04
40.00000	7.1873488E-05
50.00000	4.5860250E-05
60.00000	3.1816653E-05
70.00000	2.3357775E-05
80.00000	1.7871977E-05
90.00000	1.4115770E-05
100.0000	1.1430707E-05
110.0000	9.4498897E-06

Attachment E

RIB and SEPDB Data

The values of the material properties in Table 1 were taken from the RIB. For the matrix porosity, the values were within the range contained in the RIB, except for the Calico Hills unit for which a value of 0.01 larger than the range was used. The values of matrix porosity selected were based on R. R. Peters et al., 1984, "Fracture and Matrix Hydrologic Characteristics of Tuffaceous Materials from Yucca Mountain, Nye County, Nevada," SAND84-1471, Sandia National Laboratories, Albuquerque, New Mexico.

This report contains no candidate information for the RIB.

This report contains no candidate data for inclusion in the SEPDB.

APPENDIX B

SLTR87-2002

NUMERICAL SOLUTIONS FOR THE DISTRIBUTION OF RESIDUAL CONSTRUCTION WATER IN THE EXPLORATORY SHAFT FACILITY AT YUCCA MOUNTAIN

SLTR87-2002
Department 6310 Letter Report
Sandia National Laboratories
Nevada Nuclear Waste Storage
Investigations Project
Issued March 1987

NUMERICAL SOLUTIONS FOR THE DISTRIBUTION OF RESIDUAL CONSTRUCTION WATER IN THE EXPLORATORY SHAFT FACILITY AT YUCCA MOUNTAIN

Roger R. Eaton and Andrew C. Peterson

Introduction

The current plan for the shaft drilling and drift construction in the exploratory shaft facility (ESF) at the proposed Nevada Nuclear Waste Repository site includes the use of water for dust control and drilling purposes. During this operation, some of the water will be absorbed by the host rock. The presence of this water has generated concern about its effect on the undisturbed conditions of the rock; that is, can this water increase the saturation of the rock surrounding the shaft to a level that could have an adverse effect on in situ experiments or performance of the waste package?

Previous analyses investigating the potential change in the matrix saturation level from the residual water in the ESF were reported in SLTR87-2001 (Appendix A). This report was an initial attempt to address this issue and fulfills part of the analyses requested in Problem Definition Memo (PDM) 72-22. The hydrologic units that were included in these analyses were the Tiva Canyon welded, devitrified; Paintbrush vitric; Topopah Spring lithophysae-rich; Topopah Spring lithophysae-poor; and Calico Hills vitric. Two limiting cases were addressed to estimate the radial distance to which the rock is affected and the maximum increase in saturation that can be expected. The first analysis represents a limiting case in that the maximum radial distance that water can travel into the saturated fractures of the matrix and the resulting equilibrium saturation increase was calculated. The second analysis is a limiting case in that the maximum matrix saturation increase that may occur at any radial distance from the walls was calculated.

The results of these initial analyses, which are documented in Reference 1, indicate that the change in saturation would be quite small. Within a 10.0-m radius from the shaft center (7.8 m from the concrete liner) the largest calculated increase in saturation was 0.013 when 10% of the drilling water was retained in the Tiva Canyon unit. These changes in saturation may be less than the accuracy of in situ experiments and numerical calculations.

To investigate the effect of some of the assumptions used in the analyses discussed above, such as fracture saturation and constant radial saturation distributions, numerical time-dependent solutions for each of the four hydrologic strata have been made using the multidimensional finite element code NORIA [1]. The initial conditions for these calculations were selected to be representative of the expected conditions. The results of these calculations show the increases in saturation within a radius of 25 m from the shaft centerline for computational times ranging from 1-1000 years.

Code Requirements and Problem Definition

In these calculations, time-dependent, one-dimensional radial flow of the residual mining water in the rock matrix adjacent to the shaft liner is modeled using NORIA. In this computer code the water is assumed to be in isothermal matrix/fracture equilibrium at all times. The water is transported as a result of pressure gradients. A listing of the code used in these calculations is stored in the Sandia National Laboratories' Integrated File Storage. When using the code, it is necessary for the user to describe the material characteristics, such as saturation and permeability, as functions of pressure head. This is done in the two subroutines, PERM and FLUDIC. A listing of these two subroutines for the four different strata is given in Attachment A. The material properties used in these subroutines and for the entire analysis are based on those specified in the PDM that lists fracture and matrix hydrologic characteristics based on the psychrometer measurements of Reference 2.

An outline of the mine shaft, the shaft concrete liner, and the surrounding rock is shown in Figure 1. To calculate the one-dimensional flow in the vicinity of the liner, a row of 25 eight-node quadratical finite elements is used (Figure 2). The elements start at the outside radius of the concrete shaft liner, $R_0 = 2.21$ m, and extend to a radius of 25 m. The length of the elements increased from 0.143 m at the shaft liner to 2.78 m at 25 m.

Initial Conditions

Initial pressure head and saturation values are obtained by assuming one-dimensional, vertical, steady-state infiltration of 0.1 mm/yr through the strata shown in Figure 3. This solution was obtained using the one-dimensional, steady-state computer code LLUVIA [2]. A listing of this code is given in Attachment B. The resulting steady-state pressure head distribution, which establishes the saturation level, is given in Figure 4.

Time-dependent analysis using NORIA was made at the four axial locations indicated in Figure 3. In each case it was assumed that at time zero, residual mining water was located in the modified permeability zone, $R_0 < R < 2 * R_0$, Figure 5, as defined by Fernandez [3]. This volume was chosen because the permeability in this zone is specified in the PDM to be 80 times larger than that in the unmodified region. Thus, the mining water will most likely be nearly evenly distributed in this region before being transported into the unmodified zone through capillary action. Therefore, the initial distribution of the mining water in the modified permeability zone (MPZ) would have little effect on the time-dependent results. Based on the saturation level established by the pressure head distribution calculated with LLUVIA, the initial saturation for each strata at the axial locations shown in Figure 3 was specified such that 0.302 m^3/m of water was added to the rock, as specified by the PDM. Adding this amount of water resulted in the following changes in the initial saturation of the MPZ: Tiva Canyon increased by 0.080, Paintbrush increased by 0.017, Topopah Spring increased by 0.06, and Calico Hill increased by 0.014.

A listing of the NORIA input for each of the four calculations is given in Attachment C.

Results

NORIA was run on the CTSS computer system. Computed times out to 1000 yr required less than 25 s to run, using up to 60 time steps. In all cases, a new steady-state condition was obtained by this time. The calculations were expedient because the fractures remained unsaturated and

the computational nonlinearities that occur during fracture saturation did not exist. Figures 6-9 show the saturation profiles for 1, 2, 10, 100, and 1000 yr for the Tiva Canyon, Paintbrush, and Topopah Spring units. Because of the large permeabilities in the Calico Hills unit, solution profiles are presented for 1 mo, 0.5 yr, and 1 yr. The results for the Topopah Spring unit, shown in Figure 8, will be discussed because, except for the magnitude of the changes in saturation, the results are similar for each unit. At one year, the saturation in the MPZ for the Topopah Spring unit was still about 0.035 above the nominal value, and changes in saturation out to about 8 m from the shaft centerline were calculated. At two years, the saturation in the MPZ was 0.03 higher than the nominal, and changes in saturation out to about 10 m from the shaft centerline were calculated. At 1000 yr, the calculated saturation was uniform throughout the unit. The rate at which the saturation front penetrates the rock is in general agreement with the rates measured experimentally by Reda [4]. In that experiment, the penetration speed of the saturation front was measured using gamma ray densitometry.

For all cases, the saturation increase at radial distances greater than 5 m from the shaft centerline (0.6 m from the MPZ) was less than 0.03. The maximum increase occurred in the Topopah Spring stratum. It can be seen that for large times ($t > 100$ yr) the saturation at the extreme of the computational mesh increased. This implies that the impermeable computational boundary condition applied at $R = 25$ m affected the saturation distribution and resulted in slightly elevated saturation profiles at all radii.

Discussion and Conclusions

The results for the analyses presented indicate that the change in saturation would be quite small when the retained water was assumed to be initially located in the modified permeability zone. The largest calculated initial increase in saturation was 0.08%.

Although these calculations apply directly to the shaft geometry, similar types of saturation increases would be expected in the vicinity of

the drift. This was indicated in the analytical calculations reported in SLTR87-2001 (Appendix A).

These analyses did not consider potential effects of local variations in strata properties that could occur. Thus, under certain conditions, it can be conceived that the residual mining water could be channeled directly to an in situ experiment located at some distance, R, from the shaft. However, without detailed knowledge of the strata variations, it would be impossible to accurately model these situations.

An effect not considered in these calculations is the effect of drift ventilation on the saturation profiles. Because any drift ventilation will tend to dry the drift walls, the already extremely small saturation increases would be even smaller if ventilation was included in the analysis. The rate at which drift ventilation affects the saturation in the vicinity of drift walls was addressed in an earlier study by Hopkins and Eaton [5]. This study showed that when there is not an MPZ around the drift, ventilation would affect the saturation level to about 2 m from the drift wall within one year. The effect of the ventilation system on the movement of water when an MPZ is modeled will be addressed in a subsequent study.

It is concluded that for the problem investigated, appreciable increases in rock saturation resulting from wet mining procedures are, in general, confined to a small region in the vicinity of the walls. The conclusions are based on the current level of understanding of the material characteristics and assume homogeneous material in each stratum. If planned in situ experiments can be significantly affected by saturation increases on the order of 0.005 within 10 m of the walls, the retained water from construction could affect the results.

On the basis of the results of these calculations and the U.S. Geologic Survey evaluation of the effect on experiments of changes in initial saturation resulting from construction water, additional analyses may be identified.

References

1. N. E. Bixler, "NORIA--A Finite Element Computer Program for Analyzing Water, Vapor, Air, and Energy Transport in Porous Media," SAND84-2057, Sandia National Laboratories, Albuquerque, NM, August 1985.

2. R. R. Peters, E. A. Klavetter, I. J. Hall, S. C. Blair, P. R. Heller, and G. W. Gee, "Fracture and Matrix Hydrologic Characteristics of Tuffaceous Materials from Yucca Mountain, Nye County, Nevada," SAND84-1471, Sandia National Laboratories, Albuquerque, NM, December 1984.

3. J. A. Fernandez, T. E. Hinkebein, and J. B. Case, "Selected Analyses to Evaluate the Effect of the Exploratory Shaft on Repository Performance of Yucca Mountain," SAND85-0598, Sandia National Laboratories, Albuquerque, NM, 1988.

4. D. C. Reda, "Influence of Transverse Microfractures on the Imbibition of Water into Initially Dry Tuffaceous Rocks," Proceedings of the Symposium on Flow and Transport Through Unsaturated Fractured Rock, AGU Fall Meeting, San Francisco, CA, 1986.

5. P. L. Hopkins and R. R. Eaton, "Effect of Drift Ventilation on Repository Hydrology and Resulting Solute Transport Implications," SAND86-1571, Sandia National Laboratories, Albuquerque, NM, May 1987.

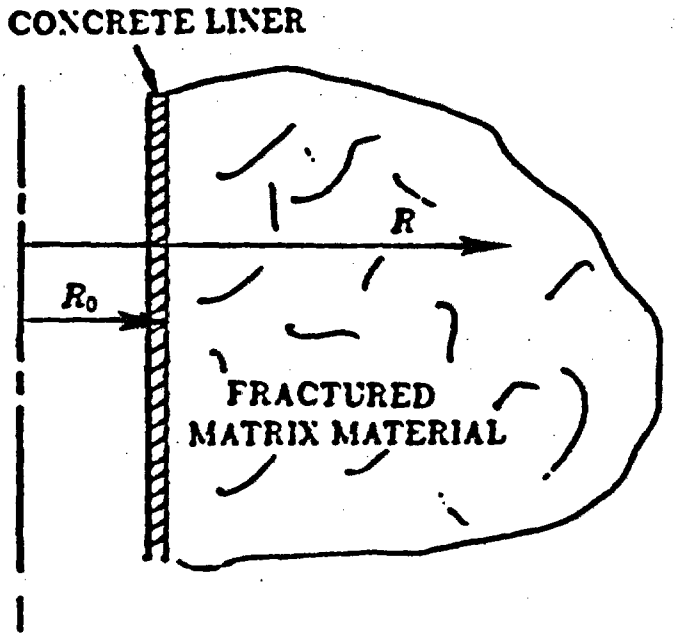

Figure 1. Outline of Problem Geometry.

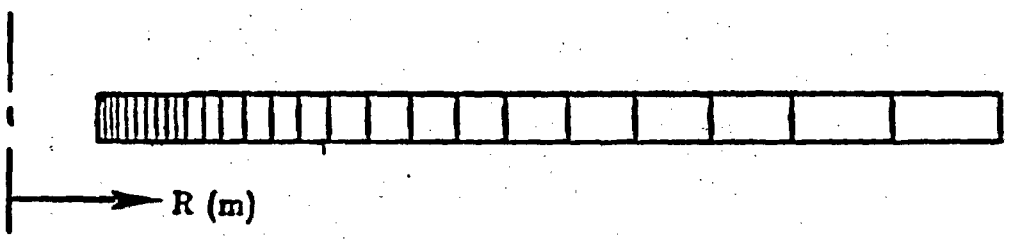

Figure 2. Finite Element Geometry.

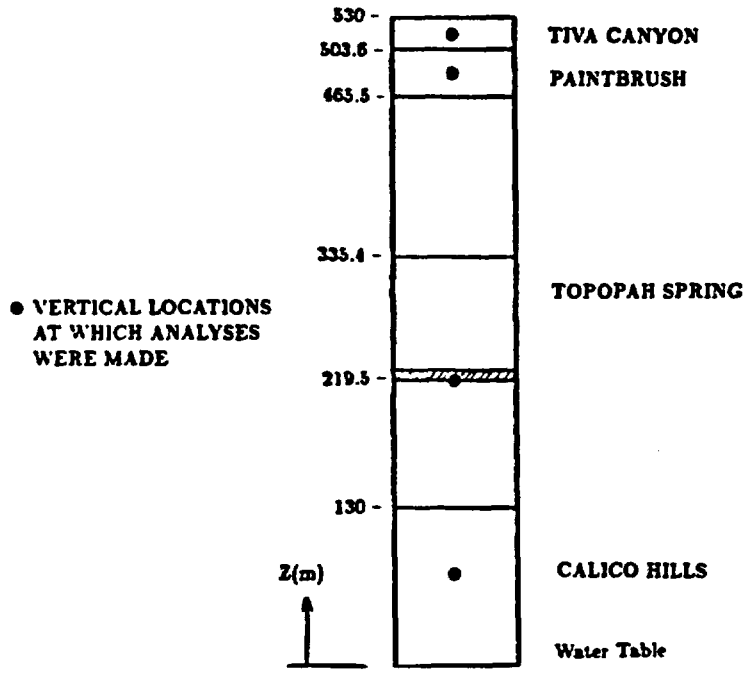

Figure 3. Vertical Geometry of Hydrologic Strata.

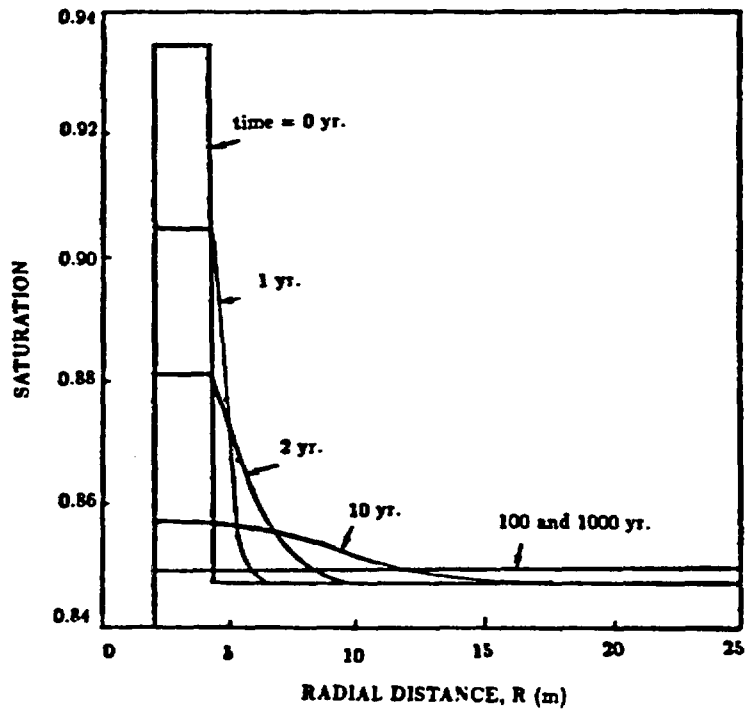

Figure 4. Vertical Distribution of Pressure Head Obtained Using Code, LLUVIA 2.

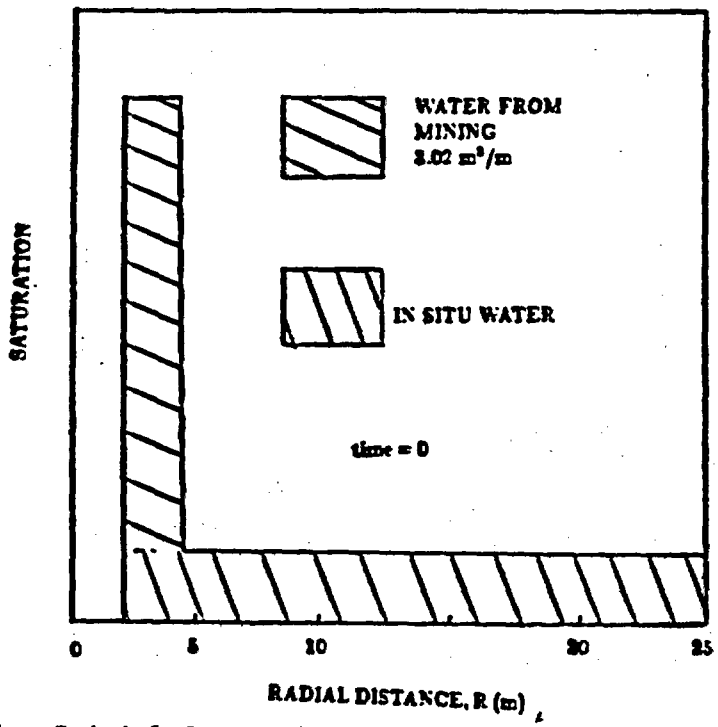

Figure 5. Initial Saturation Distribution Showing Location of Mining Water.

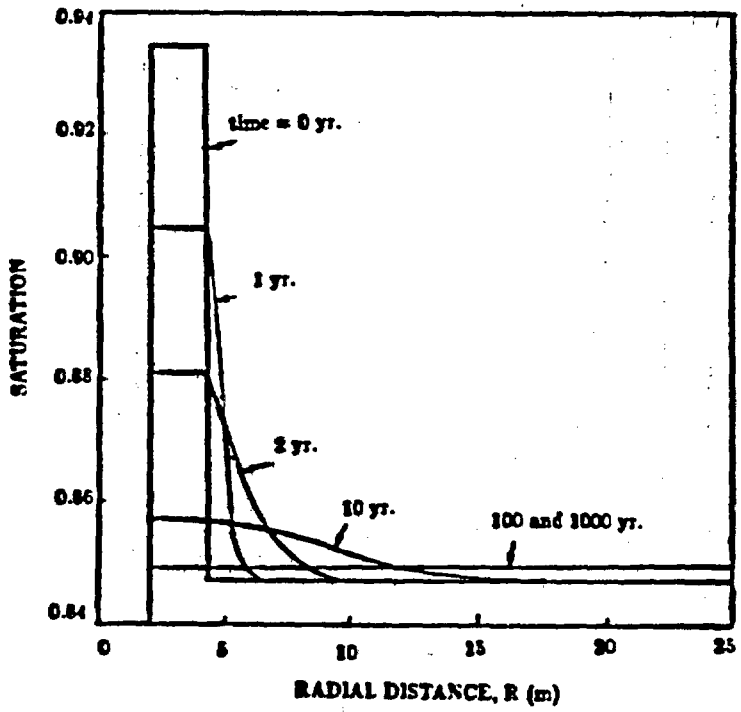

Figure 6. Saturation Profiles for Tiva Canyon for Times of 1, 2, 10, 100, and 1000 yr.

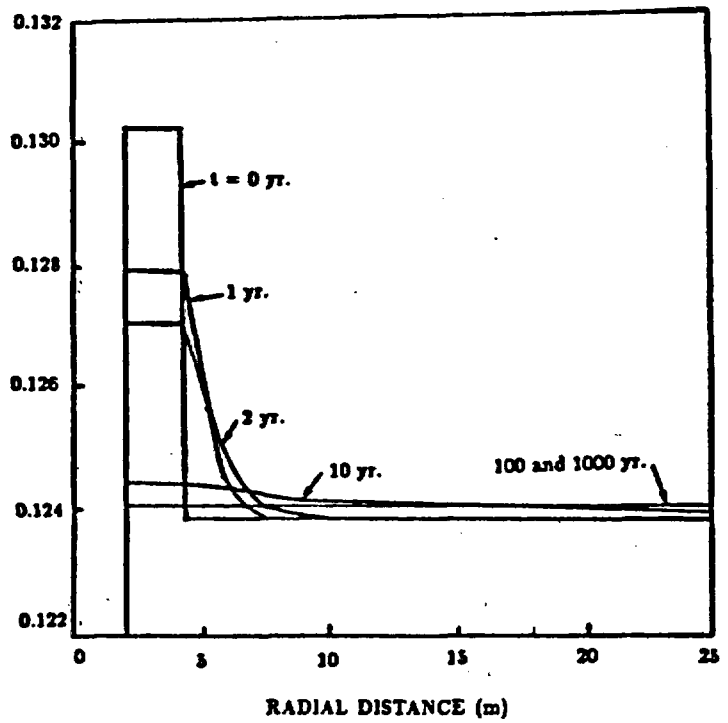

Figure 7. Saturation Profiles for Paintbrush for Times of 1, 2, 10, 100, and 1000 yr.

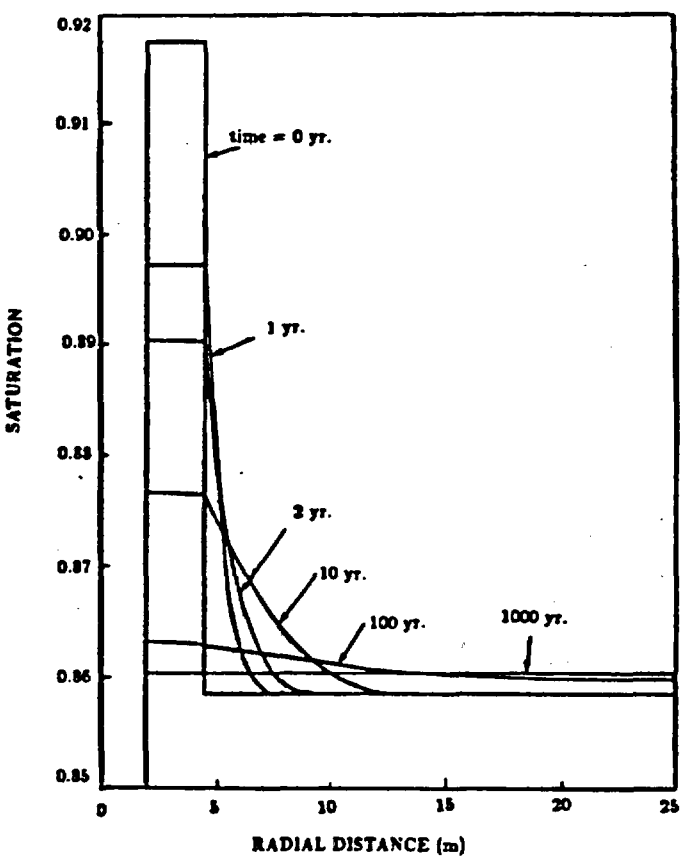

Figure 8. Saturation Profiles for Topopah Spring for Times of 1, 2, 10, 100, and 1000 yr.

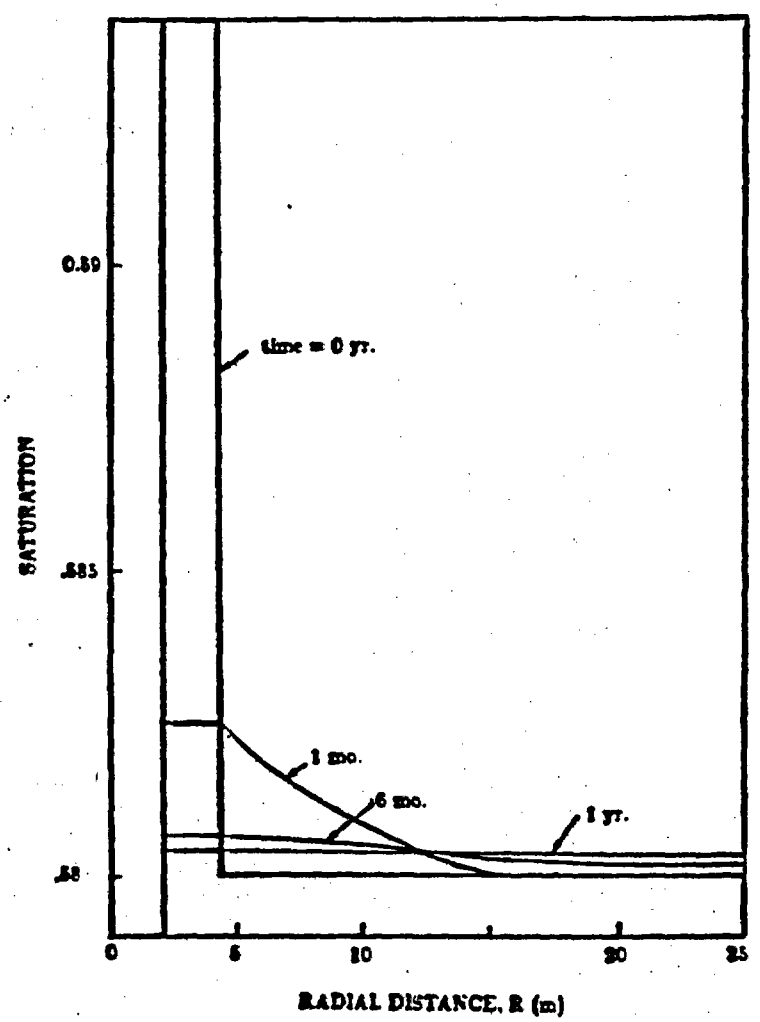

Figure 9. Saturation Profiles for Calico Hills for Times of 1, 6, and 12 mo.

Attachment A

FORTRAN listing of subroutines, PERM and FLUDIC, for Tiva Canyon.

```
c
      subroutine fluidc(th,thm,thf,cm,anml,anfl,smrl,sfr,
     1                  t,p,pv,pa,x,y,time,phi,rhog,nelem,mat,nn)
c
c     this sub calc the moisture content and der of moisture content wrt
c     p in units - kg,m,s.
c
c     mat 4, unit CHnz, Calico Hills, nonwelded, zeolitic
c     mat 5, unit CHnv, Calico Hills, nonwelded, vitric
c     mat 6, unit TSw2, Topopah Springs, welded (repository zone)
c     mat 7, unit TSw1, Topopah Springs, welded (lithophysal zone)
c     mat 8, unit PTn,  Paintbrush, nonwelded
c     mat 9, unit TCw,  Tiva Canyon, welded
c
c     variables:
c     betp      water compressibility (beta prime)
c     alpp      rock compressibility  (alpha prime)
c     anf       fracture porosity
c     anm       matrix porosity
c     phi       total porosity (phi = anf + anm * (1 - anf))
c     th        moisture content(fracture and matrix averaged)
c     thm       moisture content of the matrix
c     thf       moisture content of the fracture
c     smr       residual saturation of the matrix
c     sfr       residual saturation of the fracture
c     sm        saturation of matrix
c     sf        saturation of fracture
c     fc        fracture compressibility
c
      dimension th(8),thm(8),thf(8),cm(8),t(8),
     2          p(8),pv(8),pa(8),x(8),y(8)
      dimension smr(10),anm(10),anf(10),alpm(10),betm(10),alpp(10),
     2          fc(10)
c
c     properties
c
      data(smr(i), i=4,9)/ 0.110, 0.041,  0.080,  0.002,  0.10,  0.002/
      data(anm(i), i=4,9)/  0.28,  0.46,   0.11,   0.08,  0.40,   0.08/
      data(anf(i), i=4,9)/4.6e-5,4.6e-5, 18.e-5, 14.e-5,2.7e-5, 14.e-5/
      data(alpm(i),i=4,9)/.00308,0.0160,0.00567,0.00821,0.0150,0.00821/
      data(betm(i),i=4,9)/ 1.602, 3.872,  1.798,  1.558, 6.872,  1.558/
      data(alpp(i),i=4,9)/ 9.e-7,26.e-7, 5.8e-7, 6.2e-7,82.e-7, 6.2e-7/
      data(fc(i),  i=4,9)/2.8e-8,2.8e-8, 12.e-8, 132.e-8,19.e-8,132.e-8/
c
c     saturation function statement
c
      satfu(sr,al,ap)=(1-sr)*(1+ap)**(-al) + sr
c
c     derivative of saturation function statement
c
      chfu(sr,al,ap,bet,a,phm)=(1-sr)*al*(1.+ap)**(-al-1.)
     1 *bet*a**bet*(-phm)**(bet-1)/rhog
c
c     fracture properties
c
      sfr=3.950e-2
      alpf=1.2851
      betf=4.23
c
c     matrix properties
c
      betp=9.8e-7
c
c     evaluate moisture content
```

```
c
      alm=(1.-1/betm(mat))
      alf=(1.-1./betf)
c
c     set values for use in computing fluxes and velocities
c
      anm1=anm(mat)
      anf1=anf(mat)
      smr1=smr(mat)
c
c     loop over nodes
c
      do 100 j=1,nn
      phm=p(j)/rhog - y(j)
      if (phm.gt.-.000001) phm=-.000001
      apm=(alpm(mat)*(-phm))**betm(mat)
      apf=(alpf*    (-phm))**betf
      sm=satfu(smr(mat),alm,apm)
      sf=satfu(sfr     ,alf,apf)
c
c     convert saturation to moisture content
c
      thm(j)=sm*anm(mat)*(1.-anf(mat))
      thf(j)=sf*anf(mat)
      th(j)=thm(j) + thf(j)
c
c     these effects need to be incorporated into the capacitance term
c
      watcomp=betp*th(j)/rhog
      rokcomp=alpp(mat)*th(j)/(anf(mat)+anm(mat))*(sm-anf(mat)
     2        *(sm-sf))/rhog
      fracomp=fc(mat)*th(j)/(anf(mat)+anm(mat))*(sm-sf)/rhog
c
c     compute the derivative of saturation wrt psi
c
      chm=chfu(smr(mat),alm,apm,betm(mat),alpm(mat),phm)
      chf=chfu(sfr     ,alf,apf,betf     ,alpf     ,phm)
c
c     convert to moisture content and sum terms for total capacitance
c
      cm1=chm*anm(mat)*(1.-anf(mat)) + chf*anf(mat)
      cm(j)=cm1 + watcomp + rokcomp + fracomp
c      cm(j)=cm1 + 1.0e-5
  100 continue
c
      return
      end
c
```

```
c
c
      subroutine perm(cond1,cond2,akm11,akm22,akf11,akf22,
     1                th,t,p,pv,pa,x,y,time,phi,rhog,nelem,mat,nn)
      dimension cond1(8),cond2(8),akm11(8),akm22(8),akf11(8),akf22(8),
     1          t(8),p(8),pv(8),pa(8),x(8),y(8)
      dimension th(8)
c
c     calculates permeability  (cm**2)
c     units - gm,c m,sec.
c
      dimension cond(100)
      dimension phd(100),hkd(100)
      dimension thm(10),af(10),alpm(10),betm(10)
      dimension conm(10),conf(10)
c   rock properties
      data(alpm(i),i=4,9)/.00308, 0.016,0.00567,0.00821,0.0150,0.00821/
      data(betm(i),i=4,9)/ 1.602,  3.872,  1.798,  1.558, 6.872,  1.558/
      data(af(i),  i=4,9)/4.6e-5,4.6e-5, 18.e-5, 14.e-5,2.7e-5, 14.e-5/
c note that perm for mat=7 is 80 times bigger than mat=9
      data(conm(i),i=4,9)/2.e-11,2.7e-7,152e-11,7.76e-10,3.9e-7,9.7e-12/
      data(conf(i),i=4,9)/20.e-5,20.e-5, 1.7e-5, 3.8e-5,61.e-5, 3.8e-5/
c  conductive function statement
      confu(al,ap)=(1.+ap)**(-al/2.)*(1.-(ap/(1.+ap))**al)**2
c  fracture properties
      alpf=1.285
      betf=4.23
      do 20 j=1,nn
      phm=p(j)/rhog - y(j)
      if(phm.gt. -.000001)  phm=-.000001
      apm=(alpm(mat)*(-phm))**betm(mat)
      alm=(1-1./betm(mat))
      apf=(alpf*     (-phm))**betf
      alf=(1-1/betf)
      com=confu(alm,apm)*conm(mat)
      cof=confu(alf,apf)*conf(mat)
      akm11(j)=(1.-af(mat))*com*0.001/rhog
      akm22(j)=akm11(j)
      akf11(j)=af(mat)*cof*0.001/rhog
      akf22(j)=akf11(j)
      cond1(j)=akm11(j)+akf11(j)
      cond2(j)=akm22(j)+akf22(j)
  20  continue
      return
      end
```

FORTRAN listing of subroutines, PERM and FLUDIC, for Paintbrush.

```
      subroutine fluidc(th,thm,thf,cm,anml,anfl,smrl,sfr,
     1                  t,p,pv,pa,x,y,time,phi,rhog,nelem,mat,nn)
c
c     this sub calc the moisture content and der of moisture content wrt
c     p in units - kg,m,s.
c
c     mat 4, unit CHnz, Calico Hills, nonwelded, zeolitic
c     mat 5, unit CHnv, Calico Hills, nonwelded, vitric
c     mat 6, unit TSw2, Topopah Springs, welded (repository zone)
c     mat 7, unit TSw1, Topopah Springs, welded (lithophysal zone)
c     mat 8, unit PTn,  Paintbrush, nonwelded
c     mat 9, unit TCw,  Tiva Canyon, welded
c
c     variables:
c     betp      water compressibility (beta prime)
c     alpp      rock compressibility  (alpha prime)
c     anf       fracture porosity
c     anm       matrix porosity
c     phi       total porosity (phi = anf + anm * (1 - anf))
c     th        moisture content(fracture and matrix averaged)
c     thm       moisture content of the matrix
c     thf       moisture content of the fracture
c     smr       residual saturation of the matrix
c     sfr       residual saturation of the fracture
c     sm        saturation of matrix
c     sf        saturation of fracture
c     fc        fracture compressibility
c
      dimension th(8),thm(8),thf(8),cm(8),t(8),
     2          p(8),pv(8),pa(8),x(8),y(8)
      dimension smr(10),anm(10),anf(10),alpm(10),betm(10),alpp(10),
     2          fc(10)
c
c     properties
c
      data(smr(i), i=4,9)/ 0.110, 0.041,  0.080,  0.100,  0.10,  0.002/
      data(anm(i), i=4,9)/  0.28,  0.46,   0.11,   0.40,  0.40,   0.08/
      data(anf(i), i=4,9)/4.6e-5,4.6e-5, 18.e-5, 2.7e-5,2.7e-5, 14.e-5/
      data(alpm(i),i=4,9)/.00308,0.0160,0.00567,0.0150,0.0150,0.008217/
      data(betm(i),i=4,9)/ 1.602, 3.872,  1.798,  6.872, 6.872,  1.558/
      data(alpp(i),i=4,9)/ 9.e-7,26.e-7, 5.8e-7, 82.e-7,82.e-7, 6.2e-7/
      data(fc(i),  i=4,9)/2.8e-8,2.8e-8, 12.e-8, 19.e-8,19.e-8,132.e-8/
c
c     saturation function statement
c
      satfu(sr,al,ap)=(1-sr)*(1+ap)**(-al) + sr
c
c     derivative of saturation function statement
c
      chfu(sr,al,ap,bet,a,phm)=(1-sr)*al*(1.+ap)**(-al-1.)
     1*bet*a**bet*(-phm)**(bet-1)/rhog
c
c     fracture properties
c
      sfr=3.950e-2
      alpf=1.2851
      betf=4.23
c
c     matrix properties
c
      betp=9.8e-7
```

Attachment A (continued)

```
c
cc      evaluate moisture content
c
        alm=(1.-1/betm(mat))
        alf=(1.-1./betf)
c
cc      set values for use in computing fluxes and velocities
c
        anm1=anm(mat)
        anf1=anf(mat)
        smr1=smr(mat)
c
cc      loop over nodes
c
        do 100 j=1,nn
        phm=p(j)/rhog - y(j)
        if (phm.gt.-.000001) phm=-.000001
        apm=(alpm(mat)*(-phm))**betm(mat)
        apf=(alpf*     (-phm))**betf
        sm=satfu(smr(mat),alm,apm)
        sf=satfu(sfr     ,alf,apf)
c
cc      convert saturation to moisture content
c
        thf(j)=sf*anf(mat)
        th(j)=thm(j) + thf(j)
c
cc      these effects need to be incorporated into the capacitance term
c
        watcomp=betp*th(j)/rhog
        rokcomp=alpp(mat)*th(j)/(anf(mat)+anm(mat))*(sm-anf(mat)
       2     *(sm-sf))/rhog
        fracomp=fc(mat)*th(j)/(anf(mat)+anm(mat))*(sm-sf)/rhog
c
cc      compute the derivative of saturation wrt psi
c
        chm=chfu(smr(mat),alm,apm,betm(mat),alpm(mat),phm)
        chf=chfu(sfr     ,alf,apf,betf     ,alpf     ,phm)
c
cc      convert to moisture content and sum terms for total capacitance
c
        cm1=chm*anm(mat)*(1.-anf(mat)) + chf*anf(mat)
        cm(j)=cm1 + watcomp + rokcomp + fracomp
c        cm(j)=cm1 + 1.0e-5
  100   continue
c
        return
        end
c
```

Attachment A (continued)

```
c
      subroutine perm(cond1,cond2,akm11,akm22,akf11,akf22,
     1                th,t,p,pv,pa,x,y,time,phi,rhog,nelem,mat,nn)
      dimension cond1(8),cond2(8),akm11(8),akm22(8),akf11(8),akf22(8),
     1          t(8),p(8),pv(8),pa(8),x(8),y(8)
      dimension th(8)
c
c     calculates permeability  (cm**2)
c     units - gm,c m,sec.
c
      dimension cond(100)
      dimension phd(100),hkd(100)
      dimension thm(10),af(10),alpm(10),betm(10)
      dimension conm(10),conf(10)
c   rock properties
      data(alpm(i),i=4,9)/.00308, 0.016,0.00567,0.0150,0.0150,0.00821/
      data(betm(i),i=4,9)/ 1.602,  3.872,  1.798,  6.872,  6.872,  1.558/
      data(af(i),  i=4,9)/4.6e-5,4.6e-5, 18.e-5, 2.7e-5,2.7e-5, 14.e-5/
c note that perm for mat=7 is 80 times bigger than mat=9
      data(conm(i),i=4,9)/2.e-11,2.7e-7,152e-11,3.12e-5,3.9e-7,9.7e-12/
      data(conf(i),i=4,9)/20.e-5,20.e-5, 1.7e-5, 61.e-5,61.e-5, 3.8e-5/
c  conductive function statement
      confu(al,ap)=(1.+ap)**(-al/2.)*(1.-(ap/(1.+ap))**al)**2
c  fracture properties
      alpf=1.285
      betf=4.23
      do 20 j=i,nn
      phm=p(j)/rhog - y(j)
      if(phm.gt. -.000001)  phm=-.000001
      apm=(alpm(mat)*(-phm))**betm(mat)
      alm=(1-1./betm(mat))
      apf=(alpf*     (-phm))**betf
      alf=(1-1/betf)
      com=confu(alm,apm)*conm(mat)
      cof=confu(alf,apf)*conf(mat)
      akm11(j)=(1.-af(mat))*com*0.001/rhog
      akm22(j)=akm11(j)
      akf11(j)=af(mat)*cof*0.001/rhog
      akf22(j)=akf11(j)
      cond1(j)=akm11(j)+akf11(j)
      cond2(j)=akm22(j)+akf22(j)
   20 continue
      return
      end
c
c
```

FORTRAN listing of subroutines, PERM and FLUDIC, for Topopah Spring.

```
      subroutine fluidc(th,thm,thf,cm,anml,anfl,smrl,sfr,
     1                  t,p,pv,pa,x,y,time,phi,rhog,nelem,mat,nn)
c
c     this sub calc the moisture content and der of moisture content wrt
c     p in units - kg,m,s.
c
c     mat 4, unit CHnz, Calico Hills, nonwelded, zeolitic
c     mat 5, unit CHnv, Calico Hills, nonwelded, vitric
c     mat 6, unit TSw2, Topopah Springs, welded (repository zone)
c     mat 7, unit TSw1, Topopah Springs, welded (lithophysal zone)
c     mat 8, unit PTn,  Paintbrush, nonwelded
c     mat 9, unit TCw,  Tiva Canyon, welded
c
c     variables:
c     betp      water compressibility (beta prime)
c     alpp      rock compressibility  (alpha prime)
c     anf       fracture porosity
c     anm       matrix porosity
c     phi       total porosity (phi = anf + anm * (1 - anf))
c     th        moisture content(fracture and matrix averaged)
c     thm       moisture content of the matrix
c     thf       moisture content of the fracture
c     smr       residual saturation of the matrix
c     sfr       residual saturation of the fracture
c     sm        saturation of matrix
c     sf        saturation of fracture
c     fc        fracture compressibility
c
      dimension th(8),thm(8),thf(8),cm(8),t(8),
     2          p(8),pv(8),pa(8),x(8),y(8)
      dimension smr(10),anm(10),anf(10),alpm(10),betm(10),alpp(10),
     2          fc(10)
c
c     properties
c
      data(smr(i), i=4,9)/ 0.110, 0.041,  0.081,  0.081,  0.10,  0.002/
      data(anm(i), i=4,9)/  0.28,  0.46,   0.11,   0.11,  0.40,   0.08/
      data(anf(i), i=4,9)/4.6e-5,4.6e-5, 18.e-5, 18.e-5,2.7e-5, 14.e-5/
      data(alpm(i),i=4,9)/.00308,0.0160,0.00567,0.00567,0.0150,0.00821/
      data(betm(i),i=4,9)/ 1.602,  3.872,  1.798,  1.798,  6.872,  1.558/
      data(alpp(i),i=4,9)/ 9.e-7,26.e-7, 5.8e-7, 5.8e-7,82.e-7, 6.2e-7/
      data(fc(i),  i=4,9)/2.8e-8,2.8e-8, 12.e-8, 12.e-8,19.e-8,132.e-8/
c
c     saturation function statement
c
      satfu(sr,al,ap)=(1-sr)*(1+ap)**(-al) + sr
c
c     derivative of saturation function statement
c
      chfu(sr,al,ap,bet,a,phm)=(1-sr)*al*(1.+ap)**(-al-1.)
     1*bet*a**bet*(-phm)**(bet-1)/rhog
c
c     fracture properties
c
      sfr=3.950e-2
      alpf=1.2851
      betf=4.23
c
c     matrix properties
c
      betp=9.8e-7
c
c     evaluate moisture content
```

```
c
      alm=(1.-1/betm(mat))
      alf=(1.-1./betf)
c
c     set values for use in computing fluxes and velocities
c
      anml=anm(mat)
      anfl=anf(mat)
      smrl=smr(mat)
c
c     loop over nodes
c
      do 100 j=1,nn
      phm=p(j)/rhog - y(j)
      if (phm.gt.-.000001) phm=-.000001
      apm=(alpm(mat)*(-phm))**betm(mat)
      apf=(alpf*    (-phm))**betf
      sm=satfu(smr(mat),alm,apm)
      sf=satfu(sfr     ,alf,apf)
c
c     convert saturation to moisture content
c
      thm(j)=sm*anm(mat)*(1.-anf(mat))
      thf(j)=sf*anf(mat)
      th(j)=thm(j) + thf(j)
c
c     these effects need to be incorporated into the capacitance term
c
      watcomp=betp*th(j)/rhog
      rokcomp=alpp(mat)*th(j)/(anf(mat)+anm(mat))*(sm-anf(mat)
     2      *(sm-sf))/rhog
      fracomp=fc(mat)*th(j)/(anf(mat)+anm(mat))*(sm-sf)/rhog
c
c     compute the derivative of saturation wrt psi
c
      chm=chfu(smr(mat),alm,apm,betm(mat),alpm(mat),phm)
      chf=chfu(sfr     ,alf,apf,betf     ,alpf     ,phm)
c
c     convert to moisture content and sum terms for total capacitance
c
      cml=chm*anm(mat)*(1.-anf(mat)) + chf*anf(mat)
      cm(j)=cml + watcomp + rokcomp + fracomp
c      cm(j)=cml + 1.0e-5
  100 continue
c
      return
      end
```

Attachment A (continued)

```
c
      subroutine perm(cond1,cond2,akm11,akm22,akf11,akf22,
     1                th,t,p,pv,pa,x,y,time,phi,rhog,nelem,mat,nn)
      dimension cond1(8),cond2(8),akm11(8),akm22(8),akf11(8),akf22(8),
     1          t(8),p(8),pv(8),pa(8),x(8),y(8)
      dimension th(8)
c
c     calculates permeability  (cm**2)
c     units - gm,c m,sec.
c
      dimension cond(100)
      dimension phd(100),hkd(100)
      dimension thm(10),af(10),alpm(10),betm(10)
      dimension conm(10),conf(10)
c   rock properties
      data(alpm(i),i=4,9)/.00308, 0.016,0.00567,0.00567,0.0150,0.00821/
      data(betm(i),i=4,9)/ 1.602,  3.872,  1.798,  1.798, 6.872,  1.558/
      data(af(i),  i=4,9)/4.6e-5,4.6e-5, 18.e-5, 18.e-5,2.7e-5, 14.e-5/
c note that perm for mat=6 is 80 times bigger than mat=7
      data(conm(i),i=4,9)/2.e-11,2.7e-7,152e-11,1.9e-11,3.9e-7,9.7e-12/
      data(conf(i),i=4,9)/20.e-5,20.e-5, 1.7e-5, 1.7e-5,61.e-5, 3.8e-5/
c  conductive function statement
      confu(al,ap)=(1.+ap)**(-al/2.)*(1.-(ap/(1.+ap))**al)**2
c  fracture properties
      alpf=1.285
      betf=4.23
      do 20 j=1,nn
      phm=p(j)/rhog - y(j)
      if(phm.gt. -.000001)  phm=-.000001
      apm=(alpm(mat)*(-phm))**betm(mat)
      alm=(1-1./betm(mat))
      apf=(alpf*     (-phm))**betf
      alf=(1-1/betf)
      com=confu(alm,apm)*conm(mat)
      cof=confu(alf,apf)*conf(mat)
      akm11(j)=(1.-af(mat))*com*0.001/rhog
      akm22(j)=akm11(j)
      akf11(j)=af(mat)*cof*0.001/rhog
      akf22(j)=akf11(j)
      cond1(j)=akm11(j)+akf11(j)
      cond2(j)=akm22(j)+akf22(j)
  20  continue
      return
      end
c
c
```

FORTRAN listing of subroutines, PERM and FLUDIC, for Calico Hills.

```
      subroutine fluidc(th,thm,thf,cm,anml,anfl,smrl,sfr,
     1                  t,p,pv,pa,x,y,time,phi,rhog,nelem,mat,nn)
c
cc    this sub calc the moisture content and der of moisture content wrt
cc    p in units - kg,m,s.
cc
cc    mat 4, unit CHnz, Calico Hills, nonwelded, zeolitic
cc    mat 5, unit CHnv, Calico Hills, nonwelded, vitric
cc    mat 6, unit TSw2, Topopah Springs, welded (repository zone)
cc    mat 7, unit TSw1, Topopah Springs, welded (lithophysal zone)
cc    mat 8, unit PTn,  Paintbrush, nonwelded
cc    mat 9, unit TCw,  Tiva Canyon, welded
cc
cc    variables:
cc    betp      water compressibility (beta prime)
cc    alpp      rock compressibility  (alpha prime)
cc    anf       fracture porosity
cc    anm       matrix porosity
cc    phi       total porosity (phi = anf + anm * (1 - anf))
cc    th        moisture content(fracture and matrix averaged)
cc    thm       moisture content of the matrix
cc    thf       moisture content of the fracture
cc    smr       residual saturation of the matrix
cc    sfr       residual saturation of the fracture
cc    sm        saturation of matrix
cc    sf        saturation of fracture
cc    fc        fracture compressibility
c
      dimension th(8),thm(8),thf(8),cm(8),t(8),
     2          p(8),pv(8),pa(8),x(8),y(8)
      dimension smr(10),anm(10),anf(10),alpm(10),betm(10),alpp(10),
     2          fc(10)
c
cc    properties
c
      data(smr(i), i=4,9)/ 0.041,  0.041,  0.080,  0.080,  0.10,  0.002/
      data(anm(i), i=4,9)/  0.46,   0.46,   0.11,   0.11,  0.40,   0.08/
      data(anf(i), i=4,9)/4.6e-5,4.6e-5, 18.e-5, 4.1e-5,2.7e-5, 14.e-5/
      data(alpm(i),i=4,9)/.0160,0.0160,0.00567,0.00567,0.0150,0.00821/
      data(betm(i),i=4,9)/ 3.872,  3.872,  1.798,  1.798, 6.872,  1.558/
      data(alpp(i),i=4,9)/39.e-7,39.e-7, 5.8e-7, 12.e-7,82.e-7, 6.2e-7/
      data(fc(i),  i=4,9)/2.8e-8,2.8e-8, 12.e-8, 5.6e-8,19.e-8,132.e-8/
c
cc    saturation function statement
c
      satfu(sr,al,ap)=(1-sr)*(1+ap)**(-al) + sr
c
cc    derivative of saturation function statement
c
      chfu(sr,al,ap,bet,a,phm)=(1-sr)*al*(1.+ap)**(-al-1.)
     1 *bet*a**bet*(-phm)**(bet-1)/rhog
c
cc    fracture properties
c
      sfr=3.950e-2
      alpf=1.2851
      betf=4.23
c
cc    matrix properties
c
      betp=9.8e-7
c
cc    evaluate moisture content
```

Attachment A (continued)

```
c
      alm=(1.-1/betm(mat))
      alf=(1.-1./betf)
c
c
c     set values for use in computing fluxes and velocities
c
      anm1=anm(mat)
      anf1=anf(mat)
      smr1=smr(mat)
c
c     loop over nodes
c
      do 100 j=1,nn
      phm=p(j)/rhog - y(j)
      if (phm.gt.-.000001) phm=-.000001
      apm=(alpm(mat)*(-phm))**betm(mat)
      apf=(alpf*    (-phm))**betf
      sm=satfu(smr(mat),alm,apm)
      sf=satfu(sfr     ,alf,apf)
c
c     convert saturation to moisture content
c
      thm(j)=sm*anm(mat)*(1.-anf(mat))
      thf(j)=sf*anf(mat)
      th(j)=thm(j) + thf(j)
c
c     these effects need to be incorporated into the capacitance term
c
      watcomp=betp*th(j)/rhog
      rokcomp=alpp(mat)*th(j)/(anf(mat)+anm(mat))*(sm-anf(mat)
     2       *(sm-sf))/rhog
      fracomp=fc(mat)*th(j)/(anf(mat)+anm(mat))*(sm-sf)/rhog
c
c     compute the derivative of saturation wrt psi
c
      chm=chfu(smr(mat),alm,apm,betm(mat),alpm(mat),phm)
      chf=chfu(sfr     ,alf,apf,betf     ,alpf     ,phm)
c
c     convert to moisture content and sum terms for total capacitance
c
      cm1=chm*anm(mat)*(1.-anf(mat)) + chf*anf(mat)
      cm(j)=cm1 + watcomp + rokcomp + fracomp
c      cm(j)=cm1 + 1.0e-5
  100 continue
c
      return
      end
c
```

```
c
      subroutine perm(cond1,cond2,akm11,akm22,akf11,akf22,
     1                th,t,p,pv,pa,x,y,time,phi,rhog,nelem,mat,nn)
      dimension cond1(8),cond2(8),akm11(8),akm22(8),akf11(8),akf22(8),
     1          t(8),p(8),pv(8),pa(8),x(8),y(8)
      dimension th(8)
c
c    calculates permeability  (cm**2)
c    units - gm,c m,sec.
c
      dimension cond(100)
      dimension phd(100),hkd(100)
      dimension thm(10),af(10),alpm(10),betm(10)
      dimension conm(10),conf(10)
c    rock properties
      data(alpm(i),i=4,9)/.0160, 0.0160,0.00567,0.00567,0.0150,0.00821/
      data(betm(i),i=4,9)/ 3.872, 3.872,  1.798,  1.798, 6.872,  1.558/
      data(af(i),  i=4,9)/4.6e-5,4.6e-5, 18.e-5, 4.1e-5,2.7e-5, 14.e-5/
c note that perm for mat=4 is 80 times bigger than mat=5
      data(conm(i),i=4,9)/216e-7,2.7e-7,1.9e-11,1.9e-11,3.9e-7,9.7e-12/
      data(conf(i),i=4,9)/20.e-5,20.e-5, 1.7e-5, 2.2e-5,61.e-5, 3.8e-5/
c  conductive function statement
      confu(al,ap)=(1.+ap)**(-al/2.)*(1.-(ap/(1.+ap))**al)**2
c  fracture properties
      alpf=1.285
      betf=4.23
      do 20 j=1,nn
      phm=p(j)/rhog - y(j)
      if(phm.gt. -.000001)  phm=-.000001
      apm=(alpm(mat)*(-phm))**betm(mat)
      alm=(1-1./betm(mat))
      apf=(alpf*     (-phm))**betf
      alf=(1-1/betf)
      com=confu(alm,apm)*conm(mat)
      cof=confu(alf,apf)*conf(mat)
      akm11(j)=(1.-af(mat))*com*0.001/rhog
      akm22(j)=akm11(j)
      akf11(j)=af(mat)*cof*0.001/rhog
      akf22(j)=akf11(j)
      cond1(j)=akm11(j)+akf11(j)
      cond2(j)=akm22(j)+akf22(j)
   20 continue
      return
      end
c
c
```

Attachment B

FORTRAN listing of program, LLUVIA [4].

```
      PROGRAM INFIL (tty, input=tty, output=tty)
C
CCC   The purpose of this program is to solve for steady-state pressures
CCC   in Darcy flow problems involving constant infiltration into a
CCC   1-D column of layered strata.  The permeability of each layer is
CCC   a function of pressure and given by subroutine PERM.  A Runge-Kutta
CCC   solution procedure is implemented through subroutine DEBDF which is
CCC   one of the SLATEC library routines.
CCC
CCC   Convergence for some cases will not be obtained with a single
CCC   precision version of this program.
CCC
CCC   May 1986
CCC   R. R. Eaton and P. L. Hopkins, 1511
C
      IMPLICIT REAL*8 (A-H,O-Z)
      EXTERNAL F
      CHARACTER*1 ANS,ANS2,ANS3,YESUP,YESLO
      REAL MAXDIF
      DIMENSION Y(1),INFO(15),RWORK(261)
     1 ,IWORK(56),RPAR(3),IPAR(1),TNODE(501),PHOLD(501)
      DIMENSION DUMMY(8),US(501,8)
C
      DATA IOUT/8/
      DATA TOLD,YOLD/0.,0./,MAXDIF/0./,RHOG/9.80665D3/
      DATA DUMMY/8*0.0/,TIME/0./,US/4008*0./
      DATA YESUP/'Y'/,YESLO/'y'/
C
      COMMON /RATE/ VELBC
      COMMON / MAT/MAT
C
      OPEN (unit=8,form='formatted',status='unknown')
C
CCC   Define nodal coordinates
C
      CALL MESH (NNODE,TNODE)
C
CCC   Input infiltration rate and whether or not initial condition
CCC   solution file is to be generated.
C
      PRINT *,'ENTER DOWNWARD INFILTRATION RATE (MM/YR) '
      READ *, VELBC
      VELBC=-VELBC/3.15576D10
      PRINT *,'DO YOU WANT SOLUTION FILE GENERATED ? (Y/N)'
      READ 900, ANS
  900 FORMAT(A1)
      IF (ANS.EQ.YESUP.OR.ANS.EQ.YESLO) THEN
        PRINT *,'ENTER NUMBER OF ELEMENTS ALONG VERTICAL'
        READ *,NEL1
        PRINT *,'ENTER NUMBER OF ELEMENTS ALONG HORIZONTAL'
        READ *,NEL2
        PRINT *,'WILL ELEMENT NUMBERING START AT BOTTOM ? (Y/N)'
        PRINT *,'(IF NOT, WILL ASSUME TOP)'
        READ 900,ANS2
        PRINT *,'WILL NUMBERING BE HORIZONTAL ? (Y/N)'
        PRINT *,'(IF NOT, WILL ASSUME VERTICAL)'
        READ 900,ANS3
      ENDIF
```

```
C   Initialize variables for solution procedure
C   Refer to documentation on DEBDF for details on these variables
C
      DO 10 I=1,15
10    INFO(I)=0
      RTOL=1.D-8
      ATOL=1.D-10
      Y(1)=0.
      T=0.
      NEQ=1
      LRW=261
      LIW=56
c vel must be changed in two places.
cc      VELBC=-1.5844044D-11
C
C  Begin solution procedure loop
C
      DO 50 I=1,NNODE
        TOUT=TNODE(I)
20      CALL DEBDF(F,NEQ,T,Y,TOUT,INFO,RTOL,ATOL,IDID,RWORK
     1             ,LRW,IWORK,LIW,RPAR,IPAR)
C
        IF (IDID.EQ.-7) THEN
            INFO(1)=0
            GO TO 20
        END IF
        PHOLD(I)=Y(1)
        CALL F (TOUT,Y(1),UPRIME,RPAR,IPAR)
        VEL2=-RPAR(1)/RPAR(2)*UPRIME
        DIFF=ABS(VEL2-VELBC)
        IF (DIFF.GT.MAXDIF) THEN
            MAXDIF=DIFF
            ZLOC=T
        END IF
        TOLD=T
        YOLD=Y(1)
        INFO(1)=1
        IF( I.EQ.1) WRITE(IOUT,1000)
        PHM=Y(1)/RHOG-T
        WRITE(IOUT,1010) T,Y(1),PHM,RPAR(1),VEL2, MAT ,MAT
50    CONTINUE
      PER=MAXDIF/VELBC*100.
      WRITE(IOUT,1020) MAXDIF,ZLOC
      WRITE(IOUT,1030) PER
C
C  Write solution file if requested
C
      OPEN (unit=19,form='unformatted',status='unknown')
      IF (ANS.EQ.YESUP.OR.ANS.EQ.YESLO) THEN
      NELEM=NEL1*NEL2
      IF (ANS2.EQ.YESUP.OR.ANS2.EQ.YESLO) THEN
          ITOP=0
      ELSE
          ITOP=NELEM+1
      ENDIF
      DO 100 J=1,NEL1
      IND2=(J-1)*2
      DO 100 I=1,NEL2
     IND3=(I-1)*2
      IF (ANS3.EQ.'Y') THEN
          IND1=ABS(ITOP - ((J-1)*NEL2+I))
      ELSE
          IND1=ABS(ITOP - ((I-1)*NEL1+J))
      ENDIF
      US(IND1,1)=PHOLD(IND2+1)
      US(IND1,5)=PHOLD(IND2+1)-
      US(IND1,2)=PHOLD(IND2+1)
      US(IND1,6)=PHOLD(IND2+2)
      US(IND1,8)=PHOLD(IND2+2)
      US(IND1,3)=PHOLD(IND2+3)
      US(IND1,4)=PHOLD(IND2+3)
      US(IND1,7)=PHOLD(IND2+3)
100   CONTINUE
      PMAX=-1.0E20
      PMIN=1.0E20
```

Attachment B (continued)

```
      DO 110 I=1,8
      DO 110 J=1,NELEM
      PMAX=AMAX1(PMAX,US(J,I))
      PMIN=AMIN1(PMIN,US(J,I))
  110 CONTINUE

      DUMMY(3)=PMAX
      DUMMY(4)=PMIN
       WRITE(19) TIME,DUMMY,NELEM,((US(J2,I2),I2=1,8),J2=1,NELEM)
       DO 200 J=1,NELEM
       DO 200 I=1,8
       WRITE(8,210) J,I,US(J,I)
  200 CONTINUE
  210 FORMAT(2I8,D15.6)
       ENDIF
C
      CLOSE (unit=8,status='keep')
      CLOSE (unit=19,status='keep')
C
 1000 FORMAT('      Z(M)          PRESSURE      ',
     1 '          PSI       PERMEABILITY(M^2) VELOCITY(M/S)')
 1010 FORMAT(5D16.7,I2)
 1020 FORMAT(' MAX DIFF OF ',D14.6,' OCCURS AT ',D12.5)
 1030 FORMAT(' MAX PERCENT ERROR=',D14.6)
 1040 FORMAT(T7,'DATA (PRESSR(I),I=',I3,',',I3,') /')
 1050 FORMAT(15(T6,'1',1X,5(D12.6,',')/))
      END
      SUBROUTINE F (Z,U,UPRIME,RPAR,IPAR)
C
CCC  Z = Z-LOCATION CHOSEN BY CODE
C    U = EFFECTIVE PRESSURE
C    UPRIME dP/dz
CCC
C      IMPLICIT REAL*8 (A-H,O-Z)
      COMMON /RATE/ VELBC
      DIMENSION U(1),UPRIME(1),RPAR(3),IPAR(1)
      DATA IFLAG/0/
      AMU=.01
      CALL PERM(U(1),Z,AMU,AK,PHM)

C       VELBC=-1.5844044D-11
       UPRIME(1)=-AMU*VELBC/AK
       RPAR(1)=AK
       RPAR(2)=AMU
       RPAR(3)=UPRIME(1)
       RETURN
       END
      SUBROUTINE MESH (NNODE,TNODE)
C      REAL*8 TNODE(1),ZNODE(501)
      DIMENSION TNODE(1),ZNODE(501)
C
CCC  Define the nodal points
C
      DATA (ZNODE(I),I= 1, 15) /
     1 0.0, 65.15,130.3,175,219.5,222,224.4,279.5,335.4,400.0,465.5
     2 485,503.6,517,530.47/
C
      NNODE=15
      DO 10 I=1,NNODE
        TNODE(I)=ZNODE(I)
   10 CONTINUE
C
      RETURN
      END
```

```
      SUBROUTINE PERM (P,Z,AMU,AK,PHM)
      COMMON/MAT/MAT
C       IMPLICIT REAL*8 (A-H,O-Z)
C
C     CALCULATES PERMEABILITY  (M**2)
C     UNITS - KG,M,SEC.
C     Materials are:
C     2 - CHz
C     3 - CHny
C     4 - TSw2
C     5 - TSw1
C     6 - PTn
C     7 - TCw
C
      DIMENSION AF(10),ALPM(10),BETM(10)
      DIMENSION CONM(10),CONF(10)
C   ROCK PROPERTIES
      DATA(AF(I), I=2,7)/2*4.6E-5,18.0E-5,4.1E-5,2.7E-5,14.0E-5/
      DATA(ALPM(I),I=2,7)/0.00308,0.01600,0.00567,0.00567,0.015,0.00821/
      DATA(BETM(I),I=2,7)/1.602,3.872,1.798,1.798,6.872,1.558/
      DATA(CONM(I),I=2,7)/2.E-11,2.7E-07,1.9E-11,1.9E-11,3.9E-7,9.7E-12/
      DATA(CONF(I),I=2,7)/2*20.0E-5,1.7E-5,2.2E-5,61.0E-5,3.8E-5/
C  CONDUCTIVE FUNCTION STATEMENT
      CONFU(AL,AP)=(1.+AP)**(-AL/2.)*(1.-(AP/(1.+AP))**AL)**2
C  FRACTURE PROPERTIES
      THF=3.950E-2
      ALPF=1.2851
      BETF=4.22865
C
C  Define materials according to elevation
C
        IF (Z.LE.130.3) THEN
          MAT=3
      ELSE IF (Z.GT.130.3.AND.Z.LE.335.4) THEN
         MAT=4
      ELSE IF (Z.GT.335.4.AND.Z.LE.465.5) THEN
         MAT=5
      ELSE IF (Z.GT.465.5.AND.Z.LE.503.6) THEN
         MAT=6
        ELSE
          MAT=7
        END IF
      RHOG=1000.*9.80665
      PHM=P/RHOG-Z
      IF(PHM.GT. -.000001)  PHM=-.000001
      APM=(ALPM(MAT)*(-PHM))**BETM(MAT)
      ALM=(1-1./BETM(MAT))
      APF=(ALPF*      (-PHM))**BETF
      ALF=(1-1/BETF)
      COM=CONFU(ALM,APM)*CONM(MAT)
:  NEED TO CHANGE FOR SAND
      RESULT=CONFU(ALF,APF)
      COF=RESULT*CONF(MAT)
      AK=(1-AF(MAT))*COM+AF(MAT)*COF
 NEED PERMEABILITY IN M**2
      AK=AK*AMU/RHOG
        ak=.25e-12
      RETURN
      END
```

all done

Attachment C

Input to the NORIA code for the Tiva Canyon calculation.

```
$ shaft drilling water
setup  : 1,51
water  : 1,1000.0,0.001,,,,9.8,variable
vapor  : 2
air    : 3
calicoz : 4,2230.,1.6,2.4,,,,.2800000,1.0,,,,variable,,35,.22352e7
calicov : 5,2370.,1.6,2.4,,,,.4600248,1.0,,,,variable,,35,.22352e7
topopah2: 6,2580.,1.6,2.4,,,,.110,1.0,,,,variable,,35,.1539e7
topopah1: 7,2490.,1.6,2.4,,,,.08210000,1.0,,,,variable,,35,.4716e7
paintbsh: 8,2350.,1.6,2.4,,,,.4000162,1.0,,,,variable,,35,.22352e7
tivacan : 9,2490.,1.6,2.4,,,,.082100 ,1.0,,,,variable,,35,.4322e7
end
1,1,51,3, .94 , 1 , .94 , 1
2,21,25,25,2,21
517,517,518,518
end
iloop,9,2
quad8/4,7,1,1
lend
iloop,16,2
quad8/4,9,19,1
lend
end
formkf,   axisym
output,material,all
unzipp,0.0, 3.15e10, 1.0e2 ,100, ,5,1e4,3.15e7,6.3e7,3.15e8,3.15e9
end
stop, post
```

Attachment C (continued)

Input to the NORIA code for the Paintbrush calculation.

```
$ shaft drilling water
setup  : 1,51
water  : 1,1000.0,0.001,,,,9.8,variable
vapor  : 2
air    : 3
calicoz : 4,2230.,1.6,2.4,,,,2800000,1.0,,,,variable,,35,,22352e7
calicov : 5,2370.,1.6,2.4,,,,4600248,1.0,,,,variable,,35,,22352e7
topopah2: 6,2580.,1.6,2.4,,,,110,1.0,,,,variable,,35,,1539e7
paintbsh: 7,2350.,1.6,2.4,,,,4000,1.0,,,,variable,,35,,3595e7
paintbs2: 8,2350.,1.6,2.4,,,,4000,1.0,,,,variable,,35,,3544e7
tivacan : 9,2490.,1.6,2.4,,,,082100 ,1.0,,,,variable,,35,,4322e7
end
1,1,51,3, .94 , 1 , .94 , 1
2,21,25,25,2,21
485,485,486,486
end
lloop,9,2
quad8/4,7,1,1
lend
lloop,16,2
quad8/4,8,19,1
lend
end
formkf,   axisym
output,material,all
unzipp,0.0, 3.15e10, 1.0e2 ,100, ,5,1e4,3.15e7,6.3e7,3.15e8,3.15e9
end
stop, post
```

Attachment C (continued)

Input to the NORIA code for the Topopah Spring calculation.

```
$ shaft drilling water
setup  ; 1,51
water  ; 1,1000.0,0.001,,,,9.8,variable
vapor  ; 2
air    ; 3
calicoz ; 4,2230.,1.6,2.4,,,,.2800000,1.0,,,,variable,,35,.22352e7
calicov ; 5,2370.,1.6,2.4,,,,.4600248,1.0,,,,variable,,35,.22352e7
topopah2; 6,2580.,1.6,2.4,,,,.110,1.0,,,,variable,,35,.14105e7
topopah1; 7,2580.,1.6,2.4,,,,.1100,1.0,,,,variable,,35,.106e7
paintbsh; 8,2350.,1.6,2.4,,,,.4000162,1.0,,,,variable,,35,.22352e7
tivacan ; 9,2490.,1.6,2.4,,,,.081288 ,1.0,,,,variable,,35,.22352e7
end
1,1,51,3, .94 , 1 , .94 , 1
2,21,25,25,2,21
222,222,223,223
end
iloop,9,2
quad8/4,6,1,1
lend
iloop,16,2
quad8/4,7,19,1
lend
end
formkf,   axisym
output,material,all
unzipp,0.0, 3.15e10, 1.0e2 ,100, ,5,1e4,3.15e7,6.3e7,3.15e8,3.15e9
end
stop, post
```

Input to the NORIA code for the Calico Hills calculation.

```
$ shaft drilling water calico hills vitric use materials 4 and 5
setup  : 1,51
water  : 1,1000.0,0.001,,,,9.8,variable
vapor  : 2
air    : 3
calicoz : 4,2370.,1.6,2.4,,,.4600000,1.0,,,,variable,,35,,107e5
calico2 : 5,2370.,1.6,2.4,,,.4600000,1.0,,,,variable,,35,19.6
topopah2: 6,2580.,1.6,2.4,,,.110,1.0,,,,variable,,35,.1539e7
paintbsh: 7,2350.,1.6,2.4,,,.4000,1.0,,,,variable,,35,.3595e7
paintbs2: 8,2350.,1.6,2.4,,,.4000,1.0,,,,variable,,35,.3544e7
tivacan : 9,2490.,1.6,2.4,,,.082100 ,1.0,,,,variable,,35,.4322e7
end
1,1,51,3, .94 , 1 , .94 , 1
2,21,25,25,2,21
65.15,65.15,66.15,66.15
end
iloop,9,2
quad8/4,4,1,1
lend
iloop,16,2
quad8/4,5,19,1
lend
end
formkf,   axisym
output,material,all
unzipp,0.0, 3.15e7, 1.0e0 ,200, ,4,1e2,2.63e6,1.57e7,3.15e7
end
stop, post
```

Attachment D

RIB and SEPDB Data

The values of the material properties in Figure 1 were taken from the RIB. For the matrix porosity, the values were within the range contained in the RIB, except for the Calico Hills unit for which a value 0.01 larger than the range was used. The values of matrix porosity selected were based on R. R. Peters et al., 1984, "Fracture and Matrix Hydrologic Characteristics of Tuffaceous Materials from Yucca Mountain, Nye County, Nevada," SAND84-1471, Sandia National Laboratories, Albuquerque, New Mexico.

This report contains no candidate information for the RIB.

This report contains no candidate data for inclusion in the SEPDB.

APPENDIX C

SLTR87-2003

NUMERICAL SOLUTIONS FOR THE DISTRIBUTION OF RESIDUAL CONSTRUCTION WATER AND IN SITU PORE WATER IN THE EXPLORATORY SHAFT FACILITY AT YUCCA MOUNTAIN, INCLUDING EFFECTS OF DRIFT VENTILATION

SLTR87-2003
Department 6310 Letter Report
Sandia National Laboratories
Nevada Nuclear Waste Storage
Investigations Project
Issued April 1988

NUMERICAL SOLUTIONS FOR THE DISTRIBUTION OF RESIDUAL CONSTRUCTION WATER AND IN SITU PORE WATER IN THE EXPLORATORY SHAFT FACILITY AT YUCCA MOUNTAIN, INCLUDING EFFECTS OF DRIFT VENTILATION

Roger R. Eaton and Andrew C. Peterson

Introduction

The current plan for the shaft drilling and drift construction in the exploratory shaft facility (ESF) at the proposed Nevada Nuclear Waste Repository site includes the use of water for dust control and drilling purposes. During this operation, some of the water will be absorbed by the host rock. The presence of this water has generated concern about its effect on the undisturbed conditions of the rock; that is; can this water increase the saturation of the rock surrounding the shaft to a level which could have an adverse effect on in situ experiments or performance of the waste package?

Previous analyses investigating the potential change in the matrix saturation level from the residual water in the ESF were reported in SLTR87-2001 and SLTR87-2002 (Appendix A and Appendix B, respectively). The hydrologic units that were included in these analyses were the Tiva Canyon welded, devitrified; Paintbrush vitric; Topopah Spring lithophysae-rich; Topopah Spring lithophysae-poor; and Calico Hills vitric. SLTR87-2001 was an initial attempt to address this issue, using analytical procedures, and fulfilled part of the analyses requested in problem definition memo (PDM) 72-22. Two limiting cases were addressed to estimate the radial distance to which the rock is affected and the maximum increase in saturation that can be expected.

The first analysis (SAND87-2001) represents a limiting case in that the maximum radial distance that water can travel into the saturated fractures of the matrix and the resulting equilibrium saturation increase was calculated. The second analysis (SAND87-2001) is a limiting case in that the maximum matrix saturation increase that may occur at any radial distance from the walls was calculated. The results of these initial analytical analyses indicate that the change in saturation would be quite small. The largest calculated increase in saturation was 0.013, when 10% of the drilling water was uniformly retained in the Tiva Canyon unit in a 10.0-m radius from the shaft center (7.8 m from concrete liner). These changes in saturation may be less than the accuracy of in situ experiments and numerical calculations.

To investigate the effect of some of the assumptions used in the analyses discussed above, such as fracture saturation and constant radial saturation distributions, numerical, time-dependent solutions for each of the four hydrologic strata were made (SLTR87-2002) using the multidimensional finite element code NORIA [1]. The initial conditions for these calculations were selected to be representative of the expected conditions. The results of these calculations show the increases in saturation within a radius of 25 m from the shaft centerline for computational times ranging from 1-1000 yr.

Neither the analytical analysis (SLTR87-2001) nor the numerical analysis (SLTR87-2002) included the possible influence of the ventilation system on the movement of residual construction water and in situ pore water. The effect of drift ventilation is included in this study. Numerical calculations have been made that include the effects of drift ventilation for drifts located in the Topopah Spring and Calico Hills vitric strata. These are the only strata that are currently planned to have drifts in the ESF.

Code Requirements and Problem Definition

In these calculations, time-dependent, one-dimensional flow of the residual mining water and in situ pore water in the rock matrix adjacent to the drift walls is modeled using the numerical code NORIA. In this computer code, the flow is assumed to be in isothermal and matrix/fracture equilibrium at all times. The development of the matrix/fracture equilibrium model was discussed in Reference 2. The water is transported as a result of pressure gradients. A listing of the code used in these calculations is stored in the Sandia National Laboratories' internal file storage (ISF). When using the code, it is necessary for the user to describe the material characteristics, such as saturation and permeability, as functions of pressure head. This is done in the two subroutines, PERM and FLUDIC. A listing of these two subroutines for the two different strata is given in Attachment A. The material properties used in these subroutines and for the entire analysis are based on those specified in the

PDM, which lists fracture and hydrologic characteristics based on the psychrometer measurement of Reference 3 (see also Attachment D).

An outline of the mine drift and the surrounding rock is shown in Figure 1. To calculate the one-dimensional flow in the vicinity of the drift wall, a row of 25 eight-node, quadratic finite elements are used (Figure 2). The elements start at the drift wall, X = 0 m, and extend to 25 m. The distance was selected to be large enough that it would not significantly affect the conclusions of these analyses. The length of the elements increased from 0.187 m at the drift wall to 2.85 m at X = 25 m.

Initial and Boundary Conditions

Initial pressure head and saturation values are obtained by assuming one-dimensional, vertical, steady-state infiltration of Q = 0.1 mm/yr through the strata shown in Figure 3. This solution was obtained using LLUVIA, the one-dimensional, steady-state computer code. A listing of this code is given in Attachment B. The resulting steady-state pressure head distribution, which establishes the saturation level, is given in Figure 4.

Time-dependent analysis, using NORIA, was made at the two vertical locations indicated in Figure 3. In each case it was assumed that at time zero residual mining water was located in the modified permeability zone ($0 < X < 2.76$ m), Figure 5, as defined by Fernandez [4]. This volume was chosen because the permeability in this zone is specified in the PDM to be 80 times larger than that in the unmodified region. Thus, the mining water will most likely be nearly evenly distributed in this region before being transported into the unmodified zone through capillary action. Therefore, the initial distribution of the mining water in the modified permeability zone (MPZ) would have little effect on the time-dependent results. Based on the saturation level established by the pressure head distribution calculated with LLUVIA, the initial saturation for each stratum at the axial locations shown in Figure 3 was specified such that 0.165 m^3/m^2 of water was added to the rock for each square meter of drift wall surface, as specified by the PDM. Adding this amount of water to the modified zone

resulted in the following changes in the initial saturation: Topopah Spring increased by 0.0285, and Calico Hill increased by 0.00682.

A pressure boundary condition is imposed at the X = 0 boundary to represent the ventilation condition in the drift. The procedure for calculating a pore water potential is discussed in the ventilation study done by Hopkins et al. [5]. The equation given is

$$W = \frac{RT}{Mg} \ln \frac{u}{100} \quad ,$$

where W = pressure head (m); R = universal gas constant, 8.314×10^3; T = Kelvin temperature, 299.15; M = molecular weight of water, 18.0; g = gravitational constant, 9.8; and u = relative humidity (%), 10.0.

For these prescribed conditions the calculated pressure head is -3.25×10^4 m. The corresponding saturation for the Topopah Spring and the Calico Hills strata is 0.0943 and 0.041, respectively. (Note that if the relative humidity was assumed to be 90%, the calculated pressure head would be -1.48×10^3 m and the corresponding saturation for the Topopah Spring and Calico Hills strata would be 0.133 and 0.041, respectively.)

Listings of the NORIA input for both calculations are given in Attachment C.

Results

NORIA was run on the Cray XMP computer. Computed times out to 1000 yr required less than 30 s to run, using up to 60 time steps. The calculations were expedited because the fractures remained unsaturated and the computational nonlinearities that occur during fracture saturation did not exist.

Figure 6 shows the saturation profiles for the Topopah Spring drift for times of 1 wk, 2 wk, 4 wk, 0.5 yr, 1 yr, 10 yr, and 100 yr. The assumed initial location of the residual construction water and in situ

water is shown by the t = 0 curve. The increment in saturation located between $0 < X < 2.76$ m represents the residual construction water.

The saturation boundary condition at the drift wall creates a considerable amount of drying in the vicinity of the wall. At approximately 4 wk, drying resulting from the drift ventilation completely dominates any effect of residual construction water. By t = 100 yr the effect of drift ventilation on the rock is significant to a distance of 25 m from the drift wall and the effect of the no flow condition imposed at the right computational boundary influences the calculations. Therefore, results for times larger than 100 yr are not presented. The discontinuous slope in the saturation curves is a result of the increased permeability of the MPZ, which extends to 2.76 m. Enhanced drying occurs in this zone as a result of its permeability value, which is 80 times the undisturbed zone value. At 1 yr the effect of drying has penetrated approximately 2 m into the undisturbed rock. This is similar to the results presented in Reference 5.

Figure 7 shows the effect of drift ventilation on saturation profiles adjacent to the Calico Hills drift. Because the permeability of the Calico Hills material is several orders of magnitude larger than that of the Topopah Spring material, the time scale for drying is considerably shorter. The figure shows that after one day of ventilation the residual construction water has been completely drawn into the drift by the ventilation process. By 0.5 yr, drift ventilation affects the saturation in the Calico Hills rock to a distance of 25 m, and the no flow condition imposed at the right boundary influences the results. Therefore, results for times longer than 0.5 yr are not presented.

Discussion and Conclusions

The results for the analyses discussed in this document indicate that the change in saturation is completely dominated by the effects of the ventilation system. This ventilation removes the residual water from the drift walls before the capillary forces can transport it away from the drift walls and into the undisturbed rock.

These analyses did not consider potential effects of local variations in strata properties that could occur. Thus, under certain conditions, it can be conceived that the residual mining water could be channeled directly to an in situ experiment located at some distance, X, from the drift. However, without detailed knowledge of the strata variations, it would be impossible to accurately model these situations.

References

1. N. E. Bixler, "NORIA--A Finite Element Computer Program for Analyzing Water, Vapor, Air, and Energy Transport in Porous Media," SAND84-2057, Sandia National Laboratories, Albuquerque, NM, August 1985.

2. E. A. Klavetter and R. R. Peters, "Estimation of Hydrologic Properties of an Unsaturated, Fractured Rock Mass," SAND84-2642, Sandia National Laboratories, Albuquerque, NM, July 1986.

3. R. R. Peters, E. A. Klavetter, I. J. Hall, S. C. Blair, P. R. Heller, and G. W. Gee, "Fracture and Matrix Hydrologic Characteristics of Tuffaceous Materials from Yucca Mountain, Nye County, Nevada," SAND84-1471, Sandia National Laboratories, Albuquerque, NM, December 1984.

4. J. A. Fernandez, T. E. Hinkebein, and J. B. Case, "Selected Analyses to Evaluate the Effect of the Exploratory Shaft on Repository Performance of Yucca Mountain," SAND85-0598, Sandia National Laboratories, Albuquerque, NM, 1988.

5. P. L. Hopkins and R. R. Eaton, "Effect of Drift Ventilation on Repository Hydrology and Resulting Solute Transport Implications," SAND86-1571, Sandia National Laboratories, Albuquerque, NM, May 1987.

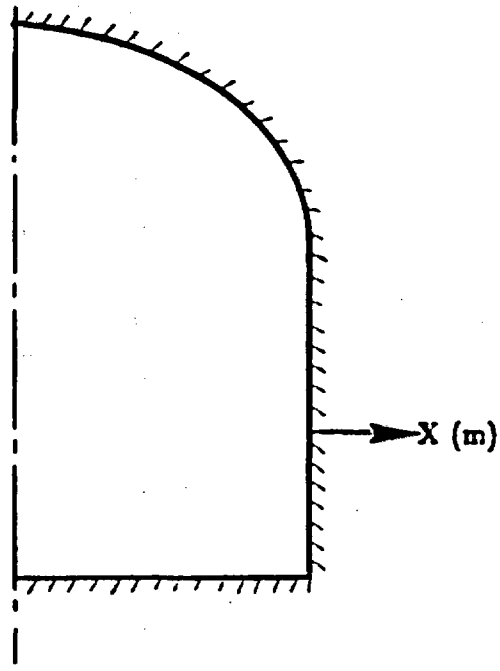

Figure 1. Outline of Problem Geometry.

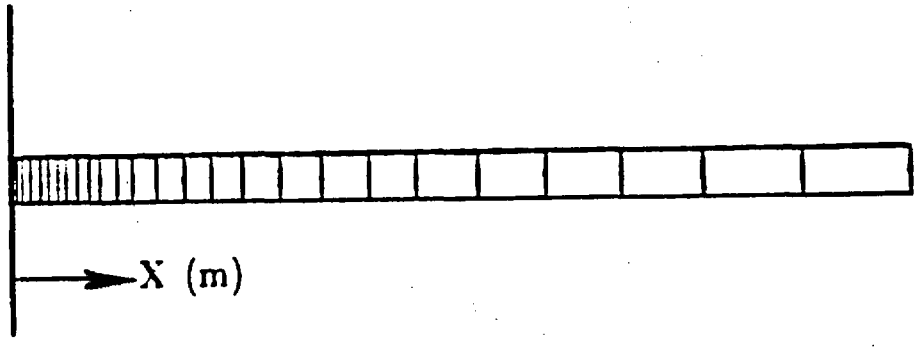

Figure 2. Finite Element Geometry.

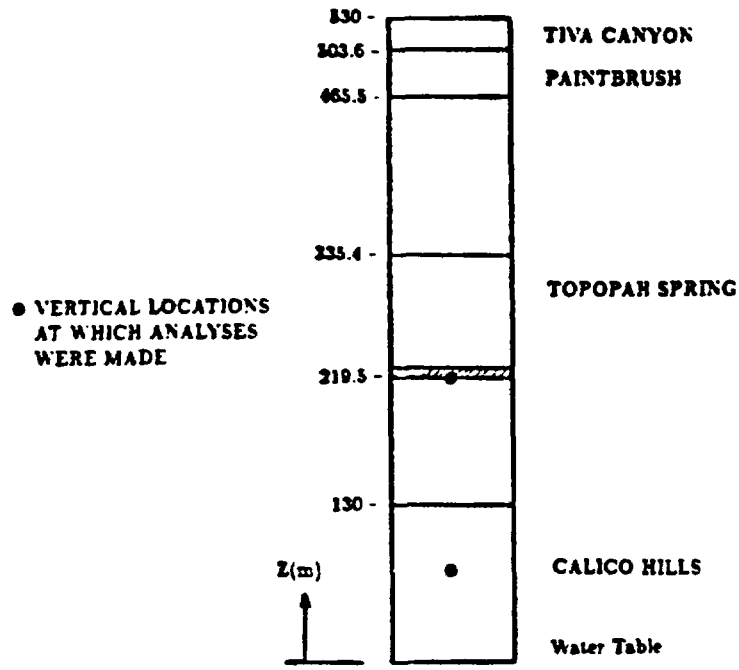

Figure 3. Vertical Geometry of Hydrologic Strata.

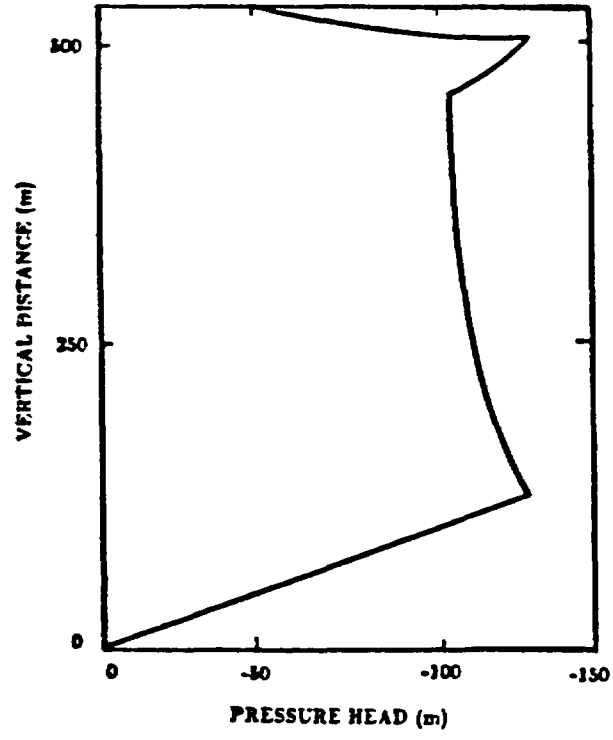

Figure 4. Vertical Distribution of Pressure Head Obtained Using Code, LLUVIA.

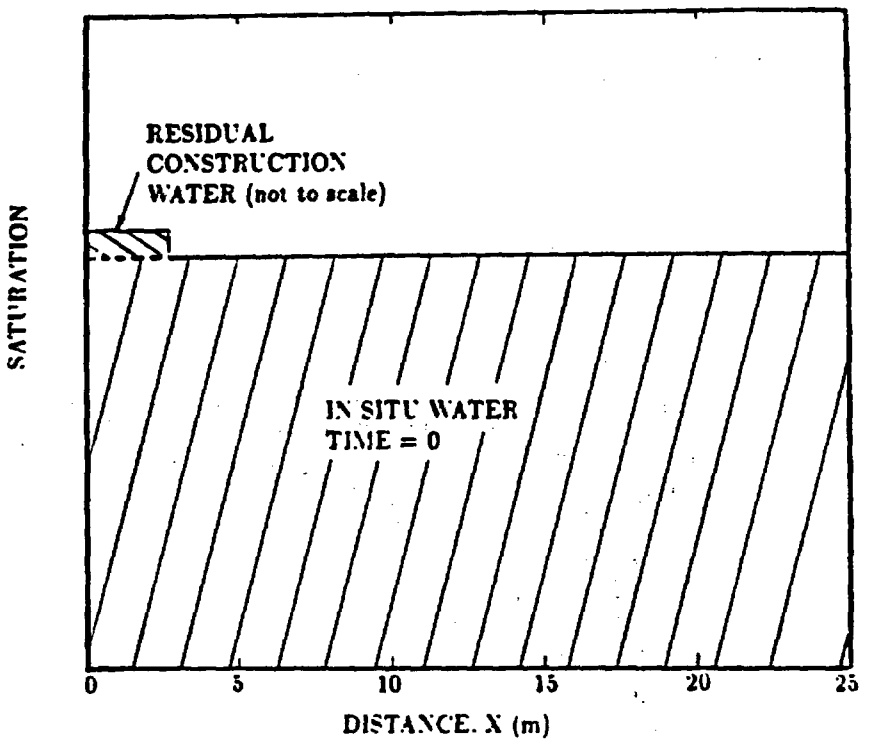

Figure 5. Initial Saturation Distribution Showing Location of Mining Water.

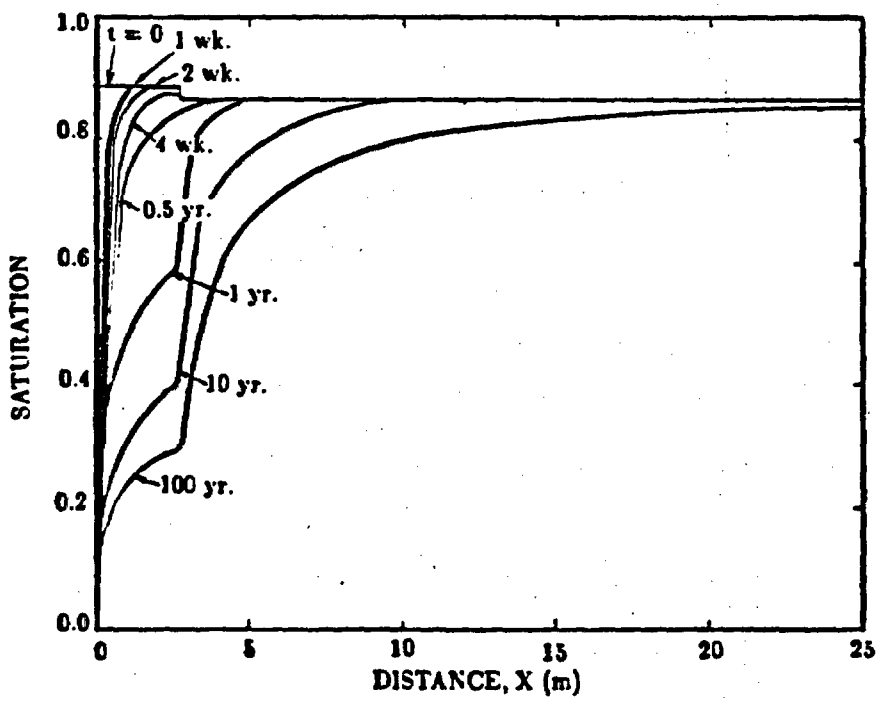

Figure 6. Saturation Profiles for Topopah Spring for Times up to 100 yr.

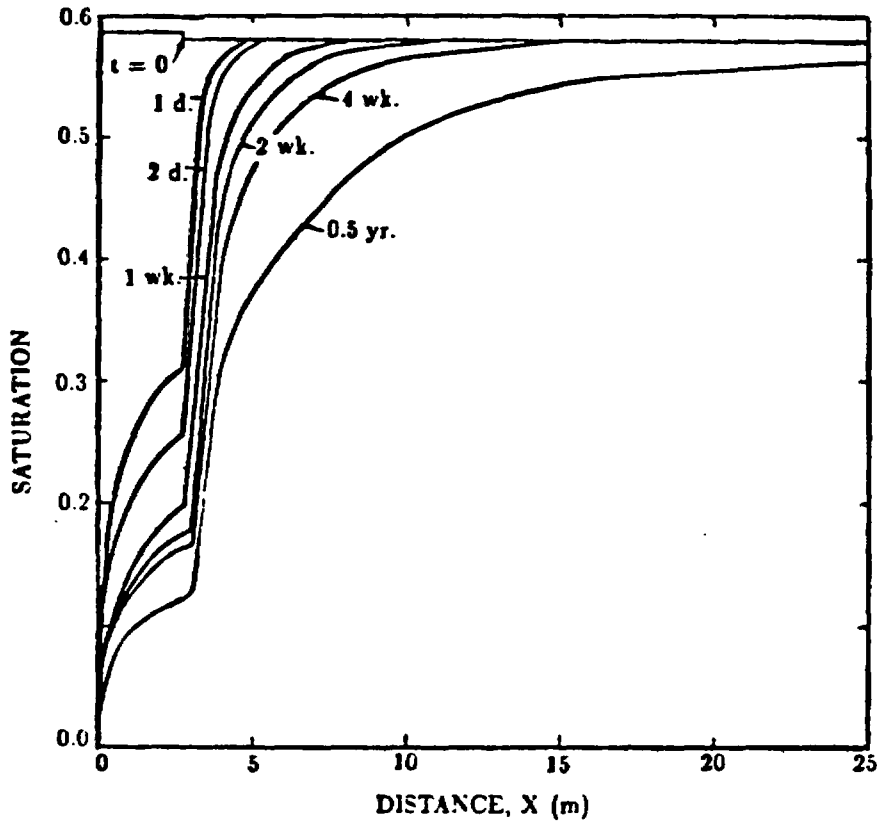

Figure 7. Saturation Profiles for Calico Hills for Times up to 0.5 yr.

Attachment A

FORTRAN listing of subroutines, PERM and FLUDIC, for Topopah Spring.

```
c
      subroutine fluidc(th,thm,thf,cm,anm1,anf1,smr1,sfr,
     1                  t,p,pv,pa,x,y,time,phi,rhog,nelem,mat,nn)
c
c     this sub calc the moisture content and der of moisture content wrt
c     p in units - kg,m,s.
c
c     mat 4, unit CHnz, Calico Hills, nonwelded, zeolitic
c     mat 5, unit CHnv, Calico Hills, nonwelded, vitric
c     mat 6, unit TSw2, Topopah Springs, welded (repository zone)
c     mat 7, unit TSw1, Topopah Springs, welded (lithophysal zone)
c     mat 8, unit PTn,  Paintbrush, nonwelded
c     mat 9, unit TCw,  Tiva Canyon, welded
c
c    variables:
c    betp       water compressibility (beta prime)
c    alpp       rock compressibility   (alpha prime)
c    anf        fracture porosity
c    anm        matrix porosity
c    phi        total porosity (phi = anf + anm * (1 - anf))
c    th         moisture content(fracture and matrix averaged)
c    thm        moisture content of the matrix
c    thf        moisture content of the fracture
c    smr        residual saturation of the matrix
c    sfr        residual saturation of the fracture
c    sm         saturation of matrix
c    sf         saturation of fracture
c    fc         fracture compressibility
c
      dimension th(8),thm(8),thf(8),cm(8),t(8),
     2          p(8),pv(8),pa(8),x(8),y(8)
      dimension smr(10),anm(10),anf(10),alpm(10),betm(10),alpp(10),
     2          fc(10)
c
c     properties
c
      data(smr(i), i=4,9)/ 0.110, 0.041,  0.080,  0.080,  0.10,  0.002/
      data(anm(i), i=4,9)/  0.28,  0.46,   0.11,   0.11,  0.40,   0.08/
      data(anf(i), i=4,9)/4.6e-5,4.6e-5, 18.e-5, 18.e-5,2.7e-5, 14.e-5/
      data(alpm(i),i=4,9)/.00308,0.0160,0.00567,0.00567,0.0150,0.00821/
      data(betm(i),i=4,9)/ 1.602, 3.872,  1.798,  1.798, 6.872,  1.558/
      data(alpp(i),i=4,9)/ 9.e-7,26.e-7, 5.8e-7, 5.8e-7,62.e-7, 6.2e-7/
      data(fc(i),  i=4,9)/2.8e-8,2.8e-8, 12.e-8, 12.e-8,19.e-8,132.e-8/
c
c     saturation function statement
c
      satfu(sr,al,ap)=(1-sr)*(1+ap)**(-al) + sr
c
c     derivative of saturation function statement
c
      chfu(sr,al,ap,bet,a,phm)=(1-sr)*al*(1.+ap)**(-al-1.)
     1 *bet*a**bet*(-phm)**(bet-1)/rhog
c
c     fracture properties
c
      sfr=3.850e-2
      alpf=1.2851
      betf=4.23
c
c     matrix properties
```

Attachment A (continued)

```
c
      betp=9.8e-7
c
c     evaluate moisture content
c
      alm=(1.-1/betm(mat))
      alf=(1.-1./betf)
c
c     set values for use in computing fluxes and velocities
c
      anm1=anm(mat)
      anf1=anf(mat)
      smr1=smr(mat)
c
c     loop over nodes
c
      do 100 j=1,nn
      phm=p(j)/rhog - y(j)
      if (phm.gt.-.000001) phm=-.000001
      apm=(alpm(mat)*(-phm))**betm(mat)
      apf=(alpf*     (-phm))**betf
      sm=satfu(smr(mat),alm,apm)
      sf=satfu(sfr     ,alf,apf)
c
c     convert saturation to moisture content
c
      thm(j)=sm*anm(mat)*(1.-anf(mat))
      thf(j)=sf*anf(mat)
      th(j)=thm(j) + thf(j)
c
c     these effects need to be incorporated into the capacitance term
c
      watcomp=betp*th(j)/rhog
      rokcomp=alpp(mat)*th(j)/(anf(mat)+anm(mat))*(sm-anf(mat)
     2       *(sm-sf))/rhog
      fracomp=fc(mat)*th(j)/(anf(mat)+anm(mat))*(sm-sf)/rhog
c
c     compute the derivative of saturation wrt psi
c
      chm=chfu(smr(mat),alm,apm,betm(mat),alpm(mat),phm)
      chf=chfu(sfr     ,alf,apf,betf     ,alpf     ,phm)
c
c     convert to moisture content and sum terms for total capacitance
c
      cm1=chm*anm(mat)*(1.-anf(mat)) + chf*anf(mat)
      cm(j)=cm1 + watcomp + rokcomp + fracomp
c      cm(j)=cm1 + 1.0e-5
  100 continue
c
      return
      end
```

Attachment A (continued)

```
c
c
c
      subroutine perm(cond1,cond2,akm11,akm22,akf11,akf22,
     1                th,t,p,pv,pa,x,y,time,phi,rhog,nelem,mat,nn)
      dimension cond1(8),cond2(8),akm11(8),akm22(8),akf11(8),akf22(8),
     1          t(8),p(8),pv(8),pa(8),x(8),y(8)
      dimension th(8)
c
c    calculates permeability  (cm**2)
c    units - gm,c m,sec.
c
      dimension cond(100)
      dimension phd(100),hkd(100)
      dimension thm(10),af(10),alpm(10),betm(10)
      dimension conm(10),conf(10)
c   rock properties
      data(alpm(i),i=4,9)/.00308, 0.016,0.00567,0.00567,0.0160,0.00821/
      data(betm(i),i=4,9)/ 1.602, 3.872,  1.798,  1.798, 6.872,  1.558/
      data(af(i),  i=4,9)/4.6e-5,4.6e-5, 18.e-5, 18.e-5,2.7e-5, 14.e-5/
c note that perm for mat=6 is 80 times bigger than mat=7
      data(conm(i),i=4,9)/2.e-11,2.7e-7,152e-11,1.8e-11,3.9e-7,9.7e-12/
      data(conf(i),i=4,9)/20.e-5,20.e-5, 1.7e-5, 1.7e-5,61.e-5, 3.8e-5/
c  conductive function statement
      confu(al,ap)=(1.+ap)**(-al/2.)*(1.-(ap/(1.+ap))**al)**2
c  fracture properties
      alpf=1.285
      betf=4.23
      do 20 j=1,nn
      phm=p(j)/rhog - y(j)
      if(phm.gt. -.000001)  phm=-.000001
      apm=(alpm(mat)*(-phm))**betm(mat)
      alm=(1-1./betm(mat))
      apf=(alpf*      (-phm))**betf
      alf=(1-1/betf)
      com=confu(alm,apm)*conm(mat)
      cof=confu(alf,apf)*conf(mat)
      akm11(j)=(1.-af(mat))*com*0.001/rhog
      akm22(j)=akm11(j)
      akf11(j)=af(mat)*cof*0.001/rhog
      akf22(j)=akf11(j)
      cond1(j)=akm11(j)+akf11(j)
      cond2(j)=akm22(j)+akf22(j)
   20 continue
      return
      end
c
c
c
```

Attachment A (continued)

```
c
      subroutine fluidc(th,thm,thf,cm,anm1,anf1,smr1,sfr,
     1                  t,p,pv,pa,x,y,time,phi,rhog,nelem,mat,nn)
c
c     this sub calc the moisture content and der of moisture content wrt
c     p in units - kg,m,s.
c
c     mat 4, unit CHnz, Calico Hills, nonwelded, zeolitic
c     mat 5, unit CHnv, Calico Hills, nonwelded, vitric
c     mat 6, unit TSw2, Topopah Springs, welded (repository zone)
c     mat 7, unit TSw1, Topopah Springs, welded (lithophysal zone)
c     mat 8, unit PTn,  Paintbrush, nonwelded
c     mat 9, unit TCw,  Tiva Canyon, welded
c
c     variables:
c     betp      water compressibility (beta prime)
c     alpp      rock compressibility   (alpha prime)
c     anf       fracture porosity
c     anm       matrix porosity
c     phi       total porosity (phi = anf + anm * (1 - anf))
c     th        moisture content(fracture and matrix averaged)
c     thm       moisture content of the matrix
c     thf       moisture content of the fracture
c     smr       residual saturation of the matrix
c     sfr       residual saturation of the fracture
c     sm        saturation of matrix
c     sf        saturation of fracture
c     fc        fracture compressibility
c
      dimension th(8),thm(8),thf(8),cm(8),t(8),
     2          p(8),pv(8),pa(8),x(8),y(8)
      dimension smr(10),anm(10),anf(10),alpm(10),betm(10),alpp(10),
     2          fc(10)
c
c     properties
c
      data(smr(i), i=4,9)/ 0.041, 0.041,  0.080,  0.080,  0.10,  0.002/
      data(anm(i), i=4,9)/  0.46,  0.46,   0.11,   0.11,  0.40,   0.08/
      data(anf(i), i=4,9)/4.6e-5,4.6e-5, 18.e-5, 4.1e-5,2.7e-5, 14.e-5/
      data(alpm(i),i=4,9)/.0160,0.0160,0.00567,0.00567,0.0150,0.00821/
      data(betm(i),i=4,9)/ 3.872, 3.872,  1.798,  1.798, 5.872,  1.558/
      data(alpp(i),i=4,9)/39.e-7,39.e-7, 5.8e-7, 12.e-7,82.e-7, 6.2e-7/
      data(fc(i),  i=4,9)/2.8e-8,2.8e-8, 12.e-8, 5.6e-8,19.e-8,132.e-8/
c
c     saturation function statement
c
      satfu(sr,al,ap)=(1-sr)*(1+ap)**(-al) + sr
c
c     derivative of saturation function statement
c
      chfu(sr,al,ap,bet,a,phm)=(1-sr)*al*(1.+ap)**(-al-1.)
     1 *bet*a**bet*(-phm)**(bet-1)/rhog
c
c     fracture properties
c
      sfr=3.950e-2
      alpf=1.2851
      betf=4.23
c
c     matrix properties
```

Attachment A (continued)

```
      betp=9.8e-7
c
c     evaluate moisture content
c
      alm=(1.-1/betm(mat))
      alf=(1.-1./betf)
c
c     set values for use in computing fluxes and velocities
c
      anm1=anm(mat)
      anf1=anf(mat)
      smr1=smr(mat)
c
c     loop over nodes
c
      do 100 j=1,nn
      phm=p(j)/rhog - y(j)
      if (phm.gt.-.000001) phm=-.000001
      apm=(alpm(mat)*(-phm))**betm(mat)
      apf=(alpf*     (-phm))**betf
      sm=satfu(smr(mat),alm,apm)
      sf=satfu(sfr     ,alf,apf)
c
c     convert saturation to moisture content
c
      thm(j)=sm*anm(mat)*(1.-anf(mat))
      thf(j)=sf*anf(mat)
      th(j)=thm(j) + thf(j)
c
c     these effects need to be incorporated into the capacitance term
c
      watcomp=betp*th(j)/rhog
      rokcomp=alpp(mat)*th(j)/(anf(mat)+anm(mat))*(sm-anf(mat)
     2       *(sm-sf))/rhog
      fracomp=fc(mat)*th(j)/(anf(mat)+anm(mat))*(sm-sf)/rhog
c
c     compute the derivative of saturation wrt psi
c
      chm=chfu(smr(mat),alm,apm,betm(mat),alpm(mat),phm)
      chf=chfu(sfr     ,alf,apf,betf     ,alpf     ,phm)
c
c     convert to moisture content and sum terms for total capacitance
c
      cm1=chm*anm(mat)*(1.-anf(mat)) + chf*anf(mat)
      cm(j)=cm1 + watcomp + rokcomp + fracomp
c      cm(j)=cm1 + 1.0e-5
  100 continue
c
      return
      end
c
```

Attachment A (concluded)

```
      subroutine perm(cond1,cond2,akm11,akm22,akf11,akf22,
     1                th,t,p,pv,pa,x,y,time,phi,rhog,nelem,mat,nn)
      dimension cond1(8),cond2(8),akm11(8),akm22(8),akf11(8),akf22(8),
     1          t(8),p(8),pv(8),pa(8),x(8),y(8)
      dimension th(8)
c
c     calculates permeability  (cm**2)
c     units - gm,c m,sec.
c
      dimension cond(100)
      dimension phd(100),hkd(100)
      dimension thm(10),af(10),alpm(10),betm(10)
      dimension conm(10),conf(10)
c   rock properties
      data(alpm(i),i=4,9)/.0180, 0.0180,0.00567,0.00567,0.0150,0.00821/
      data(betm(i),i=4,9)/ 3.872, 3.872,  1.798,  1.798, 6.872,  1.558/
      data(af(i),  i=4,9)/4.5e-5,4.5e-5, 18.e-5, 4.1e-5,2.7e-5, 14.e-5/
c note that perm for mat=4 is 80 times bigger than mat=5
      data(conm(i),i=4,9)/216e-7,2.7e-7,1.9e-11,1.9e-11,3.9e-7,9.7e-12/
      data(conf(i),i=4,9)/20.e-5,20.e-5, 1.7e-5, 2.2e-5,61.e-5, 3.8e-5/
c  conductive function statement
      confu(ai,ap)=(1.+ap)**(-ai/2.)*(1.-(ap/(1.+ap))**ai)**2
c  fracture properties
      alpf=1.285
      betf=4.23
      do 20 j=1,nn
      phm=p(j)/rhog - y(j)
      if(phm.gt. -.000001)  phm=-.000001
      apm=(alpm(mat)*(-phm))**betm(mat)
      aim=(1-1./betm(mat))
      apf=(alpf*     (-phm))**betf
      aif=(1-1/betf)
      com=confu(aim,apm)*conm(mat)
      cof=confu(aif,apf)*conf(mat)
      akm11(j)=(1.-af(mat))*com*0.001/rhog
      akm22(j)=akm11(j)
      akf11(j)=af(mat)*cof*0.001/rhog
      akf22(j)=akf11(j)
      cond1(j)=akm11(j)+akf11(j)
      cond2(j)=akm22(j)+akf22(j)
   20 continue
      return
      end
```

Attachment B

FORTRAN listing of program, LLUVIA.

```
      PROGRAM INFIL (tty, input=tty, output=tty)
C
CCC   The purpose of this program is to solve for steady-state pressures
CCC   in Darcy flow problems involving constant infiltration into a
CCC   1-D column of layered strata.  The permeability of each layer is
CCC   a function of pressure and given by subroutine PERM.  A Runge-Kutta
CCC   solution procedure is implemented through subroutine DEBDF which is
CCC   one of the SLATEC library routines.
CCC
CCC   Convergence for some cases will not be obtained with a single
CCC   precision version of this program.
CCC
CCC   May 1986
CCC   R. R. Eaton and P. L. Hopkins, 1511
C
      IMPLICIT REAL*8 (A-H,O-Z)
      EXTERNAL F
      CHARACTER*1 ANS,ANS2,ANS3,YESUP,YESLO
      REAL MAXDIF
      DIMENSION Y(1),INFO(15),RWORK(261)
     1 ,IWORK(56),RPAR(3),IPAR(1),TNODE(501),PHOLD(501)
      DIMENSION DUMMY(8),US(501,8)
C
      DATA IOUT/8/
      DATA IOLD,YOLD/0,.0./,MAXDIF/0./,RHOG/9.80665D3/
      DATA DUMMY/8*0.0/,TIME/0./,US/4008*0./
      DATA YESUP/'Y'/,YESLO/'y'/
C
      COMMON /RATE/ VELBC
      COMMON / MAT/MAT
C
      OPEN (unit=8,form='formatted',status='unknown')
C
CCC   Define nodal coordinates
C
      CALL MESH (NNODE,TNODE)
C
CCCC  Input infiltration rate and whether or not initial condition
CCCC  solution file is to be generated.
C
      PRINT *,'ENTER DOWNWARD INFILTRATION RATE (MM/YR) '
      READ *,VELBC
      VELBC=-VELBC/3.15576D10
      PRINT *,'DO YOU WANT SOLUTION FILE GENERATED ? (Y/N)'
      READ 900, ANS
  900 FORMAT(A1)
      IF (ANS.EQ.YESUP.OR.ANS.EQ.YESLO) THEN
       PRINT *,'ENTER NUMBER OF ELEMENTS ALONG VERTICAL'
       READ *,NEL1
       PRINT *,'ENTER NUMBER OF ELEMENTS ALONG HORIZONTAL'
       READ *,NEL2
       PRINT *,'WILL ELEMENT NUMBERING START AT BOTTOM ? (Y/N)'
       PRINT *,'(IF NOT, WILL ASSUME TOP)'
       READ 900,ANS2
       PRINT *,'WILL NUMBERING BE HORIZONTAL ?,(Y/N)'
       PRINT *,'(IF NOT, WILL ASSUME VERTICAL)'
       READ 900,ANS3
      ENDIF
```

Attachment B (continued)

```
C   Initialize variables for solution procedure
C   Refer to documentation on DEBDF for details on these variables
C
      DO 10 I=1,15
10    INFO(I)=0
      RTOL=1.D-8
      ATOL=1.D-10
      Y(1)=0.
      T=0.
      NEQ=1
      LRW=261
      LIW=56
C vel must be changed in two places.
C       VELBC=-1.5844044D-11
C
C  Begin solution procedure loop
C
      DO 50 I=1,NNODE
        IOUT=TNODE(I)
20      CALL DEBDF(F,NEQ,T,Y,TOUT,INFO,RTOL,ATOL,IDID,RWORK
     1            ,LRW,IWORK,LIW,RPAR,IPAR)
C
        IF (IDID.EQ.-7) THEN
            INFO(1)=0
            GO TO 20
        END IF
        DUMMY=Y(1)
        CALL F (TOUT,Y(1),UPRIME,RPAR,IPAR)
        VEL2=-RPAR(1)/RPAR(2)*UPRIME
        DIFF=ABS(VEL2-VELBC)
        IF (DIFF.GT.MAXDIF) THEN
            MAXDIF=DIFF
            ZLOC=T
        END IF
        TOLD=T
        YOLD=Y(1)
        INFO(1)=1
        IF( I.EQ.1) WRITE(IOUT,1000)
        PHM=Y(1)/RHOG-T
        WRITE(IOUT,1010) T,Y(1),PHM,RPAR(1),VEL2, MAT ,MAT
50    CONTINUE
      PER=MAXDIF/VELBC*100.
      WRITE(IOUT,1020) MAXDIF,ZLOC
      WRITE(IOUT,1030) PER
C
C  Write solution file if requested
C
      OPEN (unit=19,form='unformatted',status='unknown')
      IF (ANS.EQ.YESUP.OR.ANS.EQ.YESLO) THEN
      NELEM=NEL1*NEL2
      IF (ANS2.EQ.YESUP.OR.ANS2.EQ.YESLO) THEN
          ITOP=0
      ELSE
          ITOP=NELEM+1
      ENDIF
      DO 100 J=1,NEL1
      IND2=(J-1)*2
      DO 100 I=1,NEL2
     IND3=(I-1)*2
      IF (ANS3.EQ.'Y') THEN
          IND1=ABS(ITOP - ((J-1)*NEL2+I))
      ELSE
```

Attachment B (continued)

```
            IND1=ABS(ITOP - ((I-1)*NEL1+J))
          ENDIF
          US(IND1,1)=PHOLD(IND2+1)
          US(IND1,5)=PHOLD(IND2+1)-
          US(IND1,2)=PHOLD(IND2+1)
          US(IND1,6)=PHOLD(IND2+2)
          US(IND1,8)=PHOLD(IND2+2)
          US(IND1,3)=PHOLD(IND2+3)
          US(IND1,4)=PHOLD(IND2+3)
          US(IND1,7)=PHOLD(IND2+3)
  100     CONTINUE
          PMAX=-1.0E20
          PMIN=1.0E20
          DO 110 I=1,8
          DO 110 J=1,NELEM
          PMAX=AMAX1(PMAX,US(J,I))
          PMIN=AMIN1(PMIN,US(J,I))
  110     CONTINUE
          DUMMY(3)=PMAX
          DUMMY(4)=PMIN
           WRITE(19) TIME,DUMMY,NELEM,((US(J2,I2),I2=1,8),J2=1,NELEM)
           DO 200 J=1,NELEM
           DO 200 I=1,8
           WRITE(8,210) J,I,US(J,I)
  200     CONTINUE
  210     FORMAT(2I8,D15.6)
           ENDIF
C
          CLOSE (unit=8,status='keep')
          CLOSE (unit=19,status='keep')
C
 1000     FORMAT('      Z(M)          PRESSURE      '
     1    ,'PSI          PERMEABILITY(M^2) VELOCITY(M/S)')
 1010     FORMAT(5D16.7,I2)
 1020     FORMAT(' MAX DIFF OF ',D14.6,' OCCURS AT ',D12.5)
 1030     FORMAT(' MAX PERCENT ERROR=',D14.6)
 1040     FORMAT(T7,'DATA (PRESSR(I),I=',I3,',',I3,') /')
 1050     FORMAT(15(T6,'1',1X,5(D12.6,',')/))
          END
          SUBROUTINE F (Z,U,UPRIME,RPAR,IPAR)
C
C  Z = Z-LOCATION CHOSEN BY CODE
C  U = EFFECTIVE PRESSURE
C  UPRIME dP/dz
C
C
           IMPLICIT REAL*8 (A-H,O-Z)
          COMMON /RATE/ VELBC
          DIMENSION U(1),UPRIME(1),RPAR(3),IPAR(1)
          DATA IFLAG/0/
          AMU=.01
          CALL PERM(U(1),Z,AMU,AK,PHM)


C          VELBC=-1.5844044D-11
          UPRIME(1)=-AMU*VELBC/AK
          RPAR(1)=AK
          RPAR(2)=AMU
          RPAR(3)=UPRIME(1)
          RETURN
          END
          SUBROUTINE MESH (NNODE,TNODE)
C          REAL*8 TNODE(1),ZNODE(501)
          DIMENSION TNODE(1),ZNODE(501)
C
C  Define the nodal points
C
          DATA (ZNODE(I),I=  1, 15) /
         1 0.0, 65.15,130.3,175,219.5,222,224.4,279.5,335.4,400.0,465.5
         2 485,503.6,517,530.47/
C
```

Attachment B (concluded)

```
      NNODE=15
      DO 10 I=1,NNODE
         TNODE(I)=ZNODE(I)
   10 CONTINUE
C
      RETURN
      END
      SUBROUTINE PERM (P,Z,AMU,AK,PHM)
      COMMON/MAT/MAT
C      IMPLICIT REAL*8 (A-H,O-Z)
CCCCC
CCCCC CALCULATES PERMEABILITY  (M**2)
CCCCC UNITS - KG,M,SEC.
CCCCC Materials are:
CCCCC 2 - CHz
CCCCC 3 - CHnv
CCCCC 4 - TSw2
CCCCC 5 - TSw1
CCCCC 6 - PTn
CCCCC 7 - TCw
C
      DIMENSION AF(10),ALPM(10),BETM(10)
      DIMENSION CONM(10),CONF(10)
C   ROCK PROPERTIES
      DATA(AF(I), I=2,7)/2*4.6E-5,18.0E-5,4.1E-5,2.7E-5,14.0E-5/
      DATA(ALPM(I),I=2,7)/0.00308,0.01600,0.00567,0.00567,0.015,0.00821/
      DATA(BETM(I),I=2,7)/1.602,3.872,1.798,1.798,6.872,1.558/
      DATA(CONM(I),I=2,7)/2.E-11,2.7E-07,1.9E-11,1.9E-11,3.9E-7,9.7E-12/
      DATA(CONF(I),I=2,7)/2*20.0E-5,1.7E-5,2.2E-5,61.0E-5,3.8E-5/
C  CONDUCTIVE FUNCTION STATEMENT
      CONFU(AL,AP)=(1.+AP)**(-AL/2.)*(1.-(AP/(1.+AP))**AL)**2
C  FRACTURE PROPERTIES
      THF=3.950E-2
      ALPF=1.2851
      BETF=4.22865
C
CC  Define materials according to elevation
C
       IF (Z.LE.130.3) THEN
          MAT=3
      ELSE IF (Z.GT.130.3.AND.Z.LE.335.4) THEN
          MAT=4
       ELSE IF (Z.GT.335.4.AND.Z.LE.465.5) THEN
          MAT=5
       ELSE IF (Z.GT.465.5.AND.Z.LE.503.6) THEN
          MAT=6
        ELSE
          MAT=7
        END IF
       RHOG=1000.*9.80665
       PHM=P/RHOG-Z
       IF(PHM.GT. -.000001)  PHM=-.000001
       APM=(ALPM(MAT)*(-PHM))**BETM(MAT)
       ALM=(1-1./BETM(MAT))
       APF=(ALPF*      (-PHM))**BETF
       ALF=(1-1/BETF)
       COM=CONFU(ALM,APM)*CONM(MAT)
C  NEED TO CHANGE FOR SAND
       RESULT=CONFU(ALF,APF)
       COF=RESULT*CONF(MAT)
       AK=(1-AF(MAT))*COM+AF(MAT)*COF
C NEED PERMEABILITY IN M**2
      AK=AK*AMU/RHOG
C      ak=.25e-12
      RETURN
      END
```

Attachment C

Input to the NORIA code for the Topopah Spring calculation.

Input to the NORIA code for the Calico Hills calculations.

```
$ shaft drilling water with ventilation
setup  , 1 ,51
water  , 1,1000.0,0.001,,,,9.8,variable
vapor  , 2
air    , 3
calicoz , 4,2370.,1.6,2.4,,,.4600000,1.0,,,,variable,,35,,51e4
calicov , 5,2370.,1.6,2.4,,,.4600000,1.0,,,,variable,,35,19.6
topopah2, 6,2580.,1.6,2.4,,,.110,1.0,,,,variable,,35,.1225e7
topopah1, 7,2580.,1.6,2.4,,,.1100,1.0,,,,variable,,35,.106e7
paintbsh, 8,2350.,1.6,2.4,,,.4000162,1.0,,,,variable,,35,.22352e7
tivacan , 9,2490.,1.6,2.4,,,.081288 ,1.0,,,,variable,,35,.22352e7
end
1,1,51,3, .9448, 1 , .9448 ,1
0.00,25,25,0.00
65.15,65.15,66.15,66.15
end
iloop,9,2
quad8/4,4,1,1
iend
iloop,16,2
quad8/4,5,19,1
iend
bc,peffvary,1,1,4,1
end
formkf,
output,material,all
unzipp,0.0,.315e10, 1.0e-5 ,500,,10,1e-4,.864e5,.1728e6,.6e6,.12e7,.24e7*
.157e8,.315e8,.315e9,.315e10
end
stop
stop, post
```

Attachment D

RIB and SEPDB Data

The values of the material properties in Reference 3 were taken from the RIB. For the matrix porosity, the values were within the range contained in the RIB, except for the Calico Hills unit for which a value 0.01 larger than the range was used. The values of matrix porosity selected were based on R. R. Peters et al., 1984, "Fracture and Matrix Hydrologic Characteristics of Tuffaceous Materials from Yucca Mountain, Nye County, Nevada," SAND84-1471, Sandia National Laboratories, Albuquerque, New Mexico.

This report contains no candidate information for the RIB.

This report contains no candidate data for inclusion in the SEPDB.

APPENDIX D

SLTR88-3001

SATURATION PULSE IMBIBITION EXPERIMENT

SLTR88-3001
Department 6310 Letter Report
Sandia National Laboratories
Nevada Nuclear Waste Storage
Investigations Project
Issued February 1988

SATURATION PULSE IMBIBITION EXPERIMENT

A. J. Russo and J. A. Lewin

Introduction

The purpose of this experiment was to obtain data relevant to the movement of water into tuff when a short (100 min) pulse of water pressure is applied to the end surface of a core sample and then allowed to isothermally redistribute itself. The response of the hydrological conditions (primarily matrix saturation) to a saturation pulse can be used to estimate the response of larger configurations, such as a repository, to temporary flooding conditions such as in wet mining operations. In addition, this information can be used in the design of future hydrologic experiments.

Description of the Experiment

A cylindrical welded tuff core (Busted Butte 10-F), which was 26.7 cm long and 5.08 cm in diameter and had not previously been used in any other experiments, was initially found to weigh 1248.9 g. The round surface of the core was completely covered by a Kynar sleeve and sealed near each end. The core was installed in a cylindrical pressure vessel having access ports at each end of the core, so that a confining pressure (1.5 MPa) could be applied to the Kynar sleeve to prevent movement of water across any surfaces except the core ends (Figure 1). A traversible gamma-beam densitometer was calibrated [1] and positioned to scan along the centerline of the core in 0.635-cm increments. Data was taken before, during, and after the application of the water pulse (0.2 MPa) to the top of the core while the bottom of the core was maintained at atmospheric pressure. The data was stored on 7-in. floppy disks in files INTERM.112 through INTERM.137.[a] After 21 days, the change in subsequent readings was well below the noise level of the measurements and the test was stopped.

The temperature of the pressure vessel and its contents was raised to 40 ± 3°C and a vacuum (< 0.005 MPa) was applied to the core ends for 14

[a]All INTERM data files will be stored at the NNWSI records center in file 51/L07-12/04/85/Q3.

days in order to dry it out. When gamma-beam measurements were no longer changing a scan (INTERM.145) was taken and assumed to be the dry reference scan used in subsequent data reduction. To obtain the saturated scan, water pressure (≈0.41 MPa) was reapplied to the top of the core and gamma-beam scans were taken for 85 days. It was found that only half of the core had saturated and the movement of the front was extremely slow. To saturate the core, the pressure at the top was raised to 6.1 MPa (equal to the confining pressure) for 23 days.

Although the gamma-beam indicated the saturation front had reached the end of the core near November 6, 1987, about 16 days after the pressure was raised, no water was observed to be leaving the core. Estimates of the amount of water that should have left the core, based on the movement of the front before it reached the end, indicated that a measurable amount (≈1 cc/day) should have been observed. Because a measurement of hydraulic conductivity was planned from the measured water flux, this portion of the experiment could not be completed. It appears that the capillary pressure near the core end may have been greater than the applied pressure, and it was not possible to force water completely out of the rock. After seven days of no observed flow, an attempt was made to reverse the pressure gradient to see if water could flow in the reverse direction (from bottom to top) but in the process of relieving the core pressure there was apparently some movement of the core and the seal between the core, and the confining pressure cavity developed a leak. The conductivity portion of the experiment was terminated at that point. Because the applied pressure was changed during the imbibition portion of the experiment, a saturated reference file was made up from a combination of INTERM.194 (for $x/L > 0.6$) and INTERM.206 (for $x/L < 0.6$).

The core was removed from the pressure vessel and weighed on January 25, 1988, and found to be 1300.8 g. This was taken to be the saturated value. After bake-out of 1 wk at 40°C and 1 wk at 100°C, the core was found to weigh 1245.2 g. The difference of 55.6 g was compared to the core total volume of 541.16 cc and, assuming a water density of 1 g/cc, corresponds to an average porosity of 0.1027. The initial weight of the core was 1248.9 g and corresponds to an initial saturation of 6.65%. The

average porosity of the core from the gamma-beam measurements was 0.1037, which differs from the weight-derived value by 1.0%.

Results

The gamma-beam count rate data was corrected for electronic drift by comparisons with a reference count rate and was used to calculate the diameter-averaged core porosity and the saturation (as in Reference 2) for various times during the experiment. Figure 2 shows the porosity values obtained from the saturated and dry reference scans used.

The calculated saturation values are estimated to be accurate to ± 0.03. Figure 3 shows the initial saturation profile, and Figures 4-8 show the saturation in the upper 2.6 cm of the core for the first 2 hr of the experiment. Scans were only taken over that portion of the core because a full scan (42 points) required more than an hour to complete and it was expected that nothing of interest would occur outside the region adjacent to the saturation pulse during this time period. The core saturation, averaged over the top 0.635 cm of the core, was found to peak near 0.7 at 80 min after the start of the pulse.

Figures 9-13 show the saturation over the whole core at various times to 21 days when the pulse portion of the experiment was terminated. It is clear that the water is slowly diffusing into the core. Calculations performed by R. R. Eaton, with the code NORIA, to simulate this experiment gave good agreement with the saturation values obtained, for assumed conditions of initial saturation = 0.05, residual saturation = 0.0194, porosity = 0.109, hydraulic conductivity = 0.53 E-11 m/s, and Van Genuchten coefficient values of α = 0.0227 and β = 1.624. These values were supplied by J. H. Gauthier, 6312, as representing typical properties of Busted Butte core of the type tested.

Similar calculations for the imbibition portion of the experiment, with a constant applied water pressure of 0.413 MPa at one end of the core, showed a saturation front movement that was slightly faster than the

observed front. After seven weeks, the calculated S = 0.5 location was x/L = 0.47 and the measured value of x/L was 0.39, a 17% difference. The observed value of porosity, shown in Figure 2, is slightly lower than the 0.109 value used in the calculation, so that the hydraulic conductivity estimate used in the calculation is probably slightly too high.

In a previous imbibition experiment[2] a saturation precursor wave at approximately the 10% level was observed and it was postulated that a vapor front moved through the rock at a faster rate than the liquid front and sorbed on the rock. During this experiment, there was a considerable amount of scatter in the data at the 10% level from unknown causes but nothing that could be reasonably interpreted as a sorbing precursor was observed. One significant difference in the initial conditions of the two experiments was that the first experiment involved water flowing into an evacuated core from both ends, whereas the present experiment used a core at atmospheric pressure with one end open to atmosphere and capable of passing gas or vapor either way. A gas compression flow therefore must precede the liquid front and this flow could redistribute any moisture that is present in the downstream pore spaces. This may be a partial contributor to the larger than expected data scatter in that region.

Conclusions

Measurements of the saturation of welded tuff core, subjected to a rapid (100 min) pulse of water at the surface, show that very little penetration takes place during the pulse and that diffusion into the core at later times is very slow.

References

1. A. J. Russo and D. C. Reda, "Drying of an Initially Saturated Fractured Volcanic Tuff," ASME Winter Meeting, December 13-18, 1987, Boston, MA.

2. D. C. Reda, "Influence of Transverse Microfracture on the Imbibition of Water into Initially Dry Tuffaceous Rock," AGU Fall Meeting, San Francisco, December 1986.

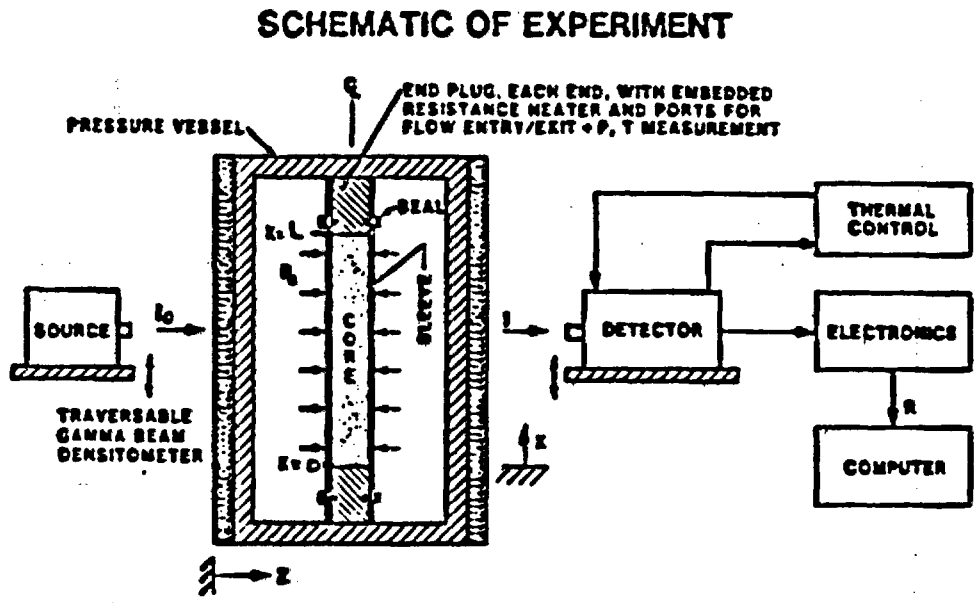

boundary conditions: confining pressure > 1.3 MPa
$0 < x < L$: no flux condition
$x = L$: water pressure = 0.2 MPa from time $t = 0$ to $t = 100$ minutes;
no liquid flux condition for $t > 100$ minutes
air pressure = 1 atm
$x = 0$: no liquid flux condition for $t > 0$
air pressure = 1 atm

Figure 1. A Schematic of the Experiment Geometry.

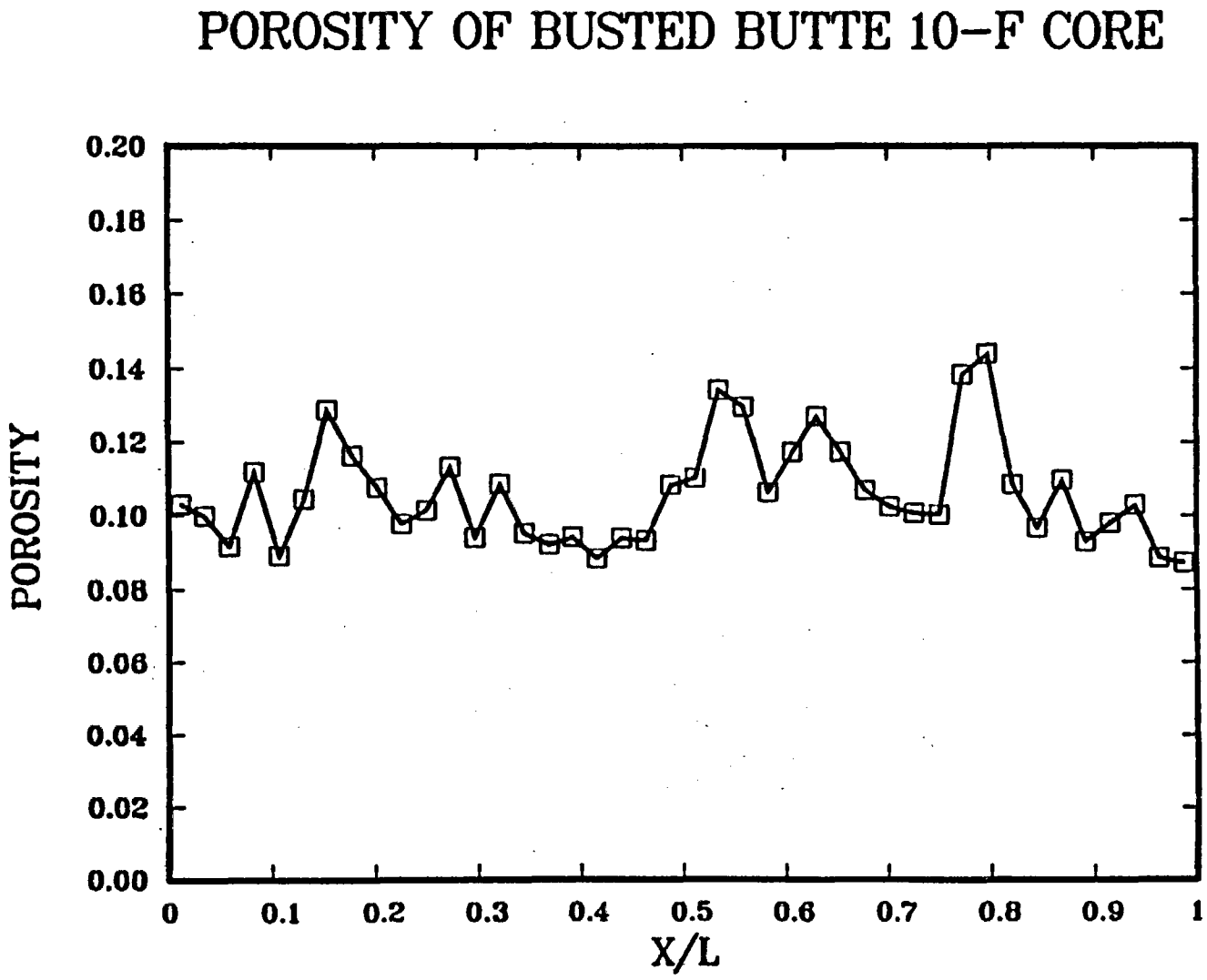

Figure 2. Porosity of the Busted Butte 10-F Core

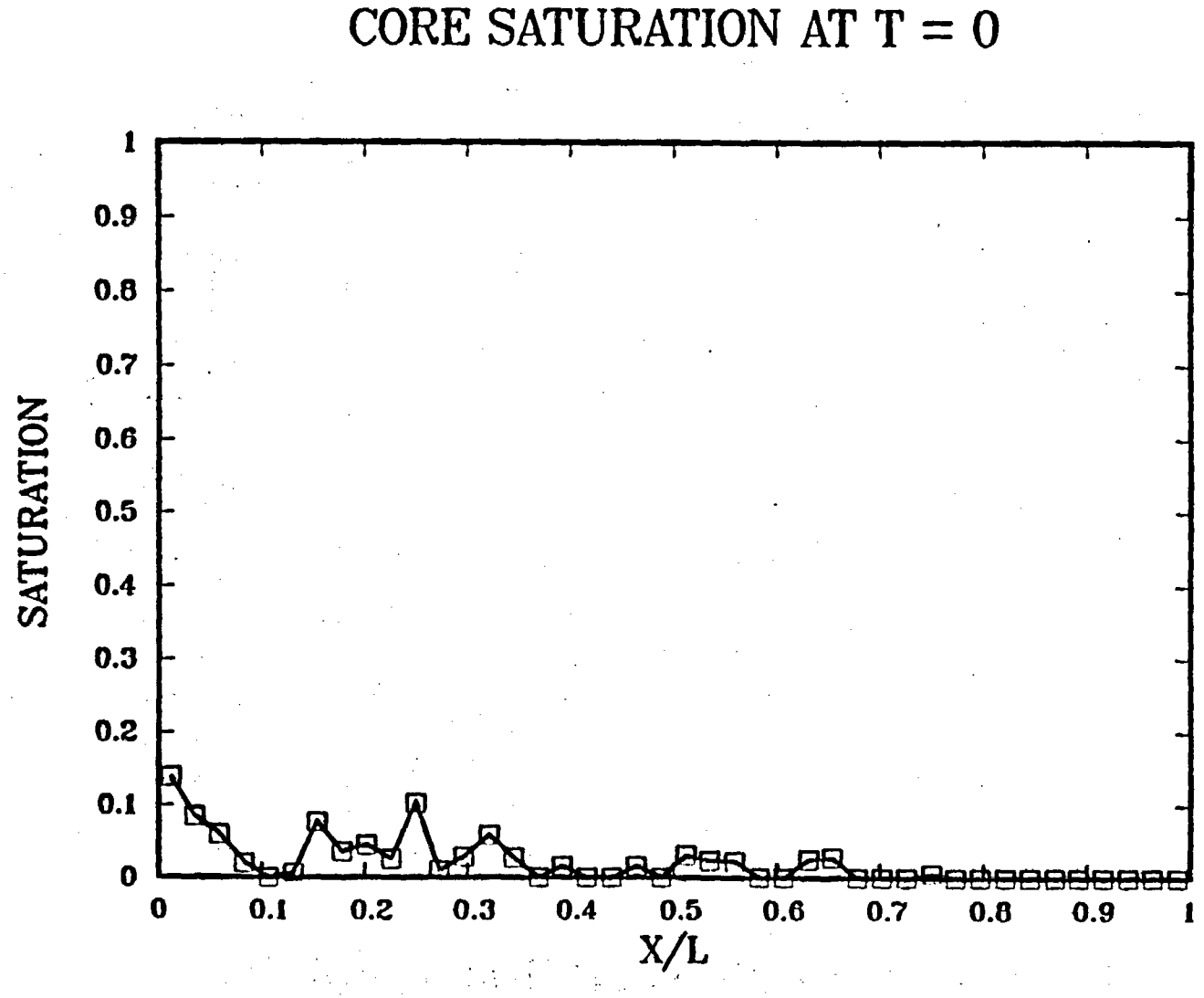
CORE SATURATION AT T = 0
SATURATION
1
0.9
0.8
0.7
0.6
0.5
0.4
0.3
0.2
0.1
0
0
0.1
0.2
0.3
0.4
0.5
0.6
0.7
0.8
0.9
1
X/L

Figure 3.

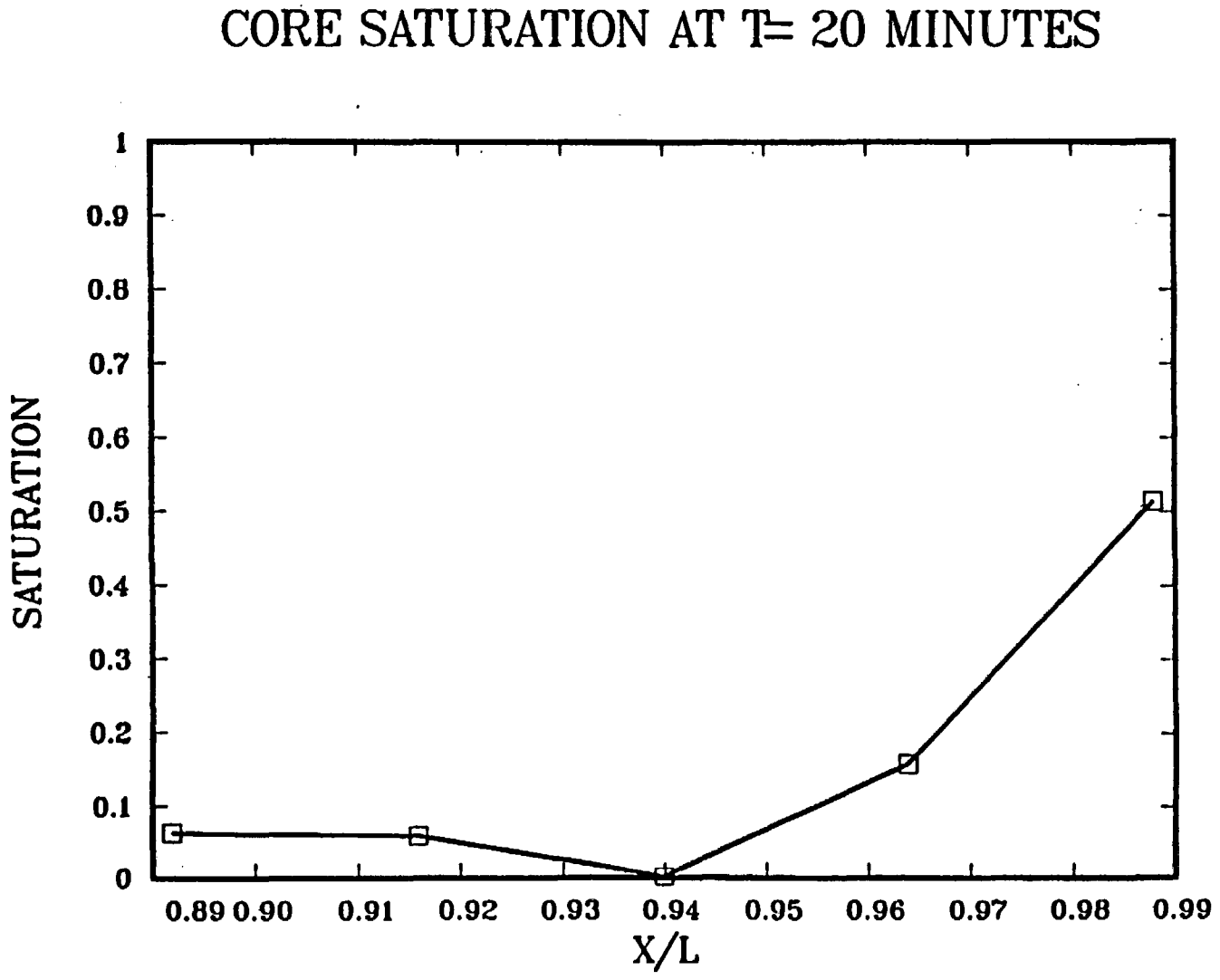
CORE SATURATION AT T= 20 MINUTES
SATURATION
1
0.9
0.8
0.7
0.6
0.5
0.4
0.3
0.2
0.1
0
0.89 0.90 0.91 0.92 0.93 0.94 0.95 0.96 0.97 0.98 0.99
X/L

Figure 4.

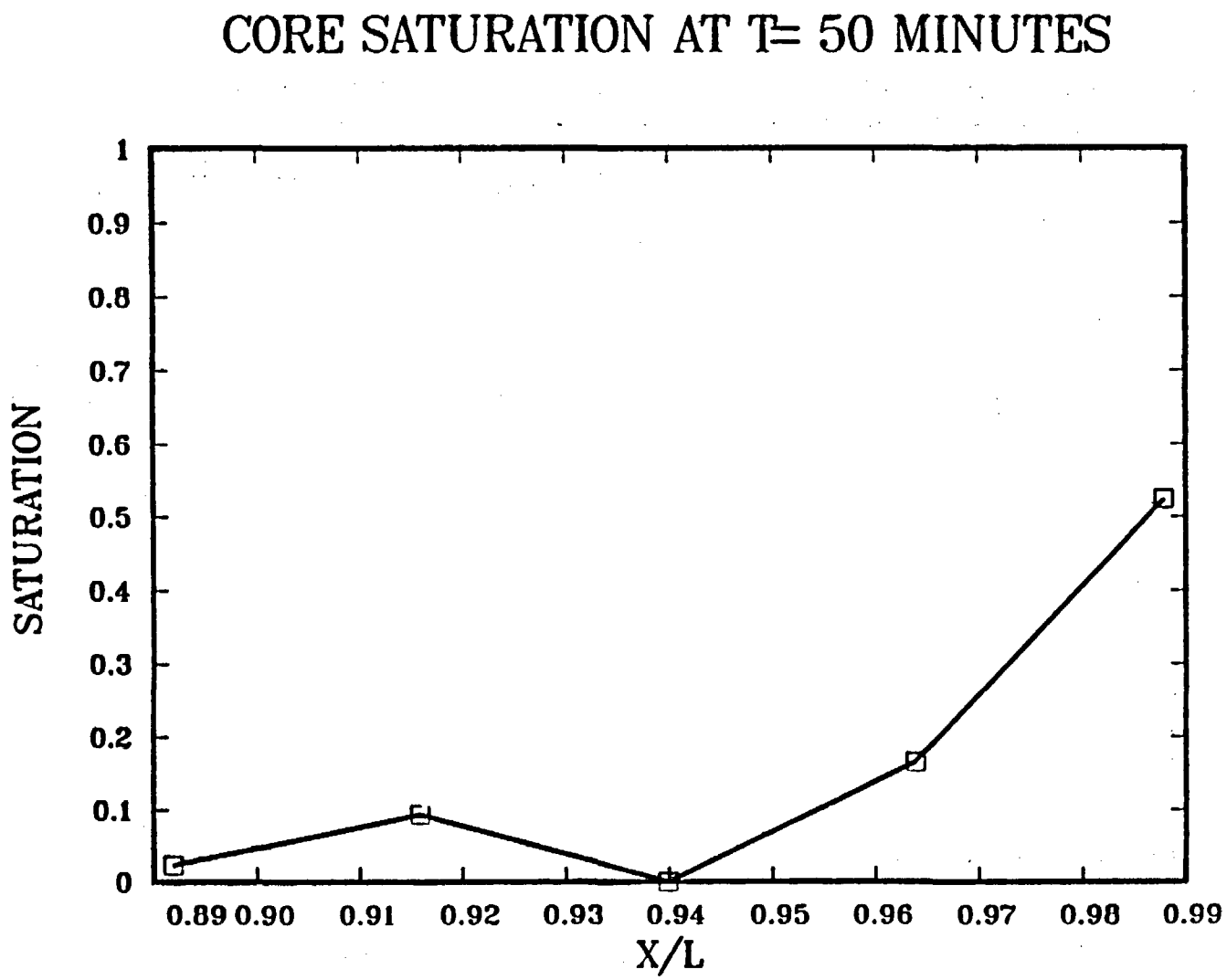
CORE SATURATION AT T= 50 MINUTES
SATURATION
1
0.9
0.8
0.7
0.6
0.5
0.4
0.3
0.2
0.1
0
0.89 0.90 0.91 0.92 0.93 0.94 0.95 0.96 0.97 0.98 0.99
X/L

Figure 5.

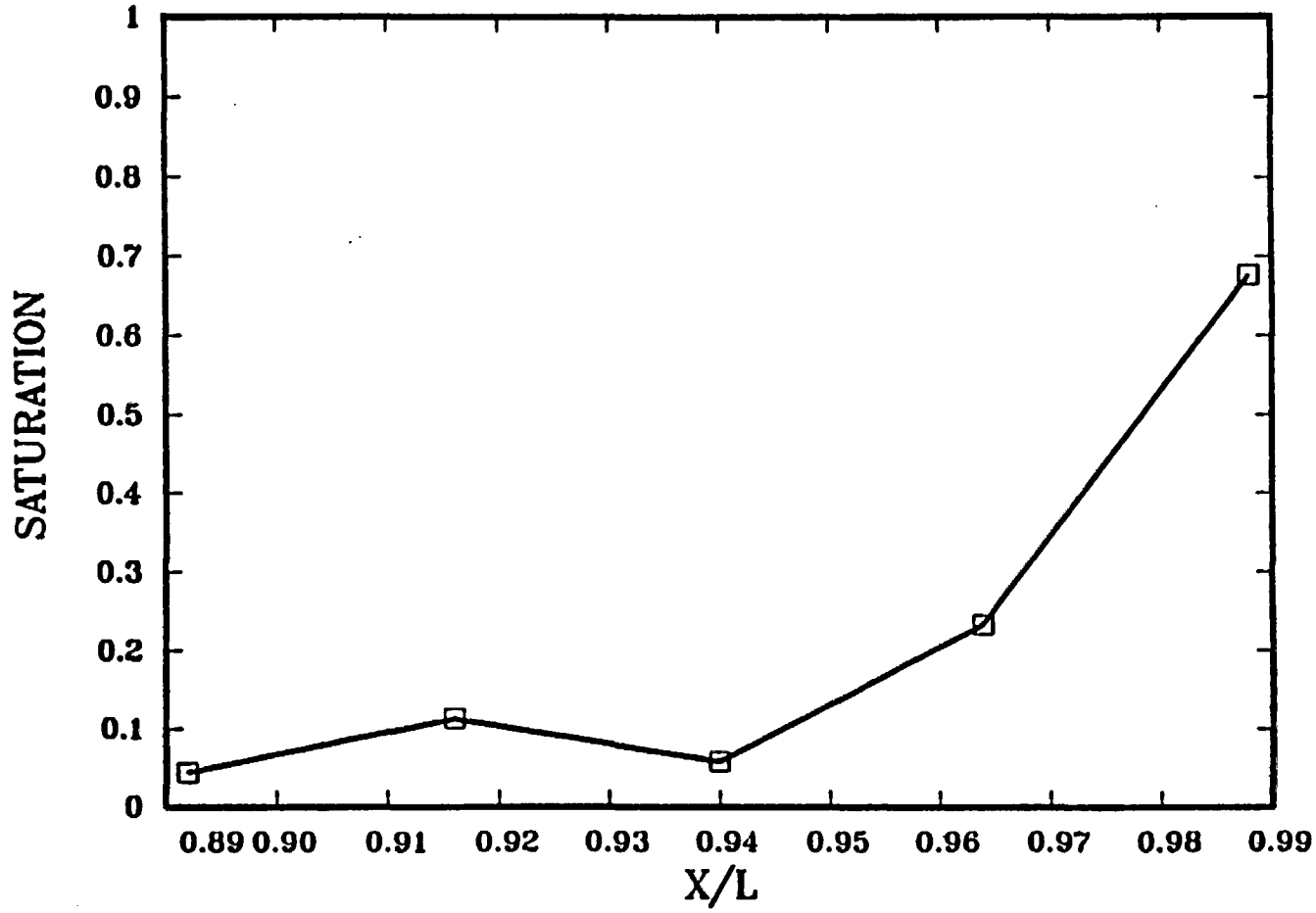
CORE SATURATION AT T = 80 MINUTES
SATURATION
1
0.9
0.8
0.7
0.6
0.5
0.4
0.3
0.2
0.1
0
0.89 0.90 0.91 0.92 0.93 0.94 0.95 0.96 0.97 0.98 0.99
X/L

Figure 6.

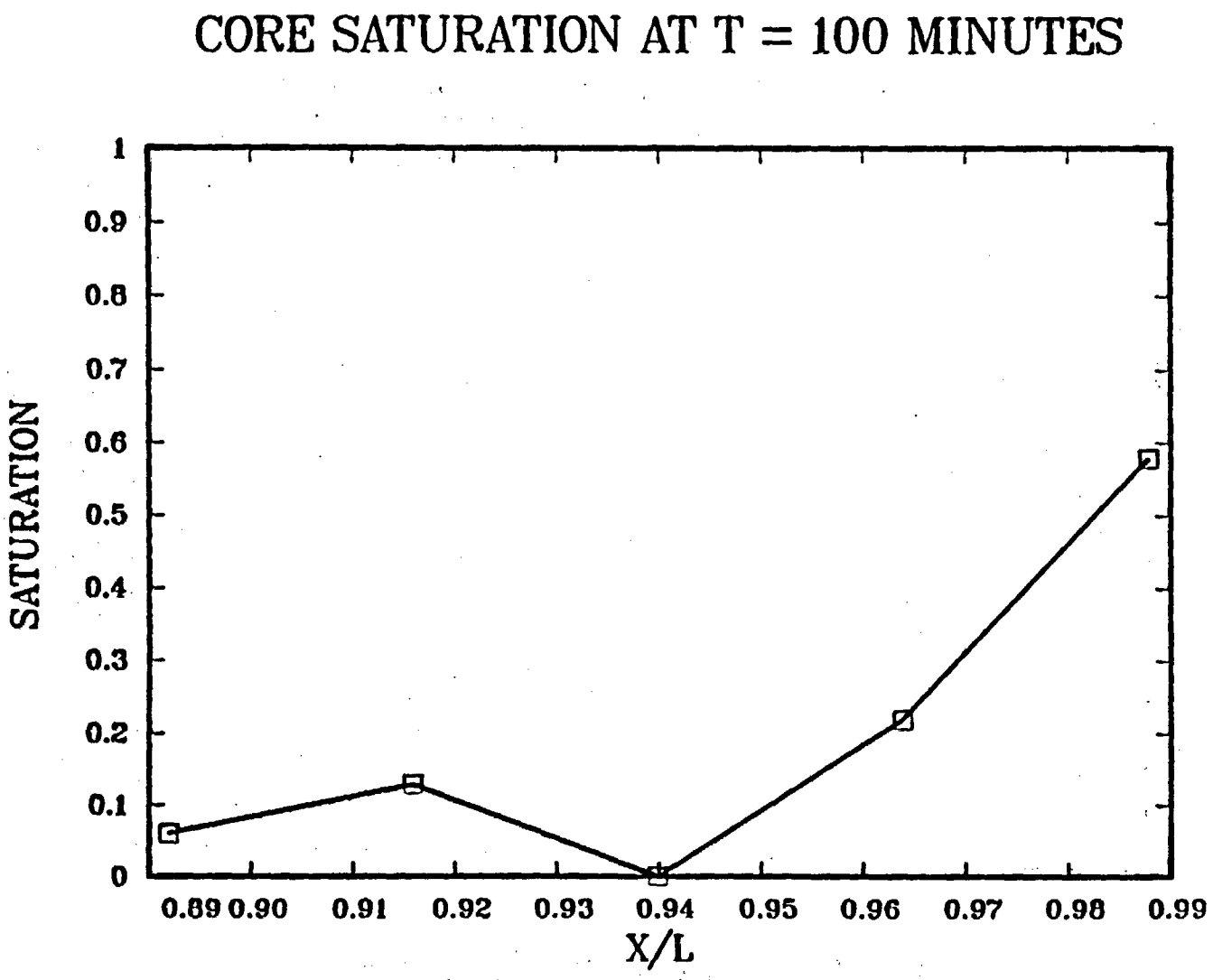
CORE SATURATION AT T = 100 MINUTES
SATURATION
1
0.9
0.8
0.7
0.6
0.5
0.4
0.3
0.2
0.1
0
0.89 0.90 0.91 0.92 0.93 0.94 0.95 0.96 0.97 0.98 0.99
X/L

Figure 7.

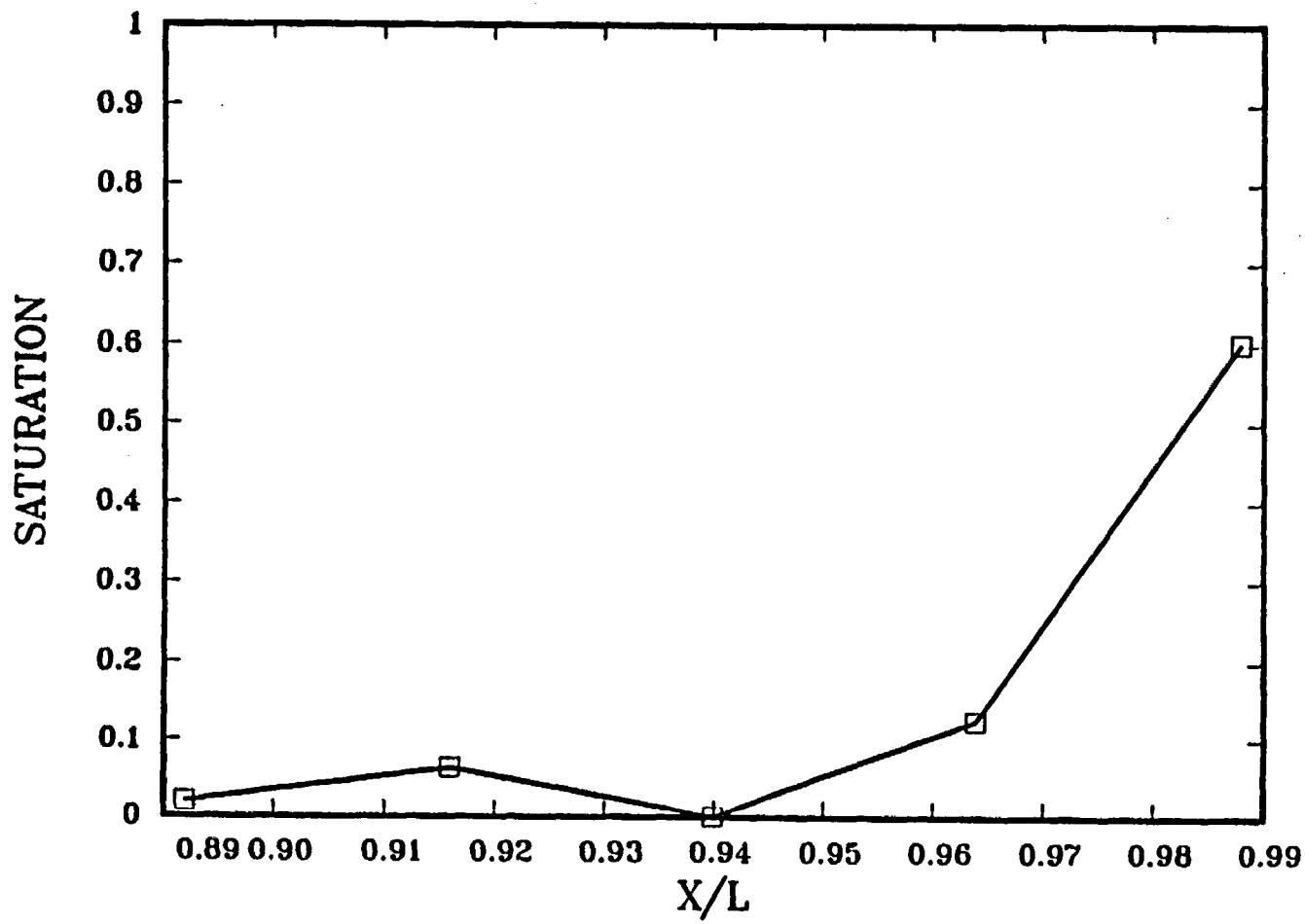
CORE SATURATION AT T = 2 HOURS
SATURATION
1
0.9
0.8
0.7
0.6
0.5
0.4
0.3
0.2
0.1
0
0.89 0.90 0.91 0.92 0.93 0.94 0.95 0.96 0.97 0.98 0.99
X/L

Figure 8.

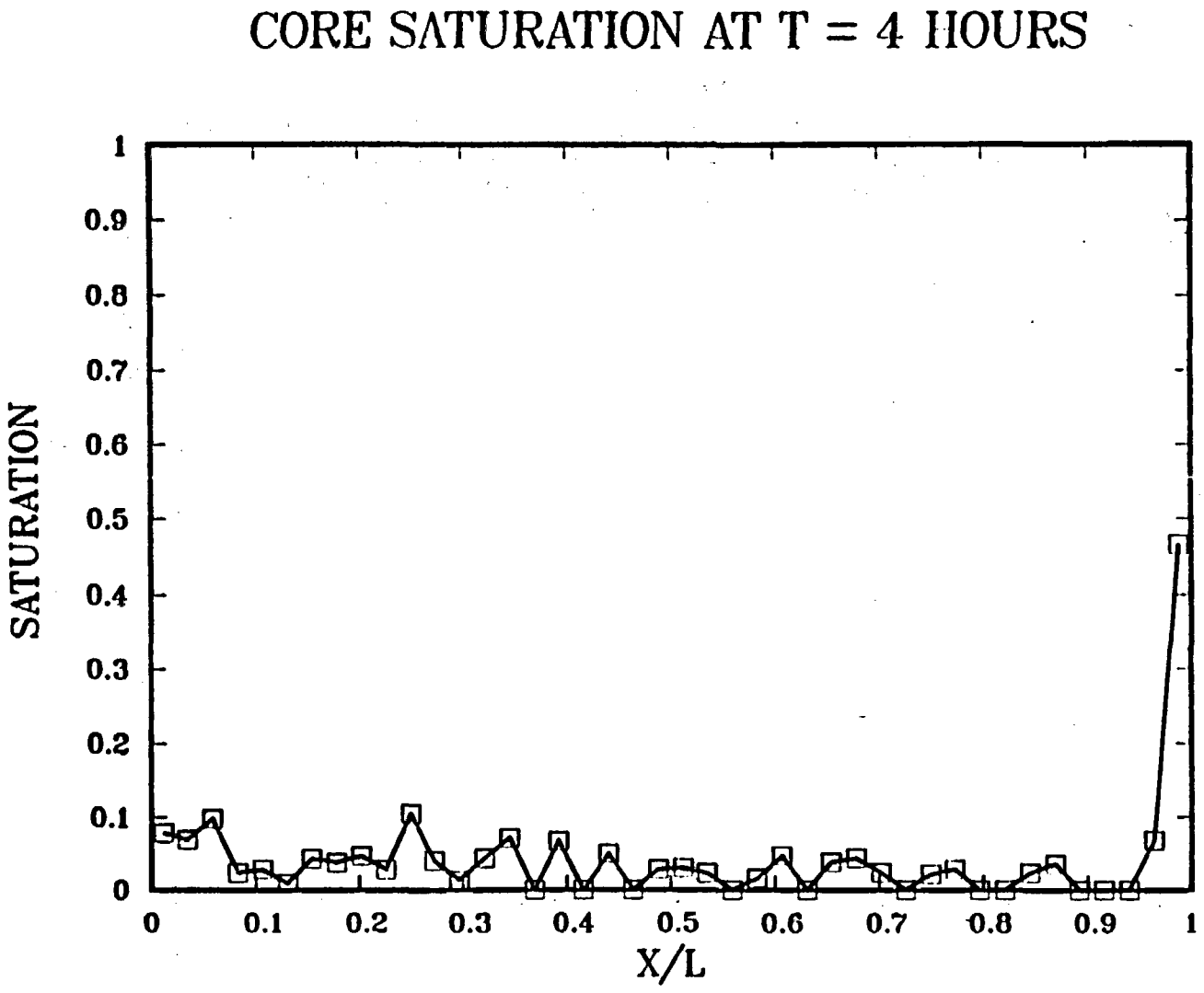
CORE SATURATION AT T = 4 HOURS
SATURATION
1
0.9
0.8
0.7
0.6
0.5
0.4
0.3
0.2
0.1
0
0
0.1
0.2
0.3
0.4
0.5
0.6
0.7
0.8
0.9
1
X/L

Figure 9.

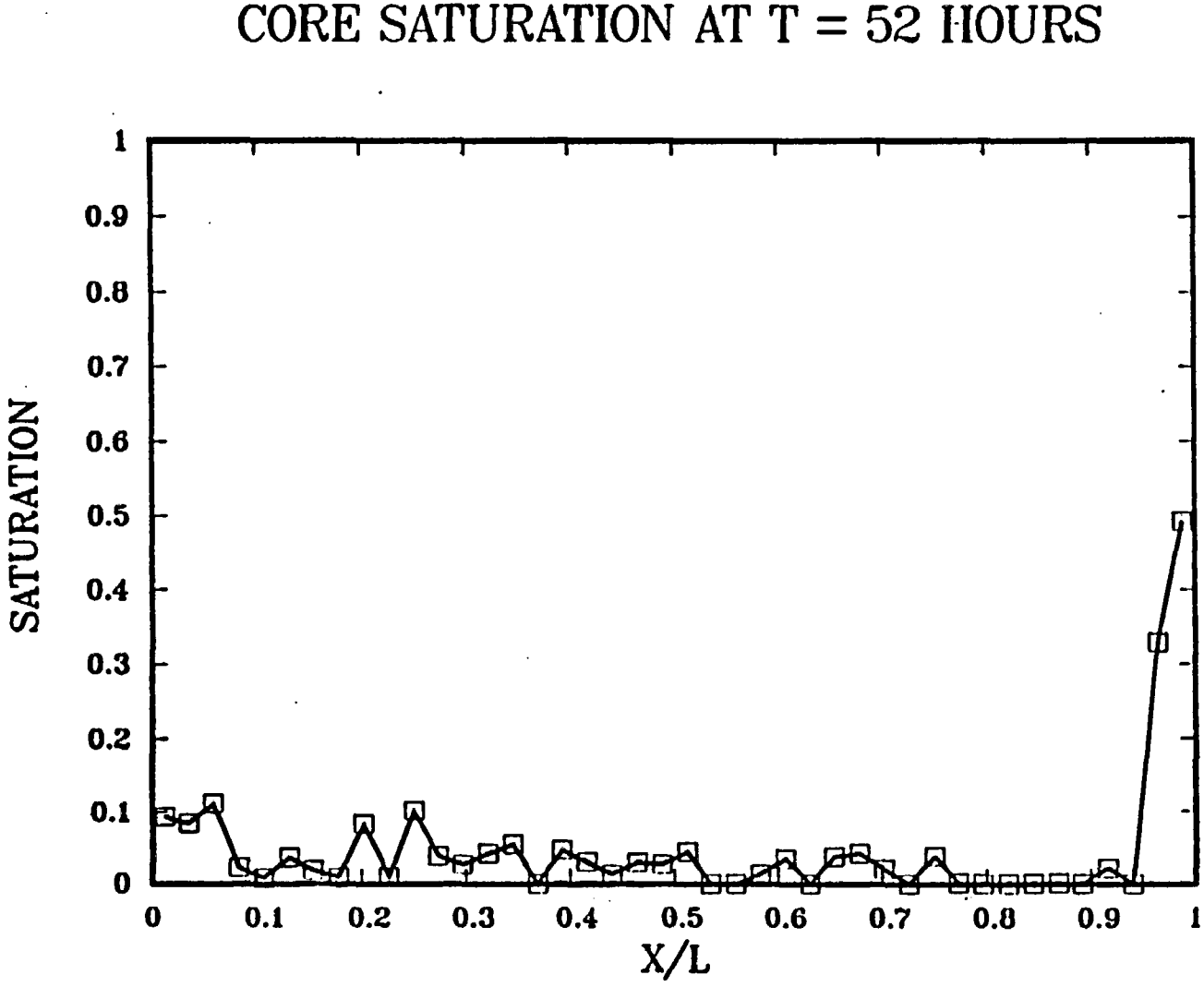
CORE SATURATION AT T = 52 HOURS
SATURATION
1
0.9
0.8
0.7
0.6
0.5
0.4
0.3
0.2
0.1
0
0
0.1
0.2
0.3
0.4
0.5
0.6
0.7
0.8
0.9
1
X/L

Figure 10.

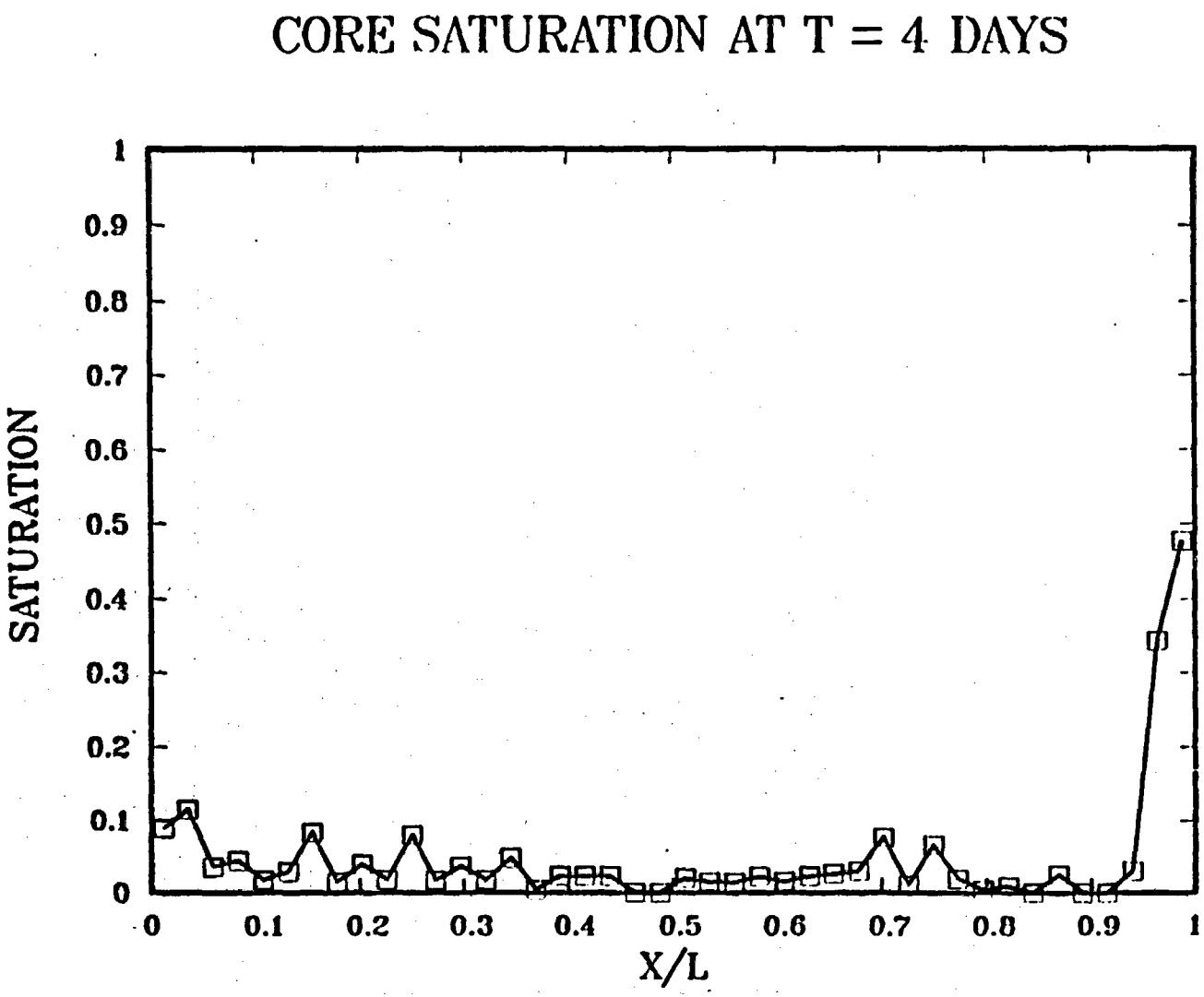
CORE SATURATION AT T = 4 DAYS
SATURATION
1
0.9
0.8
0.7
0.6
0.5
0.4
0.3
0.2
0.1
0
0
0.1
0.2
0.3
0.4
0.5
0.6
0.7
0.8
0.9
1
X/L

Figure 11.

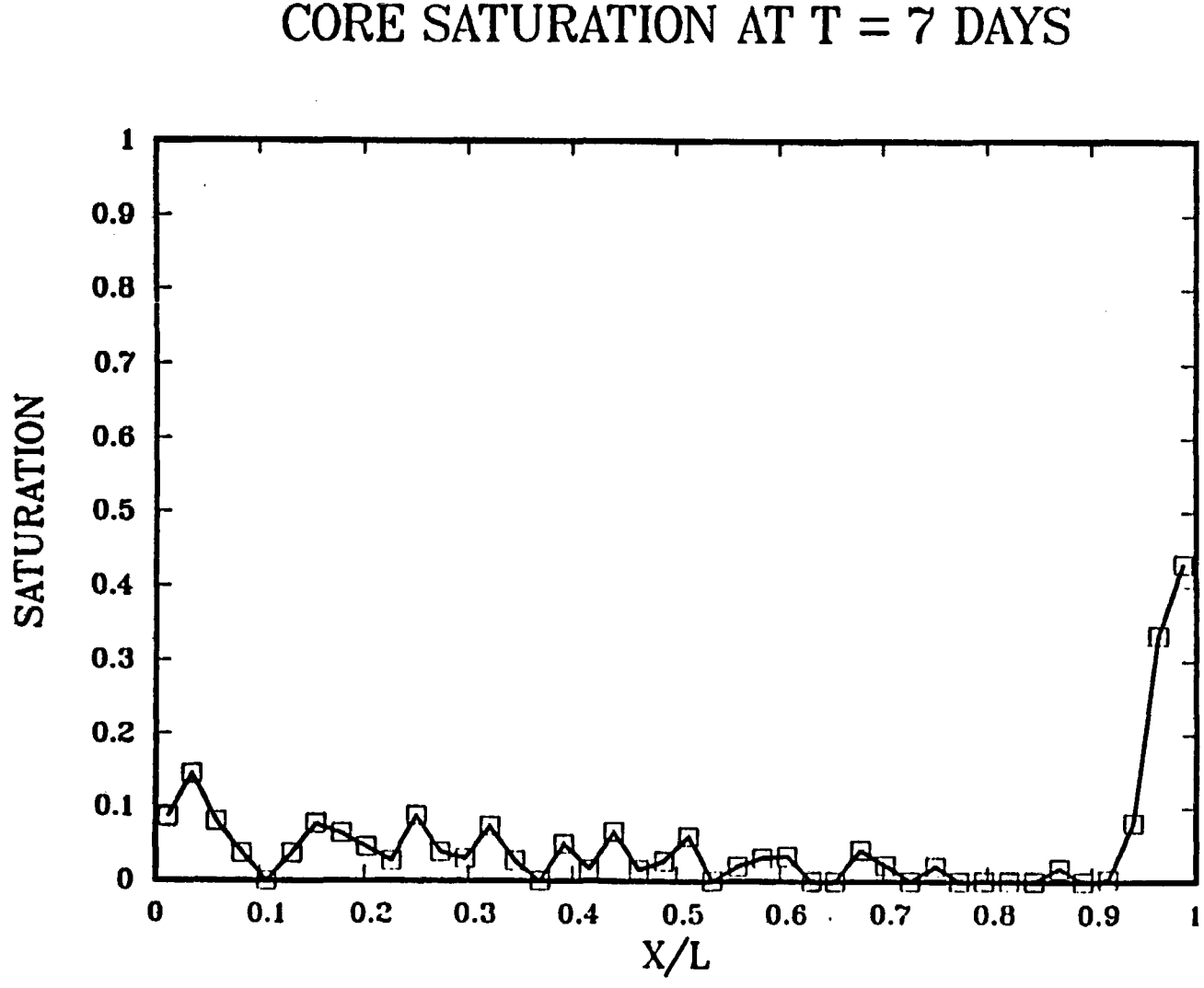
CORE SATURATION AT T = 7 DAYS
SATURATION
1
0.9
0.8
0.7
0.6
0.5
0.4
0.3
0.2
0.1
0
0
0.1
0.2
0.3
0.4
0.5
0.6
0.7
0.8
0.9
1
X/L

Figure 12.

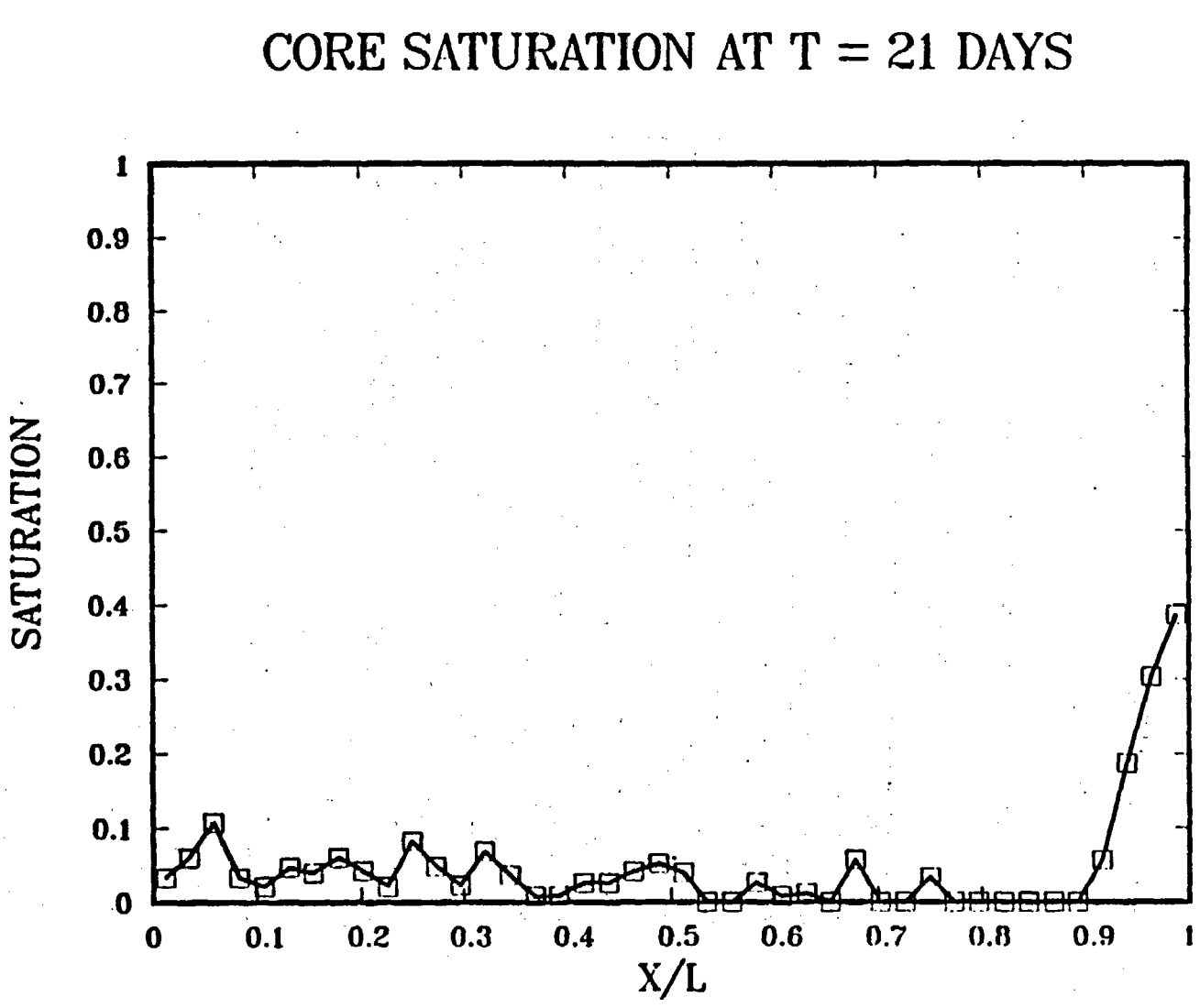
CORE SATURATION AT T = 21 DAYS
SATURATION
1
0.9
0.8
0.7
0.6
0.5
0.4
0.3
0.2
0.1
0
0
0.1
0.2
0.3
0.4
0.5
0.6
0.7
0.8
0.9
1
X/L

Figure 13.

ATTACHMENT A

RIB and SEPDB Data

This letter report contains the following data that is considered candidate information for inclusion in the SEPDB:

SAMPLE IDENTIFICATION	PROPERTY VALUE
Busted Butte Rock #10, ID 10-F	Porosity = 0.104

This letter report contains no information for inclusion in the RIB.

BULK PROPERTIES DATA COMPILATION FORM
FOR THE NNWSI PROJECT SEPDB

PART 1. SAMPLE LOCATION AND IDENTIFICATION

SAMPLE ID: BB Rock # 10-F — SAMPLE ORIGIN: Busted Butte Rock #10

SAMPLE INTERVAL (ft): N/A — TEST #: 1

PART 2. PARAMETERS

SATURATED BULK DENSITY [SBD] (g/cm^3)[a]	ESTIMATED SBD UNCERTAINTY (g/cm^3)[a]	NATURAL STATE BULK DENSITY [NSBD] (g/cm^3)[a]	ESTIMATED NSBD UNCERTAINTY (g/cm^3)[a]
N/D	N/A	N/D	N/A

DRY BULK DENSITY [DBD] (g/cm^3)[a]	ESTIMATED DBD UNCERTAINTY (g/cm^3)[a]	GRAIN DENSITY [GD] (g/cm^3)[a]	ESTIMATED GD UNCERTAINTY (g/cm^3)[a]
N/D	N/A	N/D	N/A

POROSITY (%)	ESTIMATED POROSITY UNCERTAINTY (%)
0.104	0.003

PART 3. EXPERIMENT CONDITIONS

GD EXPERIMENT TECHNIQUE	TYPE OF POROSITY	POROSITY CALCULATED USING:	BULK DENSITY TECHNIQUE
N/A	Matrix	Gamma-Beam Attenuation	N/A

SBD SAMPLE MASS (g)	NSBD SAMPLE MASS (g)	DBD SAMPLE MASS (g)	GD SAMPLE MASS (g)
N/A	N/A	N/A	N/A

PART 4. REFERENCE AND SUPPORTING INFORMATION

QA LEVEL OF DATA-GATHERING ACTIVITY: 3 — SNL NNWSI PROJECT DATA SET ID: 51/L07-12/4/85 — SNL DATA REPORT NUMBER: SAND88-2938

THIS DCF COMPLETED BY: E. A. Klevetter (Name) — 6313 (SNL Div.) — 3/20/88 (Date)

a. To convert g/cm^3 to kg/m^3, multiply by 1.000 E+03.

COMMENTS:

Unless noted, test conditions for temperature and pressure are ambient.

N/A = not applicable, N/C = not compiled, N/D = no data available, TBD = to be determined.

Nominal Sample Dimensions: 28.7 cm long; 5.08 cm diameter with cylindrical geometry.

Data originally reported in SLTR88-3001.

APPENDIX E

Reference Information Base and Site Engineering Properties Data Base

This report contains no information for inclusion in the RIB.

This report contains the following data that is considered candidate information for inclusion in the SEPDB (from attached).

Busted Butte Rock number 10-F has a porosity value of 0.104.

DISTRIBUTION

Samuel Rousso, Acting Director (RW-1)
Office of Civilian Radioactive
Waste Management
U.S. Department of Energy
Forrestal Bldg.
Washington, D.C. 20585

Ralph Stein (RW-30)
Office of Civilian Radioactive
Waste Management
U.S. Department of Energy
Forrestal Bldg.
Washington, D.C. 20585

M. W. Frei (RW-22)
Office of Civilian Radioactive
Waste Management
U.S. Department of Energy
Forrestal Bldg.
Washington, D.C. 20585

B. G. Gale (RW-23)
Office of Civilian Radioactive
Waste Management
U.S. Department of Energy
Forrestal Bldg.
Washington, D.C. 20585

F. G. Peters (RW-10)
Office of Civilian Radioactive
Waste Management
U.S. Department of Energy
Forrestal Bldg.
Washington, D.C. 20585

J. D. Saltzman (RW-20)
Office of Civilian Radioactive
Waste Management
U.S. Department of Energy
Forrestal Bldg.
Washington, D.C. 20585

S. J. Brocoum (RW-221)
Office of Civilian Radioactive
Waste Management
U.S. Department of Energy
Forrestal Bldg.
Washington, D.C. 20585

V. J. Cassella (RW-123)
Office of Civilian Radioactive
Waste Management
U.S. Department of Energy
Forrestal Bldg.
Washington, D.C. 20585

S. H. Kale (RW-20)
Office of Civilian Radioactive
Waste Management
U.S. Department of Energy
Forrestal Bldg.
Washington, D.C. 20585

T. H. Isaacs (RW-40)
Office of Civilian Radioactive
Waste Management
U.S. Department of Energy
Forrestal Bldg.
Washington, D.C. 20585

D. H. Alexander (RW-332)
Office of Civilian Radioactive
Waste Management
U.S. Department of Energy
Forrestal Bldg.
Washington, D.C. 20585

C. Bresee (RW-10)
Office of Civilian Radioactive
Waste Management
U.S. Department of Energy
Forrestal Bldg.
Washington, D.C. 20585

Gerald Parker (RW-333)
Office of Civilian Radioactive
Waste Management
U.S. Department of Energy
Forrestal Bldg.
Washington, D.C. 20585

Chief, Repository Projects Branch
Division of Waste Management
U.S. Nuclear Regulatory Commission
Washington, D.C. 20555

NTS Section Leader
Repository Project Branch
Division of Waste Management
U.S. Nuclear Regulatory Commission
Washington, D.C. 20555

Document Control Center
Division of Waste Management
U.S. Nuclear Regulatory Commission
Washington, D.C. 20555

Carl P. Gertz, Project Manager (5)
Yucca Mountain Project Office
Nevada Operatons Office
U.S. Department of Energy
Mail Stop 523
P.O. Box 98518
Las Vegas, NV 89193-8518

J. L. Fogg (12)
Technical Information Office
Nevada Operations Office
U.S. Department of Energy
P.O. Box 98518
Las Vegas, NV 89193-8518

C. L. West, Director
Office of External Affairs
U.S. Department of Energy
Nevada Operations Office
P.O. Box 98518
Las Vegas, NV 89193-8518

W. M. Hewitt, Program Manager
Roy F. Weston, Inc.
955 L'Enfant Plaza, Southwest
Suite 800
Washington, D.C. 20024

Technical Information Center
Roy F. Weston, Inc.
955 L'Enfant Plaza, Southwest
Suite 800
Washington, D.C. 20024

L. D. Ramspott (3)
Technical Project Officer for YMP
Lawrence Livermore National
Laboratory
Mail Stop L-204
P.O. Box 808
Livermore, CA 94550

M. E. Spaeth
Technical Project Officer for YMP
Science Applications International
Corp.
101 Convention Center Dr.
Suite 407
Las Vegas, NV 89109

H. N. Kalia
Exploratory Shaft Test Manager
Los Alamos National Laboratory
Mail Stop 527
101 Convention Center Dr.
Suite P230
Las Vegas, NV 89109

D. T. Oakley (4)
Technical Project Officer for YMP
Los Alamos National Laboratory
N-5, Mail Stop J521
P.O. Box 1663
Los Alamos, NM 87545

L. R. Hayes (6)
Technical Project Officer for YMP
U.S. Geological Survey
P.O. Box 25046
421 Federal Center
Denver, CO 80225

K. W. Causseaux
NHP Reports Chief
U.S. Geological Survey
P.O. Box 25046
421 Federal Center
Denver, CO 80225

R. V. Watkins, Chief
Project Planning and Management
U.S. Geological Survey
P.O. Box 25046
421 Federal Center
Denver, CO 80225

Center for Nuclear Waste
Regulatory Analyses
6220 Culebra Road
Drawer 28510
San Antonio, TX 78284

R. L. Bullock
Technical Project Officer for YMP
Fenix & Scisson, Inc.
Mail Stop 403
101 Convention Center Dr.
Suite 320
Las Vegas, NV 89109-3265

James C. Calovini
Technical Project Officer for YMP
Holmes & Narver, Inc.
101 Convention Center Dr.
Suite 860
Las Vegas, NV 89109

Dr. David W. Harris
YMP Technical Project Officer
Bureau of Reclamation
P.O. Box 25007 Bldg. 67
Denver Federal Center
Denver, CO 80225-0007

M. D. Voegele
Science Applications International Corp.
101 Convention Center Dr.
Suite 407
Las Vegas, NV 89109

J. A. Cross, Manager
Las Vegas Branch
Fenix & Scisson, Inc.
P.O. Box 93265
Mail Stop 514
Las Vegas, NV 89193-3265

P. T. Prestholt
NRC Site Representative
1050 East Flamingo Road
Suite 319
Las Vegas, NV 89109

A. E. Gurrola, General Manager
Energy Support Division
Holmes & Narver, Inc.
P.O. Box 93838
Mail Stop 580
Las Vegas, NV 89193-3838

A. M. Sastry
Technical Project Officer for YMP
MAC Technical Services
Valley Bank Center
101 Convention Center Drive
Suite P-113
Las Vegas, NV 89109

B. L. Fraser, General Manager
Reynolds Electrical & Engineering Co.
P.O. Box 98521
Mail Stop 555
Las Vegas, NV 89193-8521

P. K. Fitzsimmons, Director
Health Physics & Environmental Division
Nevada Operations Office
U.S. Department of Energy
P.O. Box 98518
Las Vegas, NV 89193-8518

Robert F. Pritchett
Technical Project Officer for YMP
Reynolds Electrical & Engineering Co.
Mail Stop 615
P.O. Box 98521
Las Vegas, NV 89193-8521

Elaine Ezra
YMP GIS Project Manager
EG&G Energy Measurements, Inc.
P.O. Box 1912
Mail Stop H-02
Las Vegas, NV 89125

SAIC-T&MSS Library (2)
Science Applications International Corp.
101 Convention Center Dr.
Suite 407
Las Vegas, NV 89109

Dr. Martin Mifflin
Desert Research Institute
Water Resource Center
2505 Chandler Avenue
Suite 1
Las Vegas, NV 89120

E. P. Binnall
Field Systems Group Leader
Building 50B/4235
Lawrence Berkeley Laboratory
Berkeley, CA 94720

J. F. Divine
Assistant Director for
Engineering Geology
U.S. Geological Survey
106 National Center
12201 Sunrise Valley Dr.
Reston, VA 22092

V. M. Glanzman
U.S. Geological Survey
P.O. Box 25046
913 Federal Center
Denver, CO 80225

C. H. Johnson
Technical Program Manager
Nuclear Waste Project Office
State of Nevada
Evergreen Center, Suite 252
1802 North Carson Street
Carson City, NV 89710

T. Hay, Executive Assistant
Office of the Governor
State of Nevada
Capitol Complex
Carson City, NV 89710

R. R. Loux, Jr. (3)
Executive Director
Nuclear Waste Project Office
State of Nevada
Evergreen Center, Suite 252
1802 North Carson Street
Carson City, NV 89710

John Fordham
Desert Research Institute
Water Resources Center
P.O. Box 60220
Reno, NV 89506

Prof. S. W. Dickson
Department of Geological Sciences
Mackay School of Mines
University of Nevada
Reno, NV 89557

J. R. Rollo
Deputy Assistant Director for
Engineering Geology
U.S. Geological Survey
106 National Center
12201 Sunrise Valley Dr.
Reston, VA 22092

Eric Anderson
Mountain West Research-Southwest
Inc.
Phoenix Gateway Center
432 North 44 Street
Suite 400
Phoenix, AZ 85008-6572

Judy Foremaster (5)
City of Caliente
P.O. Box 158
Caliente, NV 89008

A. T. Tamura
Science and Technology Division
Office of Scientific and Technical
Information
U.S. Department of Energy
P.O. Box 62
Oak Ridge, TN 37831

L. Jardine
Project Manager
Bechtel National Inc.
P.O. Box 3965
San Francisco, CA 94119

R. Harig
Parsons Brinckerhoff Quade &
Douglas
1625 Van Ness Ave.
San Francisco, CA 94109-3679

Dr. Roger Kasperson
CENTED
Clark University
950 Main Street
Worcester, MA 01610

Robert E. Cummings
Engineers International, Inc.
P.O. Box 43817
Tucson, AZ 85733-3817

Dr. Jaak Daemen
Department of Mining and
Geotechnical Engineering
University of Arizona
Tucson, AZ 85721

Department of Comprehensive Planning
Clark County
225 Bridger Avenue, 7th Floor
Las Vegas, NV 89155

Economic Development Department
City of Las Vegas
400 East Stewart Avenue
Las Vegas, NV 89109

Planning Department
Nye County
P.O. Box 153
Tonopah, NV 89049

Director of Community Planning
City of Boulder City
P.O. Box 367
Boulder City, NV 89005

Commission of the European
Communities
200 Rue de la Loi
B-1049 Brussels
BELGIUM

Lincoln County Commission
Lincoln County
P.O. Box 90
Pioche, NV 89043

Community Planning & Development
City of North Las Vegas
P.O. Box 4086
North Las Vegas, NV 89030

City Manager
City of Henderson
Henderson, NV 89015

ONWI Library
Battelle Columbus Laboratory
Office of Nuclear Waste Isolation
505 King Avenue
Columbus, OH 43201

Librarian
Los Alamos Technical
Associates, Inc.
P.O. Box 410
Los Alamos, NM 87544

1510	J. W. Nunziato
1511	D. K. Gartling
1511	N. E. Bixler
1511	R. R. Eaton (5)
1511	P. L. Hopkins
1511	M. J. Martinez
1511	A. J. Russo
1511	Day File
1512	J. C. Cummings
1513	D. W. Larson
1513	R. C. Dykhuizen
1520	L. W. Davison
1530	D. B. Hayes
1550	C. W. Peterson
1554	D. P. Aeschilman
3140	Technical Library
6230	W. C. Luth
6300	R. W. Lynch
6300-1	T. O. Hunter
6310	J. E. Stiegler, Actg.
6310	100/12142/SAND88-2936/Q3
6310	YMPCRF
6311	A. L. Stevens
6311	C. Mora
6312	F. W. Bingham
6312	P. C. Kaplan
6312	R. R. Peters
6312	R. W. Prindle
6313	T. E. Blejwas
6313	E. A. Klavetter
6313	A. W. Peterson (5)
6314	J. R. Tillerson
6315	L. E. Shephard
6316	R. P. Sandoval

6317	S. Sinnock
6332	WMT Library (20)
6410	N. R. Ortiz, Actg.
3141	S. A. Landenberger (5)
3151	W. I. Klein (3)
8524	J. A. Wackerly
3154-1	C. L. Ward (8) for DOE/OSTI

Org.	Bldg.	Name	Rec'd by	Org.	Bldg.	Name	Rec'd by

Sandia National Laboratories